CORRELATION EFFECTS IN THE TRANSITION METALS AND THE SCREENING OF NON-TRANSITION ELEMENT IMPURITIES IN IRON AND NICKEL

By

COLIN MICHAEL SAYERS

Thesis submitted
for the
Degree of Doctor of Philosophy
of the University of London
and for the
Diploma of Imperial College

Solid State Theory Group
Physics Department
Imperial College
London, S.W.7.

December 1976

ABSTRACT

The screening of a non-transition element impurity in iron is studied in Koster-Slater theory with only the 4s electrons being considered to participate in the screening, the 3d electrons being assumed to be correlated and localised on the iron sites as suggested by saturation magnetisation measurements. Assuming about one 4s electron per atom in pure iron and a positive polarisation of the 4s band, the impurity hyperfine field is found to cross from negative to positive values as the potential becomes strong enough to form a bound state. Such a change in sign is observed between Al and Si in iron and soft X-ray emission measurements confirm the presence of a bound state on Al in iron. No such bound state is seen on Al in Ni and in contrast to iron the screening in nickel is dominated by the 3d electrons.

The effect of electron interactions are studied in the one-band model using Gutzwiller's method and are found to give a lower cohesive energy than that obtained by Friedel, the difference being greatest for a half filled band. This extends qualitatively to the transition metals, the effect of electron interactions on the itineracy being greatest for a half-filled band, and in the middle of the 3d series the elastic moduli, melting point and heat of fusion indicate a much weaker bonding than expected from Friedel's model, which works well for the 4d and 5d series.

The Stoner criterion is derived in the single band Gutzwiller model and the properties of the Stoner parameter are discussed. A transition to a partially aligned state is possible if the density of states at the Fermi level $n(E_F)$ of the uncorrelated non-magnetic state is large and for a given value of $n(E_F)$, the critical interaction energy at which a ferromagnetic transition first occurs decreases with the number of states α within this high density of states region, although the results are not strongly dependent upon α, particularly for large $n(E_F)$. The magnetisation dependence of the ground state energy is discussed, and the magnetic moment and magnetisation energy of the lowest energy state are found to increase with α, provided that the interaction strength is sufficient to cause a ferromagnetic transition. Thus Ni, with a sharp peak at the Fermi level, is a strong ferromagnet despite the narrowness of this peak because of the small number of holes in the d band, whilst Fe, with 2.9 holes per atom in the d band, is a weak ferromagnet although intra-atomic exchange is a strong stabilising influence.

ACKNOWLEDGEMENTS

The work presented in this thesis was carried out under the supervision of Professor N.H. March, with the financial support of the Science Research Council.

To Professor March I would like to express my thanks for many useful conversations, comments and suggestions during this work and for enabling me to work in close contact with experiment. I am grateful to all members of the Solid State Group at Imperial College and in particular to Dr. N. Rivier for many stimulating conversations and to Professor B.R. Coles for useful comment.

It is a pleasure to thank Professor D.J. Fabian and Dr. L.M. Watson (Strathclyde) for useful comments and correspondence concerning the soft X-ray emission experiments discussed in Chapter 3, Professor J. Friedel (Orsay) for valuable comments on the work presented in Chapter 4, Dr. R.D. Lowde (Harwell) for introducing me to the theory of magnetism and for stimulating my interest in the present subject, and Dr. T.E. Cranshaw (Harwell) for discussions on the hyperfine field problems.

Special thanks go to my wife, Zehra, for much encouragement and good advice and for several valuable comments on the manuscript, and to my parents for encouragement and moral support.

Finally I wish to thank Mrs. T. Wright and Mrs. J. Morris for typing the thesis.

CONTENTS

Contents (Continued)

INTRODUCTION

The problem of the nature of the d electrons in the transition metals has been a persistent one in the theory of the solid state with both the localised and itinerant models having had considerable success. Some of the experimental evidence which has been taken in support of one or the other of these models is discussed in § 1.1. In particular it appears that in contrast to nickel, which behaves in a way characteristic of an itinerant ferromagnet, iron behaves as if there are two spins localised on the atom coupled ferromagnetically by Hund's rule exchange. Much has been learnt about the nature of electron interactions in the transition metals by studying the structure of an isolated transition metal atom in a metal such as Cu or Au, but the difficulty in treating the electronic structure of a transition metal such as iron arises from the delicate balance between the intra-atomic interaction and the hopping integral, which determines the bandwidth, and can only be studied in the pure matrix. In § 1.5 we discuss experiments on alloys of iron and nickel with non-transition metal impurities and calculate the change in saturation magnetisation with impurity concentration in a simple charge screening model. It is found that whilst in Ni the screening is dominated by the 3d electrons, in Fe the screening of a non-transition element impurity is largely by the 4s electrons. In Chapter 2 we present a simple model of the screening of a non-transition element impurity in iron in which only the part played by the 4s electrons in the screening is considered, the 3d electrons being considered to be correlated and localised on the iron sites. This model, which is capable of treating different spatial wavefunctions for $\uparrow$ and $\downarrow$ electrons, represents an extension of the one-band model of Koster and Slater (1954) to the spin polarised case. The model is used to calculate the hyperfine field at the

impurity nucleus and, assuming a positive polarisation of the 4s electrons and about one 4s electron per atom in the pure matrix, the impurity hyperfine field is found to cross from negative to positive values as the impurity potential becomes strong enough to form a bound state at the bottom of the band. The results are found to be in good qualitative agreement with experiment, the hyperfine field crossing from negative to positive values between Al and Si, Ga and Ge, Sn and Sb, and between Tl and Pb in iron in the 3rd, 4th, 5th and 6th periods respectively, and are compared with those of Daniel and Friedel (1963) who represented the 4s electrons by a spin polarised free electron gas. The interest of examining the electronic structure of impurities in iron in the region of the cross-over is pointed out, and in Chapter 3 soft X-ray emission spectra of such alloys are discussed. The covalent admixture between the impurity state and neighbouring 3d states is considered in § 3.5 and a simple explanation of the saturation magnetisation measurements of Aldred on alloys of iron with non-transition element impurities is proposed.

In Chapter 4 the effect of electron interactions on the cohesion in the one band model is investigated using Gutzwiller's model, and is found to give a lower cohesive energy than that obtained by Friedel (1969), who neglected the energy cost of intra-atomic charge fluctuations, the difference being greatest for a half filled band. The applicability of the results to the case of five d bands is discussed in § 4.4 with particular reference to the difference in electronic structure between iron and nickel. In § 4.6 we discuss the implications of these results for the surface properties of the transition metals, and the role of correlation in the catalytic properties of the 3d series.

Chapter 5 discusses the magnetic properties of the single band Gutzwiller model. A partially aligned state becomes stable relative to the non-magnetic state if $1 - C_{EFF}\, n(E_F) < 0$, where $n(E_F)$ is the density of states at the Fermi level, and the properties of C_{EFF}

are discussed. As the number of electrons (holes) per atom in the band $\bar{n} \rightarrow 0$, C_{EFF} behaves with the bare interaction C in a qualitatively similar way to the effective interaction C_{HF} between opposite spin electrons in the non-magnetic ground state. As $\bar{n} \rightarrow 1$, however, $C_{HF} - C_{EFF}$ is found to increase in magnitude with C_{HF} being greater than C_{EFF}. We therefore expect that Kanamori's theory, which replaces the Stoner parameter C_{EFF} with the effective interaction between opposite spin electrons in the non-magnetic ground state, evaluated in the ladder approximation, would overestimate the tendency to ferromagnetism, particularly in the limit $\bar{n} \rightarrow 1$. This is shown to be the case and for the triangular density of states, for example, Gutzwiller's model is found to offer a better description of the correlated ground state if $\bar{n} \gtrsim 0.035$. The dependence of the ground state energy on the magnetisation is discussed and it is found that the important criterion for ferromagnetism is the presence of a region of high density of states at the Fermi level. For a given height of this peak y/ω, where 2ω is the bandwidth, the critical values of the interaction strength at which a transition to a partially aligned state occurs decreases as the number of states within this peak α decreases, but the dependence upon α is not strong, particularly for large y. On the other hand, it is found that the magnetisation and energy of magnetisation of the lowest energy state is greatest for a large value of α provided that the interaction strength is sufficient to cause a transition to ferromagnetism. It is argued that a similar behaviour is to be expected in the case of the transition metals with five d bands, although intra-atomic exchange will, of course, be an additional important factor in stabilising the ferromagnetic state. In Ni it is well known from band structure calculations that there is a sharp peak in the density of states at the Fermi level, and since the number of holes in the d band of Ni is small, strong

ferromagnetism is possible despite the narrowness of this peak. In iron, however, with 2.9 holes per atom in the d band, it is unlikely that a peak of sufficient width will occur and iron is a weak ferromagnet, despite the strong stabilising influence of intra-atomic exchange. Finally the absence of ferromagnetism in Pd and Pt is discussed.

Some of the work in this thesis has been presented in the following:

C.M. Sayers, N.H. March, A. Dev, D.J. Fabian and L.M. Watson (1975). J.Phys.F.5, L207.

C.M. Sayers, N.H. March, A. Dev, D.J. Fabian and L.M. Watson (1976), Paper presented at the 13th Annual Solid State Physics Conference (Manchester).

C.M. Sayers (1976), J.Phys.F. 6, 1939.

C.M. Sayers (1976), To be published in J.Phys.F.

C.M. Sayers, N.H. March, D.J. Fabian and L.M. Watson (1976). To be submitted to J.Phys.F.

J. Friedel and C.M. Sayers (1976). To be submitted to J.Physique.

CHAPTER I

EVIDENCE FOR CORRELATION EFFECTS IN THE TRANSITION METALS

1.1 Introduction and Experimental Survey

When compared with s and p states of about the same energy, atomic d states are rather tightly bound around the nucleus due to the term $\ell(\ell+1)/r^2$ in the radial Schrodinger equation. Consequently, when the atoms come together to form the solid, the s and p states overlap strongly and form a broad band, but the d states are not strongly perturbed by the lattice potential and do not overlap strongly with d states on neighbouring atoms. This is particularly true of the 3d series, there being $(n - \ell - 1)$ spherical nodal surfaces centred at the origin, and it is not clear whether a description of the electronic structure based on localised atomic orbitals, as used for the even more localised f states in the rare earth metals, or a molecular orbital description, as used for simple metals, would be the more appropriate. Indeed, this has been a question of considerable controversy with much experimental information in support of both these points of view (Herring, 1966)

1.1.1 Evidence in favour of a localised model

(i) The temperature dependence of the initial susceptibility, χ_o, of iron and nickel above the Curie temperature T_c varies as $A(T-T_c)^{-\gamma}$ with $\gamma = 1.37 \pm 0.04$ for iron (Noakes and Arrot, 1964) and $\gamma = 1.35 \pm 0.02$ for nickel (Kouvel and Fisher, 1964) in excellent agreement with the 4/3 power relation obtained from the exact series for the Heisenberg model.

(ii) The energy distribution of neutrons critically scattered from iron is found to be several times smaller than that expected on the basis of a simple itinerant model, but close to that expected from a localised model (Erikson and Jacrot, 1960).

(iii) The magnetic entropy of iron is about $k \ln 3$ per atom (Hofmann et al. 1956, Mott and Stevens 1957) indicating that there are two spins per atom coupled by intra-atomic exchange, which remain coupled well above the Curie point despite becoming decoupled from the moments on neighbouring iron atoms.

(iv) Whilst the resistivity of nickel above T_c behaves very much like that of palladium with a curvature satisfactorily explained by an itinerant model, the resistivity of iron varies linearly with a strong temperature independent contribution, a similar behaviour being observed in the magnetic rare earth metals (White and Woods 1958, Coles 1958). This suggests that spin disorder plays a different role in iron than in nickel, and a strong spin disorder term occurs also in the resistivity of manganese (White and Woods 1958).

1.1.2 Evidence in favour of an itinerant model

(i) Whilst the saturation moment of iron is 2.2 μ_B/atom in agreement with there being two spins per atom coupled ferromagnetically by Hund's rule exchange, and in agreement with the value of $k \ln 3$ for the magnetic entropy, the saturation moment of Ni is 0.61 μ_B/atom and that of Co 1.72 μ_B/atom. This indicates that in Ni and Co some, at least, of the d electrons are itinerant.

(ii) The electronic specific heat of the transition metals (Cheng et al. 1960) is five to ten times greater than that of the simple metals indicating a high density of states at the Fermi energy, and strongly suggesting the existence of a Fermi surface for d electrons.

(iii) Experimental studies of the de Hans-van Alphen effect (Joseph and Thorsen 1963, Gold et al. 1971, Baraff 1973) and the magnetoresistance (Coleman et al. 1973, Angadi et al. 1974) clearly demonstrate the existence of a Fermi surface for d electrons in iron and nickel, and are in excellent agreement with the band structure calculations of Callaway and co-workers (Tawil and Callaway 1973, Wang and Callaway 1974).

(iv) Soft X-ray emission spectroscopy (SXS) and X-ray photoemission spectroscopy (XPS) give d electron bandwidths similar to those obtained in band structure calculations.

There is therefore considerable evidence that the d electrons in the transition metals are collective, but it is clear that, in the 3d series at least, correlation effects are important in determining the electronic structure. We note in particular the striking difference between iron and nickel. Thus, whilst nickel behaves very much like an itinerant ferromagnet, iron has many of the properties of a system of localised spins. This difference is perhaps surprising at first sight since the nuclear charge of nickel is greater than that of iron, so we would expect the 3d shell in Ni to be more tightly bound around the nucleus and consequently would expect electron interactions to be stronger than in iron. We might therefore expect correlation effects to be more important in nickel than in iron, in disagreement with experiment. This important fact will be discussed in Chapter 4.

1.2 Density Functional Theory

Despite the importance of correlations in the electronic structure of the transition metals there is an exact treatment of the ground state energy in a method in which the many-body system is characterised by the electron density. This allows the inclusion of correlation effects, while retaining the conceptual and computational simplicity of the band picture. This density functional approach is based on two fundamental theorems proved by Hohenberg and Kohn (1964) namely that the ground state wavefunction is a unique functional of the density, and that there exists a ground state energy functional which is stationary with respect to variations in the charge density. This was extended to the spin dependent case by Stoddart and March (1971) and by von Barth and Hedin (1972), the proof of the theorems being given in Appendix A.

If the electrons move in an external potential $V^{\sigma}_{EXT}(\underline{r})$ we write the total energy in density functional language as

$$E[\rho_{\uparrow},\rho_{\downarrow}] = T_S[\rho_{\uparrow}] + T_S[\rho_{\downarrow}] + \frac{1}{2}\int d\underline{r}\, d\underline{r}' \frac{\rho(\underline{r})\,\rho(\underline{r}')}{|\underline{r}-\underline{r}'|} \tag{1.1}$$
$$+ \int d\underline{r}\,[V^{\uparrow}_{EXT}(\underline{r})\rho_{\uparrow}(\underline{r}) + V^{\downarrow}_{EXT}(\underline{r})\rho_{\downarrow}(\underline{r})] + E_{XC}[\rho_{\uparrow},\rho_{\downarrow}]$$

where $T_S[\rho_\sigma]$ is the kinetic energy of a non-interacting gas of density ρ_σ and E_{XC} is the exchange and correlation contribution to the total energy. We require $E[\rho_{\uparrow},\rho_{\downarrow}]$ to be stationary with respect to arbitrary variations in $\rho_{\uparrow}$ and $\rho_{\downarrow}$ subject to the conservation of the total number of electrons. The spin density is then given by

$$\rho_\sigma(\underline{r}) = \sum_{\substack{\text{OCC}\\ \text{STATES}}} |\phi_{i\sigma}(\underline{r})|^2 \tag{1.2}$$

where the functions $\phi_{i\sigma}$ are solutions of the Schrodinger-like equation

$$\left[\frac{-\hbar^2}{2m}\nabla^2 + V^{\sigma}_{EXT}(\underline{r}) + \int d\underline{r}' \frac{\rho(\underline{r}')}{|\underline{r}-\underline{r}'|} + V^{\sigma}_{XC}\right]\phi_{i\sigma}(\underline{r}) = \epsilon_{i\sigma}\phi_{i\sigma}(\underline{r}) \tag{1.3}$$

where $V^{\sigma}_{XC}(r) = \delta E_{XC}/\delta\rho_\sigma(r)$ is a functional of $\rho_{\uparrow}$ and $\rho_{\downarrow}$. Equations (1.2) and (1.3) are in principle exact. It is clear however that to obtain the functional form of $V^{\sigma}_{XC}(r)$ is equivalent to solving the many body problem and in practice approximations for the exchange and correlation potential are necessary. In most of the applications of the density functional scheme a local dependence on the density has been assumed. This approximation is exact in the limit of slow and weak spatial variations of the spin density. Various attempts have been suggested to improve the local density approximation such as the use of gradient corrections. It is doubtful, however, whether gradient corrections can be viewed as improvements in practical calculations. Thus the inclusion of the two lowest terms gives wrong corrections for spatial variations with characteristic wave vectors of the order or

larger than the Fermi wavevector (Geldart et al. 1972) and therefore give no improvement when the local density approximation certainly needs to be corrected. The $\epsilon_{i\sigma}$ in (1.3) are Lagrange multipliers and should not be confused with the quasi-particle energies $E_{\underset{\sim}{k}\sigma}$ which must be obtained from the Dyson equation

$$\left[-\frac{k^2\nabla^2}{2m} + V^{\sigma}_{EXT}(\underset{\sim}{r}) + \int d\underset{\sim}{r}' \frac{\rho(\underset{\sim}{r}')}{|\underset{\sim}{r}-\underset{\sim}{r}'|} \right] \psi_{\underset{\sim}{k}\sigma}(\underset{\sim}{r}) + \int \Sigma_{\sigma}(\underset{\sim}{r},\underset{\sim}{r}'; E_{\underset{\sim}{k}\sigma}) \psi_{\underset{\sim}{k}\sigma}(\underset{\sim}{r}') d\underset{\sim}{r}' = E_{\underset{\sim}{k}\sigma} \psi_{\underset{\sim}{k}\sigma}(\underset{\sim}{r}) \tag{1.4}$$

where Σ_{σ} is the spin dependent non-local quasi particle self energy (Hedin and Lundquist, 1969). Thus although equation (1.1) offers in principle an exact treatment of the ground state energy, the $\epsilon_{i\sigma}$ and $\phi_{i\sigma}$ in (1.3) do not represent the quasi particle energies and wavefunctions and little can be learnt about the nature of the wavefunction in the presence of electron interactions from these calculations. There have therefore been several semi-empirical discussions of the nature of the wavefunctions and density of states in a strongly correlated electron system, particularly with reference to iron, and these usually assume that some, at least, of the electrons are localised in nature.

1.3 Theories with combined localised and itinerant character

(i) Pauling (1938) on the basis of a study of the behaviour of the melting points, compressibilities and atomic volumes of the transition metals was the first to recognise the importance of the d electrons in the bonding, but pointed out that in the middle right of the 3d series the d electrons do not contribute as fully as might be expected to the binding. To explain this, Pauling assumed that the five d-orbitals can be partitioned into 2.44 non-bonding or atomic like d-orbitals, and 2.56 bonding d-orbitals which, together with one s and three p orbitals hybridise to give 6.56 bonding hybrid (spd) orbitals. The behaviour of the physical properties within the 3d series was then taken to indicate

that on passing from potassium to vanadium the number of bonding electrons per atom increases from one to five, after which the electrons begin to enter the atomic, or localised, d orbitals where they retain parallel spin as long as possible. Thus Cr, Mn, Fe, Co and Ni are assumed to have 5.78 bonding electrons and 0.22, 1.22, 2.22, 3.22 and 4.22 atomic like d electrons respectively.

(ii) Mott and Stevens (1957) and Bates and Stevens (1961) suggested that both localised and itinerant electrons may be simultaneously present in iron because of the anisotropy of the d orbitals. The effect of a cubic field is to split the five fold degeneracy of the d electrons into a triply degenerate set, labelled T_{2g}, and a doubly degenerate set, labelled Eg. Mott and Stevens assumed that the T_{2g} orbitals, which are directed towards nearest neighbours in the body centred cubic structure, are itinerant but that the distance between next nearest neighbours in iron was greater than the critical distance at which a Mott transition occurs so that the Eg states must be described by 'non-conducting' wave-functions. The three T_{2g} functions, possibly much hybridised with the 4sp electrons, and perhaps with radii greatly different from the atomic Eg states, were assumed to form a set of wavefunctions of the Bloch type which are strongly bonding, and it was assumed that there are two electrons per atom in the non-conducting Eg states coupled by intra-atomic exchange giving a moment of 2.0 μ_B/atom, the difference between this and the saturation moment of 2.2 μ_B being due to a small polarisation of the itinerant d electrons.

(iii) Goodenough (1960, 1963) emphasised the two sublattice nature of the body centred cubic structure of iron in which near neighbour directed orbitals form a band in which the bonding states, corresponding to antiparallel spin correlations within the bonds, are more stable than the antibonding states with parallel spin correlations. He suggested that any inherent spin correlation between nearest neighbours, whether

it be antiferromagnetic or ferromagnetic, forces the next nearest neighbour correlations to be ferromagnetic because intra-atomic exchange interactions and nearest neighbour spin correlations are both assumed to be stronger than next nearest neighbour correlations. As a result, the Eg electrons may be assumed to be localised and to behave as if they obey Hund's rule.

(iv) Van der Woude and Sawatzky (1974), in a recent review, have analysed the hyperfine field at iron sites in iron based alloys on the basis of a modified Zener-Vonsovskii model and have concluded that the 3d magnetic moments in iron are highly localised and are coupled ferromagnetically by a small percentage of itinerant d electrons. Stearns (1973, 1976) has proposed a similar model and from a study of the concentration dependence of the hyperfine field at successive neighbour shells to the impurity has concluded that at most 4% of the 3d electrons in iron are itinerant.

(v) Edwards (1970) and Sakoh and Edwards (1975) proposed that a Hubbard splitting occurs in iron, the upper Hubbard band containing two states per atom, and that the two holes per atom in this band may be treated as localised spins coupled by Hunds' rule. A model Hamiltonian was suggested in which the localised spins interact with one another via a superexchange term, and with the remaining 0.9 3d holes per atom in the lower Hubbard band which are taken as itinerant. This model was found to offer a reasonable description of the temperature dependence of the spontaneous magnetisation and spin paramagnetic susceptibility of iron.

From the nature of the assumptions involved, these theories should be regarded as interpretations rather than as explanations of the experimental facts. These models attempt to explain why the electrons in iron sometimes behave as localised and sometimes as itinerant by assuming the presence of both itinerant electrons and localised electrons

or holes. With the exception of the theory of Edwards (1970) and Sakoh and Edwards (1974), which assumes a Hubbard splitting with the localised holes being in the upper Hubbard band, all of these theories assume that the localised electrons or holes lie within the energy range occupied by the itinerant electrons. This seems most unreasonable since a localised state lying within an itinerant band must surely hybridise with this band and broaden in energy to become a resonance with a finite lifetime. Rather than divide the electrons into two groups, the electrons in one having localised wavefunctions, the electrons in the other having Bloch character, it would appear more reasonable that the many body wavefunctions itself should lie between these two extremes. Such a situation is known to be the case in the simplest many electron, many centre problem, namely the Hydrogen molecule which we shall now discuss.

1.4 Correlation in the Hydrogen Molecule

The first treatment of the electronic structure of the hydrogen molecule was by Heitler and London (1927) who recognised that when the atoms are well separated the ground state would correspond to the solution with one electron on each atom. If ϕ_a and ϕ_b are hydrogen wavefunctions for nucleus a and b, the space wavefunction corresponding to the solution of lowest energy in this approximation is

$$\psi(\underset{\sim}{r}_1, \underset{\sim}{r}_2) = \phi_a(1)\,\phi_b(2) + \phi_a(2)\,\phi_b(1) \qquad (1.5)$$

At the same time as Heitler and London suggested this approximation another treatment, the molecular orbital approach, was developed by Hund (1928) and by Mulliken (1928). In this method an electron is assumed to belong equally to the two nuclei, the space wavefunction corresponding to the solution of lowest energy being

$$\psi(\underset{\sim}{r}_1, \underset{\sim}{r}_2) = [\phi_a(1)\phi_b(2) + \phi_b(1)\phi_a(2)] + [\phi_a(1)\phi_a(2) + \phi_b(1)\phi_b(2)] \tag{1.6}$$

Here the first term is the Heitler London wavefunction (1.5) whilst the second represents the ionic configuration $H^+ + H^-$. This wavefunction clearly breaks down as the molecule is pulled apart, since at large interatomic distances the Coulomb repulsion would prevent two electrons coming together on the same atom to form the H^- ion. Further, it is clear that even at the equilibrium interatomic distance electron-electron interactions are not adequately introduced since according to this wavefunction the probability of a given electron being in a given atom is independent of whether another electron of opposite spin is already there. Coulson and Fisher (1949) considered the wavefunction

$$\psi(\underset{\sim}{r}_1, \underset{\sim}{r}_2) = [\phi_a(1)\phi_b(2) + \phi_b(1)\phi_a(2)] + \mu[\phi_a(1)\phi_a(2) + \phi_b(1)\phi_b(2)] \tag{1.7}$$

and found the value of μ giving the lowest energy as a function of the interatomic spacing R. At infinite distance μ is of course zero, and the Heitler-London wavefunction is exact. As R decreases μ was found to increase to a maximum value of about 0.24, a value which it takes at about the equilibrium interatomic distance. This is much smaller than the value $\mu = 1$ corresponding to the molecular orbital wavefunction which therefore greatly overestimates the ionic contribution.

In order to treat the effect of electron interactions on the wavefunction in the transition metals it seems natural, in view of the simplicity of the above scheme, to use a wavefunction in which the number of multiply occupied atoms in the ground state is used as a

varational parameter. Such a method was proposed by Gutzwiller (1963, 1965) and we shall use this in Chapters 4 and 5.

Hopefully it should be possible to obtain information about the degree of polarity in the ground state wavefunction from experiment. Perhaps the most promising way of doing so is to study the response of the d electrons to the presence of a substitutional impurity.

1.5 Correlation Effects in the screening of non-transition element impurities in iron and nickel.

Much can be learnt about the nature of the d electrons, localised versus itinerant, by examining their response to a substitutional impurity. If the d electrons were found to play no part in the screening of the impurity excess charge, a simple band picture would apparently not be sufficient to treat the electronic structure, whilst if they behave in a Thomas-Fermi manner a description of the electrons as a system of localised spins would be most inappropriate. The electronic structure of a transition element impurity in iron or nickel would, however, be determined largely by the balance between the electron-electron interactions on the impurity site and the overlap with neighbouring orbitals, and the nature of the response would therefore be rather dependent upon the impurity atom chosen. A non-transition element impurity would however approximate more closely to a simple perturbation, the d orbitals lying well above or below the d band of the host.

In the presence of an impurity such as Al or Si in iron or nickel let us define wavefunctions $\phi_{i\sigma}(\underline{r})$ with energy $E^{o}_{i\sigma}$ derived from the d band wavefunctions of the pure metal by the action of a potential which repels the d level at the impurity site well above the d band where it no longer interacts with the system. Let us then consider the response of the system to the potential

$$V_\sigma(\underline{r}) = V_1(\underline{r}) - V_2(\underline{r}) - V_3^\sigma(\underline{r}) + V_4^\sigma(\underline{r}) \tag{1.8}$$

where $V_1(\underline{r})$ is the potential of the impurity core, $V_2(\underline{r})$ the potential of the transition metal atom core originally present at the impurity site, $V_3^\sigma(\underline{r})$ the potential of the partially filled d shell removed or filled, and $V_4^\sigma(\underline{r})$ the potential due to the screening charge at the impurity site which should be obtained self-consistently. It is convenient to work in terms of the canonical density matrix $C_{o\sigma}(\underline{r},\underline{r}',\beta)$ where $\beta = 1/kT$, for spin σ electrons, which is built up from the $\phi_{i\sigma}$ and the $E_{i\sigma}$ as follows

$$C_{o\sigma}(\underline{r},\underline{r}',\beta) = \sum_i \phi_{i\sigma}^*(\underline{r})\,\phi_{i\sigma}(\underline{r}')\,e^{-\beta E_{i\sigma}} \tag{1.9}$$

Following March and Murray (1961) we define the canonical density matrix in the presence of the impurity potential (1.8) by analogy

$$C_\sigma(\underline{r},\underline{r}',\beta) = \sum_i \psi_{i\sigma}^*(\underline{r})\,\psi_{i\sigma}(\underline{r}')\,e^{-\beta E_{i\sigma}} \tag{1.10}$$

where $\psi_{i\sigma}$ is an eigenfunction of the perturbed Hamiltonian H_σ with energy $E_{i\sigma}$. $C_\sigma(\underline{r},\underline{r}',\beta)$ satisfies the Bloch equation

$$H_\sigma C_\sigma(\underline{r},\underline{r}',\beta) = -\frac{\partial}{\partial\beta} C_\sigma(\underline{r},\underline{r}',\beta) \tag{1.11}$$

subject to the initial condition $C_\sigma(\underline{r},\underline{r}',0) = \delta(\underline{r}-\underline{r}')$. A solution of (1.11) suitable for iteration is

$$C_\sigma(\underline{r},\underline{r}',\beta) = C_{o\sigma}(\underline{r},\underline{r}',\beta) - \int d\underline{r}_1 \int_0^\beta d\beta_1\, C_{o\sigma}(\underline{r},\underline{r}_1,\beta-\beta_1)\,V_\sigma(\underline{r}_1)\,C_\sigma(\underline{r}_1,\underline{r}',\beta_1) \tag{1.12}$$

Thus, using the orthonormality of the $\phi_{i\sigma}$

$$\int d\underline{r}\, \phi^{*}_{i\sigma}(\underline{r})\, \phi_{j\sigma}(\underline{r}) = \delta_{ij} \tag{1.13}$$

the response of the d electrons is, to first order in $V_{\sigma}(\underline{r})$

$$\int d\underline{r}\, C_{\sigma}(\underline{r},\underline{r},\beta) = \int d\underline{r}\, C_{0\sigma}(\underline{r},\underline{r},\beta) \tag{1.14}$$

$$- \beta \int d\underline{r}_1\, C_{0\sigma}(\underline{r},\underline{r}_1,\beta)\, V_{\sigma}(\underline{r}_1)$$

To obtain the expression for the spin density we introduce the Dirac density matrix

$$\rho_{\sigma}(\underline{r},\underline{r}',E) = \sum_i \psi^{*}_{i\sigma}(\underline{r})\, \psi_{i\sigma}(\underline{r}')\, \Theta(E - E_{i\sigma}) \tag{1.15}$$

and utilise the relationship between C and ρ which was established by March and Murray (1960)

$$C_{\sigma}(\underline{r},\underline{r}',\beta) = \beta \int_0^{\infty} \rho_{\sigma}(\underline{r},\underline{r}',E)\, e^{-\beta E}\, dE \tag{1.16}$$

$\rho_{\sigma}(\underline{r},\underline{r}',E)$ is seen to be the inverse Laplace transform of $\frac{1}{\beta} C_{\sigma}(\underline{r},\underline{r}',\beta)$ and may be written in the form

$$\rho_{\sigma}(\underline{r},\underline{r}',E) = \frac{1}{2\pi i} \int_{\alpha - i\infty}^{\alpha + i\infty} \frac{e^{\beta E}}{\beta}\, C_{\sigma}(\underline{r},\underline{r}',\beta)\, d\beta \tag{1.17}$$

where α is chosen such that the integral has no poles in the part of the complex plane for which $R(\beta) \geq \alpha$. Substituting gives

$$\int d\underset{\sim}{r}\, \rho_\sigma(\underset{\sim}{r},\underset{\sim}{r},E) = \int d\underset{\sim}{r}\, \rho_{0\sigma}(\underset{\sim}{r},\underset{\sim}{r},E) - \int d\underset{\sim}{r}_1 \frac{\partial}{\partial E} \rho_{0\sigma}(\underset{\sim}{r}_1,\underset{\sim}{r}_1,E) V_\sigma(\underset{\sim}{r}_1) \tag{1.18}$$

and defining

$$\rho_+ = \rho_\uparrow + \rho_\downarrow \qquad \rho_- = \rho_\uparrow - \rho_\downarrow \tag{1.19}$$

$$V_+ = V_\uparrow + V_\downarrow \qquad V_- = V_\uparrow - V_\downarrow$$

we obtain

$$\int d\underset{\sim}{r}\, \rho_-(\underset{\sim}{r},E) = \int d\underset{\sim}{r}\, \rho_-^0(\underset{\sim}{r},E) - \frac{1}{2}\int d\underset{\sim}{r}_1 \frac{\partial}{\partial E} \rho_+^0(\underset{\sim}{r}_1,E) V_-(\underset{\sim}{r}_1) - \frac{1}{2}\int d\underset{\sim}{r}_1 \frac{\partial}{\partial E} \rho_-^0(\underset{\sim}{r}_1,E) V_+(\underset{\sim}{r}_1) \tag{1.20}$$

$$\int d\underset{\sim}{r}\, \rho_+(\underset{\sim}{r},E) = \int d\underset{\sim}{r}\, \rho_+^0(\underset{\sim}{r},E) - \frac{1}{2}\int d\underset{\sim}{r}_1 \frac{\partial}{\partial E} \rho_+^0(\underset{\sim}{r}_1,E) V_+(\underset{\sim}{r}_1) - \frac{1}{2}\int d\underset{\sim}{r}_1 \frac{\partial}{\partial E} \rho_-^0(\underset{\sim}{r}_1,E) V_-(\underset{\sim}{r}_1) \tag{1.21}$$

So the change in magnetic moment of the system due to the impurity potential $V_\sigma(\underset{\sim}{r})$ is just

$$\mu_{\text{Screening}} \equiv \int d\underset{\sim}{r}\, \Delta\rho_-(\underset{\sim}{r},E_F)\mu_B = \frac{1}{2}\mu_B \int d\underset{\sim}{r} \frac{\partial}{\partial E}\left[\rho_+^0(\underset{\sim}{r},E)V_-(\underset{\sim}{r}) + \rho_-^0(\underset{\sim}{r},E)V_+(\underset{\sim}{r})\right]_{E_F} \tag{1.22}$$

to first order in $V_\sigma(\underline{r})$ to which we must add the change in moment due to the filling or removal of the partially filled d shell at the impurity site $-\mu_{HOST}$, where μ_{HOST} is the magnetic moment per atom in the pure matrix.

Consider now a ferromagnetic transition element into which a concentration c of impurity atoms has been placed. We shall assume that the impurities are non-interacting and have zero moment. This assumption is supported by the neutron scattering measurements of Holden, Comly and Low (1964) on dilute alloys of Al, Si, Ga, Ge, Sn and Sb in iron which indicate the absence of a local moment on the impurity site within experimental error. Thus the total moment of the perturbed system is given by

$$\mu_{TOTAL} = N\bar{\mu} \tag{1.23}$$

where $N\bar{\mu} = (1-c)N\mu_{HOST} + cN\mu_{SCREENING}$ (1.24

where $\mu_{Screening} = \int d\underline{r}\, \Delta\rho_-(\underline{r}, E_F)\, \mu_B$ is given to first order in $V_\sigma(\underline{r})$ by (1.22). The rate of change of mean magnetic moment with impurity concentration c is then

$$\frac{d\bar{\mu}}{dc} = -\mu_{HOST} + \mu_{SCREENING} \tag{1.25}$$

Equation (1.22) has the advantage of providing a simple and understandable picture of $\mu_{Screening}$. The second term results in a change in moment upon alloying because the density of states at the Fermi level in a spin polarised electron gas is different for $\uparrow$ and $\downarrow$ spins. Thus in Ni the $\uparrow$ spin 3d band is full so

$$\frac{\partial}{\partial E}\rho^0_\uparrow(\underline{r}, E)\Big|_{E_F} = 0. \quad \text{Mott (1935)}$$

suggested that because of the high density of states in the d band the screening would be dominated by the d electrons. Thus neglecting the first term in (1.22)

$$\int d\underset{\sim}{r}\, \Delta\rho_{-}(\underset{\sim}{r}, E_F) = -(Z_{IMP} - n_{COND}) \tag{1.26}$$

by Friedel's rule, where Z_{IMP} is the valence of the impurity atom and n_{COND} is the number of electrons per atom in the valence band of pure Ni. This gives

$$\frac{d\bar{\mu}}{dc} = -\mu_{Ni} - (Z_{IMP} - n_{COND})\mu_B \tag{1.27}$$

In Ni there are ten electrons per atom and the $\uparrow$ spin 3d band is filled. Consequently there are the same number of electrons in the 4s band as there are holes in the $\downarrow$ spin 3d band giving the simple relation

$$\frac{d\bar{\mu}}{dc} = -Z_{IMP}\mu_B \tag{1.28}$$

It should be noted that this relationship is valid only for nickel because the number of electrons in the 4s band is equal to the number of holes in the 3d band and is not applicable to other strong ferromagnets as has been sometimes assumed. Table 1.1 compares the values of $d\bar{\mu}/dc$ observed by Crangle and Martin (1959) for several non-transition element impurities in nickel with the prediction based on Equation (1.28).

TABLE 1.1

$d\bar{\mu}/dc$ for Ni based alloys in μ_B/Atom

Solute	Valence	Theory	Experiment
Cu	1	-1.0	-1.14
Zn	2	-2.0	-2.11
Al	3	-3.0	-2.80
Si	4	-4.0	-3.77
Ge	4	-4.0	-3.70
Sn	4	-4.0	-4.22
Sb	5	-5.0	-5.31

The agreement is seen to be excellent. It thus seems that the screening of non-transition element impurities in nickel is dominated by the 3d electrons which appear to be behaving in a way characteristic of an itinerant ferromagnet. This conclusion is entirely consistent with the experimental data presented in Table 1.1. Thus for nickel at least the 3d electrons must be treated in a model which is itinerant by nature and we expect normal band structure calculations to be applicable.

The first term in (1.22) is entirely new and arises from the exchange interaction of the d electrons with the absent magnetic moment at the impurity site. If the moment arises in part from near neighbour interactions this will lead to a depolarisation at sites neighbouring the impurity. Some evidence of the importance of this term is seen in Table (1.1) where the experimental value is frequently greater in magnitude than the theoretical prediction which, if we only took into account the second term in (1.22), would mean that more electrons than are available enter the d band. Nevertheless the strong valence dependence of $d\bar{\mu}/dc$ for non-transition element

impurities indicates that the 3d electrons in Ni are essentially itinerant in nature.

That such a conclusion would be wrong for iron is seen in Table 1.2 which gives the $d\bar{\mu}/dc$ values for iron based alloys obtained by Aldred (1968).

TABLE 1.2

$d\bar{\mu}/dc$ for Fe based alloys in μ_B/Atom

	Groups				
Period	1	2	3	4	5
2		Be -2.26			
3			Al -2.27	Si -2.28	
4	Cu -2.00	Zn -2.01	Ga -1.43	Ge -1.36	As -1.40
5				Sn -0.97	Sb -0.97
6	Au -1.09				

Al and Si are seen to obey the simple dilution model $d\bar{\mu}/dc = -2.2\,\mu_B$, a result first obtained by Fallot (1936), Parsons et al (1958) and Arrot and Sato (1959). In this model the impurities are assumed to carry no moment and not to disturb the moments on neighbouring iron atoms. This model is supported by the neutron scattering measurements of Holden et al (1967) who found no moment on Al, Si, Ga, Ge, Sn and Sb impurities in iron within experimental error. The measurements of Aldred (1966, 1968) summarised in Table 1.2 show, however, that the dilution model is only obeyed by those impurities with low atomic number, all others producing a small increase in the moment on neighbouring iron atoms. This is supported by the neutron scattering measurements (Holden et al 1967) which reveal that iron

atoms within 4-5 Å of the impurity have moments which are increased by ~ 1-2% over the value for pure iron. We see from Table 1.2 however that this increase depends only on the period of the impurity within groups 3 to 5, there being no dependence on the valence, indicating that the magnetic 3d electrons do not contribute to the screening of a non-transition element impurity. Furthermore this increase in moment is seen not to arise from the first term in (1.22) as this would imply an antiferromagnetic nearest neighbour coupling. We conclude therefore that the $d\bar{\mu}/dc$ values of iron based alloys can not be explained by the term $\mu_{\text{Screening}}$ in (1.25) as this would depend strongly on the impurity valence. There must therefore be a further contribution to $d\bar{\mu}/dc$ which we have not taken into account, and we shall discuss one such in Chapter 3.

This conclusion, that the 3d electrons in iron are not involved in the screening of a non-transition element impurity, is further supported by the specific heat measurements of Beck and co-workers (Gupta et al 1964, Beck 1964, Cheng et al 1964) on alloys of iron with Al, Si, Ge and Sb, which cannot be described in terms of the filling of a 'rigid' or a 'semi-rigid' d band by the excess valence electrons of the impurity. In addition, optical absorption measurements, which we shall discuss in Chapter 3, reveal that in Fe Al alloys the Fermi level does not change on alloying whilst in Ni Al alloys the absorption edge appears to move linearly upwards in energy with increasing Al content. Thus, in contrast to nickel, in which the screening of a non-transition element impurity is dominated by the 3d electrons, in iron the 3d electrons are ineffective in the screening of such impurities, which is largely by the 4s electrons. It is reasonable, therefore, to treat the screening of a non-transition element impurity in iron by a model in which the iron 3d electrons are assumed to be strongly correlated and localised on the iron sites, and that only the 4s electrons contribute to the screening.

CHAPTER II

Screening of non-transition element impurities in iron and the impurity hyperfine field

2.1 The Koster-Slater Model

We concluded in Chapter I that whilst in nickel the screening of a non-transition element impurity is dominated by the 3d electrons, in iron the 3d electrons are ineffective in the screening which is largely by the 4s electrons. We shall present in this chapter a simple model of the screening of a non-transition element impurity in iron in which only the 4s electrons are considered to take part in the screening, the 3d electrons being assumed to be highly correlated and localised on the iron sites. We shall assume further that s-d hybridisation effects may be neglected and shall discuss their effect in Chapter 3.

With these assumptions we may use the one-band model of Koster and Slater (Koster and Slater 1954, Wolff 1961, Clogston 1962) to treat the screening of the impurity excess charge by the 4s electrons. We write the unperturbed wavefunctions $\phi_{\underset{\sim}{k}\sigma}(\underset{\sim}{r})$ with wavevector $\underset{\sim}{k}$ and spin σ in terms of the Wannier functions $\omega_\sigma(\underset{\sim}{r}-\underset{\sim}{R}_i)$ centred on the i'th site as

$$\phi_{\underset{\sim}{k}\sigma}(\underset{\sim}{r}) = \sum_{\underset{\sim}{R}_i} e^{i\underset{\sim}{k}\cdot\underset{\sim}{R}_i}\,\omega_\sigma(\underset{\sim}{r}-\underset{\sim}{R}_i) \tag{2.1}$$

and, following Koster and Slater (1954) write the scattered wavefunction by analogy as

$$\psi_{\underset{\sim}{k}\sigma}(\underset{\sim}{r}) = \sum_{\underset{\sim}{R}_i} c_\sigma(\underset{\sim}{k},\underset{\sim}{R}_i)\,\omega_\sigma(\underset{\sim}{r}-\underset{\sim}{R}_i) \tag{2.2}$$

which is related to $\phi_{\underset{\sim}{k}\sigma}$ via the integral Schrodinger equation

$$\psi_{k\sigma}(\underset{\sim}{r}) = \phi_{k\sigma}(\underset{\sim}{r}) + \int d\underset{\sim}{r}' G_\sigma(\underset{\sim}{r}\,\underset{\sim}{r}'E) V^\sigma_{IMP}(\underset{\sim}{r}') \psi_{k\sigma}(\underset{\sim}{r}')\, d\underset{\sim}{r}' \qquad (2.3)$$

where V^σ_{IMP} is the impurity potential and the Green function for the unperturbed lattice $G_\sigma(\underset{\sim}{r}\,\underset{\sim}{r}'E)$ is given by

$$G_\sigma(\underset{\sim}{r}\,\underset{\sim}{r}'E) = \sum_{\underset{\sim}{k}'} \frac{\phi^*_{k'\sigma}(\underset{\sim}{r})\,\phi_{k'\sigma}(\underset{\sim}{r}')}{E - E_{k'\sigma} + i\eta} \qquad (2.4)$$

where $E_{k\sigma}$ is the energy of the unperturbed state $\phi_{k\sigma}$ to be abbreviated by E.

To solve (2.3) it is necessary to take a simple model for the impurity potential V^σ_{IMP} and in the method of Koster and Slater it is assumed that the matrix element of the impurity potential V^σ_{IMP} between Wannier functions $\omega_\sigma(\underset{\sim}{r} - \underset{\sim}{R}_i)$ is given by

$$\langle \omega_\sigma(\underset{\sim}{r} - \underset{\sim}{R}_i) | V^\sigma_{IMP} | \omega_\sigma(\underset{\sim}{r} - \underset{\sim}{R}_j) \rangle = V_\sigma \delta(\underset{\sim}{R}_i - \underset{\sim}{R}_0)\delta(\underset{\sim}{R}_j - \underset{\sim}{R}_0) \qquad (2.5)$$

where $\underset{\sim}{R}_0$ is the impurity site. This assumption, which effectively limits the impurity potential to the impurity site, is reasonable for iron based alloys for which neutron scattering experiments (Holden et al, 1967) reveal that the disturbance on iron atoms neighbouring the impurity is small, but would be certainly inapplicable to nickel based alloys in which an appreciable reduction in the magnetic moment extends some 5 $\mathring{A}$ into the nickel host (Comly et al, 1968).

Substitution of (2.1) and (2.2) into (2.3) with the assumption (2.5) gives an expression for the amplitude $C_\sigma(\underset{\sim}{R}_i)$ of the Wannier function centred at $\underset{\sim}{R}_i$

$$c_\sigma(\underset{\sim}{R}_i) = e^{i\underset{\sim}{k}\cdot\underset{\sim}{R}_i} + \sum_{\underset{\sim}{k}'} \frac{e^{i\underset{\sim}{k}'\cdot(\underset{\sim}{R}_0 - \underset{\sim}{R}_i)}}{E - E_{\underset{\sim}{k}'\sigma} + i\eta} c_\sigma(\underset{\sim}{R}_0) V_\sigma \tag{2.6}$$

where we have chosen the phases of the Wannier functions to be purely real; and in particular the amplitude of the Wannier function on the impurity site is given by

$$\left[1 - V_\sigma \sum_{\underset{\sim}{k}'} \frac{1}{E - E_{\underset{\sim}{k}'\sigma} + i\eta} \right] c_\sigma(\underset{\sim}{R}_0) = e^{i\underset{\sim}{k}\cdot\underset{\sim}{R}_0} \tag{2.7}$$

which can be written as

$$c_\sigma(\underset{\sim}{R}_0) = \frac{e^{i\underset{\sim}{k}\cdot\underset{\sim}{R}_0}}{[1 - V_\sigma F_\sigma(E)] + i\pi V_\sigma n_\sigma(E)} \tag{2.8}$$

where $n_\sigma(E)$ is the density of states in the 4s band and

$$F_\sigma(E) = \mathcal{P} \int \frac{n_\sigma(\epsilon)\, d\epsilon}{E - \epsilon} \tag{2.9}$$

$\mathcal{P}$ indicating that it is the principal part of the integral that is to be taken.

The density of spin σ electrons at a point $\underset{\sim}{r}$ in the alloy is then given by

$$\rho_\sigma(\underset{\sim}{r}) = \sum_{\text{OCC STATES}} |\psi_\sigma(\underset{\sim}{r})|^2 = \sum_{\substack{\text{OCC STATES} \\ \underset{\sim}{R}_i\ \underset{\sim}{R}_j}} c_\sigma^*(\underset{\sim}{R}_i)\, w_\sigma^*(\underset{\sim}{r} - \underset{\sim}{R}_i)\, c_\sigma(\underset{\sim}{R}_j)\, w_\sigma(\underset{\sim}{r} - \underset{\sim}{R}_j) \tag{2.10}$$

$$= \sum_{ij} \alpha_{ij}^\sigma\, w_\sigma^*(\underset{\sim}{r} - \underset{\sim}{R}_i)\, w_\sigma(\underset{\sim}{r} - \underset{\sim}{R}_j)$$

where $\alpha_{ij}^{\sigma} = \sum_{\text{OCC STATES}} c_{k\sigma}^{+}(R_i)\, c_{k\sigma}(R_j)$

We shall assume that the only Wannier function to have amplitude at R_0 is the one centred on the impurity site, the density of spin σ electrons at the impurity nucleus then being

$$\rho_{\sigma}(R_0) = \alpha_{\sigma} |\omega_{\sigma}(0)|^2 \tag{2.11}$$

where $\alpha_{\sigma} = \sum_{\text{OCC STATES}} |c_{\sigma}(R_0)|^2$

Whilst the density of spin σ electrons at r in the pure matrix is

$$\rho_{\sigma}^{0}(r) = \sum_{\text{OCC STATES}} e^{-ik\cdot R_i}\, \omega_{\sigma}^{+}(r - R_i)\, e^{ik\cdot R_j}\, \omega_{\sigma}(r - R_j) \tag{2.12}$$
$$= \sum_{\text{OCC STATES}} |\omega_{\sigma}(0)|^2$$

at the impurity nucleus, with the same assumption at before.

Thus, using (2.8) we have

$$\alpha_{\sigma} = \sum_{\text{OCC STATES}} \frac{1}{[1 - V_{\sigma} F_{\sigma}(E)]^2 + [\pi V_{\sigma} n_{\sigma}(E)]^2} \tag{2.13}$$
$$= \int^{E_F} \frac{n_{\sigma}(E)\, dE}{[1 - V_{\sigma} F_{\sigma}(E)]^2 + [\pi V_{\sigma} n_{\sigma}(E)]^2}$$

2.1.1 Treatment of bound and virtual bound states on the impurity

If the impurity potential V_{σ} is sufficiently large there will be an energy E_0^{σ} such that

$$1 - V_{\sigma} F_{\sigma}(E_0^{\sigma}) = 0 \tag{2.14}$$

will be satisfied. If this energy lies within the band the term $i\pi V_\sigma n_\sigma (E_0^\sigma)$ in the denominator of (2.8) will remain but $C_\sigma(\underset{\sim}{k}_0)$ will exhibit a resonance in the region of E_0^σ. This corresponds to the virtual bound state discussed by Friedel (1958). If E_0^σ lies outside the band $C_\sigma(\underset{\sim}{k}_0)$ will become infinite signalling the formation of a bound state on the impurity site. This level lies above the band if the impurity is repulsive and below it if the impurity is attractive.

In the presence of a virtual bound state we may evaluate (2.13) by expanding $F_\sigma(E)$ about the energy E_0^σ and setting $n(E) \approx n(E_0^\sigma)$ in the integral. Thus $F_\sigma(E) \approx F_\sigma(E_0^\sigma) + (E - E_0^\sigma) F_\sigma'(E_0^\sigma)$

$$= V_\sigma^{-1} + (E - E_0^\sigma) F_\sigma'(E_0^\sigma) \qquad (2.15$$

and $$[1 - V_\sigma F_\sigma(E)]^2 + [\pi V_\sigma n_\sigma(E)]^2 \qquad (2.16$$

$$\approx V_\sigma^2 (AE^2 + BE + C)$$

where $A = F_\sigma'^2(E_0^\sigma)$

$B = -2E_0^\sigma F_\sigma'^2(E_0^\sigma)$

$C = E_0^{\sigma 2} F_\sigma'^2(E_0^\sigma) + \pi^2 n^2(E_0^\sigma)$

but $$\int \frac{d\alpha}{a\alpha^2 + b\alpha + c} = \frac{2}{\sqrt{4ac - b^2}} \tan^{-1} \frac{2a\alpha + b}{\sqrt{4ac - b^2}}$$

for $4ac > b^2$ as in this case, so (2.13) becomes

$$\frac{1}{\pi V_\sigma^2 F_\sigma'(E_0^\sigma)} \left[\tan^{-1} \frac{(E - E_0^\sigma) F_\sigma'(E_0^\sigma)}{\pi n_\sigma(E_0^\sigma)} \right]. \qquad (2.17$$

If the bound state lies below the band then

$$\alpha_\sigma = \left| \frac{F_\sigma^2(E_0^\sigma)}{F_\sigma'(E_0^\sigma)} \right| + \int_{E_B^\sigma}^{E_F} \frac{n_\sigma(\epsilon)\, d\epsilon}{[1 - V_\sigma F_\sigma(\epsilon)]^2 + [\pi V_\sigma n_\sigma(\epsilon)]^2} \qquad (2.18)$$

where E_B^σ is the bottom of the band. As $V_\sigma \to -\infty$, $E_0^\sigma \to -\infty$ and we see from (2.9) that

$$\alpha_\sigma^{BOUND} = \left| \frac{F_\sigma^2(E_0^\sigma)}{F_\sigma'(E_0^\sigma)} \right| \longrightarrow 1$$ corresponding to the Wannier function $\omega_\sigma(\underline{r} - \underline{R}_0)$ becoming completely full.

2.2 Hyperfine Field at the Impurity nucleus

The hyperfine field at an iron nucleus in pure body-centred cubic iron is known from many experiments to be $-339\,kOe$ (Stearns 1973) and is the sum of several contributions. The most important of these is that due to the polarisation of the core electrons by the magnetic 3d electrons, and whilst predictions of their value have been made (Watson and Freeman, 1961) it is only recently that it has been possible to measure them individually (Song et al 1972, 1974). There appears to be considerable disagreement between experiment and theory, the measured contribution to the hyperfine field at an Fe nucleus in iron due to the 2s electrons being $-1644 \pm 391\,kOe$ (Song et al 1974) whilst the predictions of theory are of the same sign but are several times smaller in magnitude. This negative sign arises because the 3d band is spin polarised. If the majority of 3d electrons have spin $\uparrow$, a core electron with spin $\uparrow$ experiences a stronger exchange force than one with spin $\downarrow$ so $\phi_{ns\uparrow}(\underline{r})$ is pulled out relative to $\phi_{ns\downarrow}(\underline{r})$ for inner ns levels, the opposite being true for outer levels. Goodings and Heine (1960) investigated this in the case of a free atom of iron using unrestricted Hartree-Fock theory

and found that the contribution of the 1s level is small. The contribution of the 3s level was small and positive but when slightly expanded 3d wavefunctions were used, corresponding to the situation in the solid, the 3s level was found to behave more like an "inner" shell with a negative contribution at the nucleus. To be consistent with the observed total hyperfine field, therefore, the measured contribution of the 2s electrons requires a large positive contribution of order 300-1500 kOe from the 4s electrons (Duff and Das, 1975) which is at least an order of magnitude greater than current band theory (Wakoh and Yamashita 1968, Duff and Das 1971, Callaway et al. 1973). Song et al do however quote a value of +600 kOe obtained by Stearns. It is important to add that the small negative magnetisation found at interatomic positions in iron (Shull and Yamada 1962), which was originally interpreted in terms of a negative 4s polarisation, is now thought to be due to the spin dependence of the radial part of the 3d wavefunctions (Duff and Das, 1971).

At the nucleus of a non-transition element impurity in iron, however, the core polarisation is expected to be small and we shall assume that the dominant contribution to the hyperfine field is the 4s polarisation. Thus the core polarisation term is proportional to the z component of the spin of the impurity

$$H_{CORE} = g\mu_B A_{CORE} \langle \bar{S}_z \rangle \qquad (2.19$$

where A_{CORE} is the hyperfine coupling constant. Neutron scattering measurements of Holden et al (1967) indicate that there is no moment on Al, Si, Ga, Ge, Sn and Sb impurities within experimental error, so we can assume that this process is absent at a non-transition element impurity in iron. Furthermore the dipole fields produced by neighbouring iron atoms cancels in a lattice of cubic symmetry and the orbital magnetic moment is quenched. We shall assume that the external Lorentz and

demagnetising fields are relatively small and may be accounted for. Under these conditions the hyperfine field at the impurity nucleus is

$$H(\underset{\sim}{R}_0) = \frac{8\pi}{3}\mu_B\left[\rho_\uparrow(\underset{\sim}{R}_0) - \rho_\downarrow(\underset{\sim}{R}_0)\right] \tag{2.20}$$

where $\uparrow$ is the majority spin direction in the 3d band of pure iron, which we may evaluate using the Koster-Slater theory presented in §.2.1.

It is convenient to work with the quantity ξ defined by

$$\xi = \frac{H(\underset{\sim}{R}_0)}{H^0_{4s}(\underset{\sim}{R}_0)} \tag{2.21}$$

where $H^0_{4s}(\underset{\sim}{R}_0)$ is the contribution of the 4s electron polarisation to the hyperfine field at an iron nucleus in pure iron. Thus with

$H^0_{4s}(\underset{\sim}{R}_0) = \frac{8\pi}{3}\mu_B\beta$ where

$$\beta = \int_{E_B^\uparrow}^{E_F} |\omega_\uparrow(0)|^2 n_\uparrow(\epsilon)\,d\epsilon - \int_{E_B^\downarrow}^{E_F} |\omega_\downarrow(0)|^2 n_\downarrow(\epsilon)\,d\epsilon \tag{2.22}$$

$$\xi = \frac{(\kappa_\uparrow - \kappa_\downarrow)(|\omega_\uparrow(0)|^2 + |\omega_\downarrow(0)|^2)}{2\beta} + \frac{(\kappa_\uparrow + \kappa_\downarrow)(|\omega_\uparrow(0)|^2 - |\omega_\downarrow(0)|^2)}{2\beta} \tag{2.23}$$

where κ_σ is given by (2.18) in the presence of a bound state and by (2.13) otherwise.

We shall now assume that the difference between $\omega_\uparrow(\underset{\sim}{r} - \underset{\sim}{R}_0)$ and $\omega_\downarrow(\underset{\sim}{r} - \underset{\sim}{R}_0)$ may be neglected and that we can represent the 4s band by two identical subbands shifted in energy with respect to

one another by 2Δ . Thus we introduce $\omega(\underset{\sim}{r}-\underset{\sim}{R}_0)$ and $n(E)$ defined by

$$\omega_\uparrow(\underset{\sim}{r}-\underset{\sim}{R}_0) = \omega(\underset{\sim}{r}-\underset{\sim}{R}_0) = \omega_\downarrow(\underset{\sim}{r}-\underset{\sim}{R}_0)$$

$$n_\uparrow(E-\Delta) = n(E) = n_\downarrow(E+\Delta) \qquad (2.24)$$

2.2.1 The Impurity Potential

Since the magnetic 3d shell originally present at the impurity site has been either removed or filled, the impurity potential, defined with respect to the pure lattice, will be spin dependent and must be determined self-consistently. The potential acting on the 4s electrons will be

$$V^\sigma_{imp}(\underset{\sim}{r}) = V_1(\underset{\sim}{r}) - V_2(\underset{\sim}{r}) - V^\sigma_3(\underset{\sim}{r}) + V^\sigma_4(\underset{\sim}{r}) \qquad (2.25)$$

where $V_1(\underset{\sim}{r})$ is the potential of the impurity core, $V_2(\underset{\sim}{r})$ the potential of the iron core originally present at the impurity site, $V^\sigma_3(\underset{\sim}{r})$ the potential of the iron 3d shell removed or filled and V^σ_4 the potential due to the screening charge at the impurity site. Since there is no moment at the impurity site (Holden et al. 1967) and the 4s - 4s exchange interaction is small we may make the assumption $V_4^\uparrow = V_4^\downarrow = V_4$ say and write

$$\langle\omega_\sigma(\underset{\sim}{r}-\underset{\sim}{R}_0)|V^\sigma_{imp}|\omega_\sigma(\underset{\sim}{r}-\underset{\sim}{R}_0)\rangle = V+\Delta \quad \text{For Spin } \uparrow$$

$$= V-\Delta \quad \text{For Spin } \downarrow \qquad (2.26)$$

V may be obtained self-consistently by setting $\alpha_\uparrow + \alpha_\downarrow$ equal to the number of s electrons involved in the screening at the impurity

site. It is not easy to relate V to the valence of the impurity because of the increasing proportion of p states involved in the screening as the impurity becomes more attractive. These states contribute to the impurity hyperfine field via a polarisation of the core s electrons but this effect is small and may be neglected. Nevertheless the parameter V is expected to vary roughly linearly with the valence of the impurity as we may see from the following argument based on Slater orbitals. We have assumed in (2.26) that the exchange splitting 2Δ of the 4s band is due to intra-atomic exchange only, that is $2\Delta = J_{sd}\,\mu_{Fe}$ where J_{sd} is the intra-atomic s-d exchange integral and μ_{Fe} is the magnetic moment per atom in the pure matrix.

For a rough estimate of how V depends on the valence of the impurity let us take as the radial part of a one electron function in an atom of nuclear charge z the approximate form used by Slater (1930).

$$N r^{n^*-1} \; e^{-(z-s)r/n^* a_0} \qquad (2.27$$

where N is a normalisation constant given by

$$N^2 \int_0^\infty r^2 dr \; r^{2(n^*-1)} \; e^{-2(z-s)r/n^* a_0} = 1 \qquad (2.28$$

The integral is evaluated by a simple change of variable

$$\alpha = \frac{2(z-s)r}{n^* a_0}$$

$$\text{thus } 1 = N^2 \int_0^\infty \left[\frac{n^* a_0}{2(z-s)}\right]^{2n^*+1} \alpha^{2n^*} \; e^{-\alpha}$$

$$\text{but } \Gamma(z) = \int_0^\infty t^{z-1} \; e^{-t} \, dt$$

Thus $1 = N^2 \left[\frac{n^* a_0}{2(z-s)}\right]^{2n^*+1} \Gamma(2n^*+1)$

The Eigenfunctions (2.27) are solutions of the central field with

$$V(r) = -\frac{(z-s)e^2}{r} + \frac{n^*(n^*-1)\hbar^2}{2mr^2} \qquad (2.30)$$

thus an approximation to the Koster-Slater matrix element is

$$N_H^2 \int_0^\infty r^2 dr\, r^{2(n_H^*-1)} e^{-2(z_H-s_H)r/n_H^* a_0} \frac{(Z_H - Z_I - S_H + S_I)e^2}{r}$$

$$= \frac{(z_H - s_H - Z_I + S_I)(z_H - s_H)e^2}{n_H^{*2} a_0} \qquad (2.31)$$

where we have used the recurrence relation $\Gamma(z+1) = z\Gamma(z)$, and where the subscript H stands for host atom and I for impurity atom.

Values of n_H, S_H, n_I and S_I are obtained from Slater's rules as follows

n	=	1	2	3	4	5	6
n^*	=	1	2	3	3.7	4.0	4.2

thus for iron 4s electrons $n^* = 3.7$.

To determine s, the electrons are divided into groups (1s), (2s, 2p), (3s, 3p), (3d), (4s, 4p) etc. each of which has a different screening constant found in the following way

(i) nothing from any shell outside the one considered,

(ii) an amount 0.35 from each other electron in the group considered (except the 1s group, where 0.30 is used),

(iii) if the shell considered is an s or p shell an amount 0.85

for each electron with total quantum number less by one, and an amount 1.00 for each electron still further in; but if the shell is d or f, an amount 1.00 for every electron inside it.

Values of Z_I and S_I have been evaluated for Cu, Zn, Ga, Ge, As, Se, Br and Kr assuming that the electronic structure is the same in the solid as in the free atom and are given in Table 2.1.

TABLE 2.1

Slater constants for non-transition elements

	Z	n^*	S	Z-S
Cu	29	3.7	25.30	3.70
Zn	30	3.7	25.65	4.55
Ga	31	3.7	26.00	5.00
Ge	32	3.7	26.35	5.65
As	33	3.7	26.70	6.30
Se	34	3.7	27.05	6.95
Br	35	3.7	27.40	7.60
Kr	36	3.7	27.75	8.25

To investigate the dependence on the configuration of the pure matrix calculations were performed for the Fe $3d^6\ 4s^2$ and Fe $3d^7\ 4s^1$ configurations, the values of the matrix element (2.31) so obtained being plotted in Figure 2.1 in units of e^2/a_0, the binding energy of the hydrogen atom being $e^2/2a_0 \sim 13.6$ eV. These values are seen not to depend strongly on the assumed configuration of iron in the solid and vary linearly with the valence of the impurity. We note that for Ga (2.31) is of the order of the bandwidth of pure iron. It is clear, therefore, that a perturbative treatment of the screening of a non-transition element impurity in iron would be quite wrong. The Koster-Slater method presented in § 2.1 is, however, ideally suited for the treatment of such a problem.

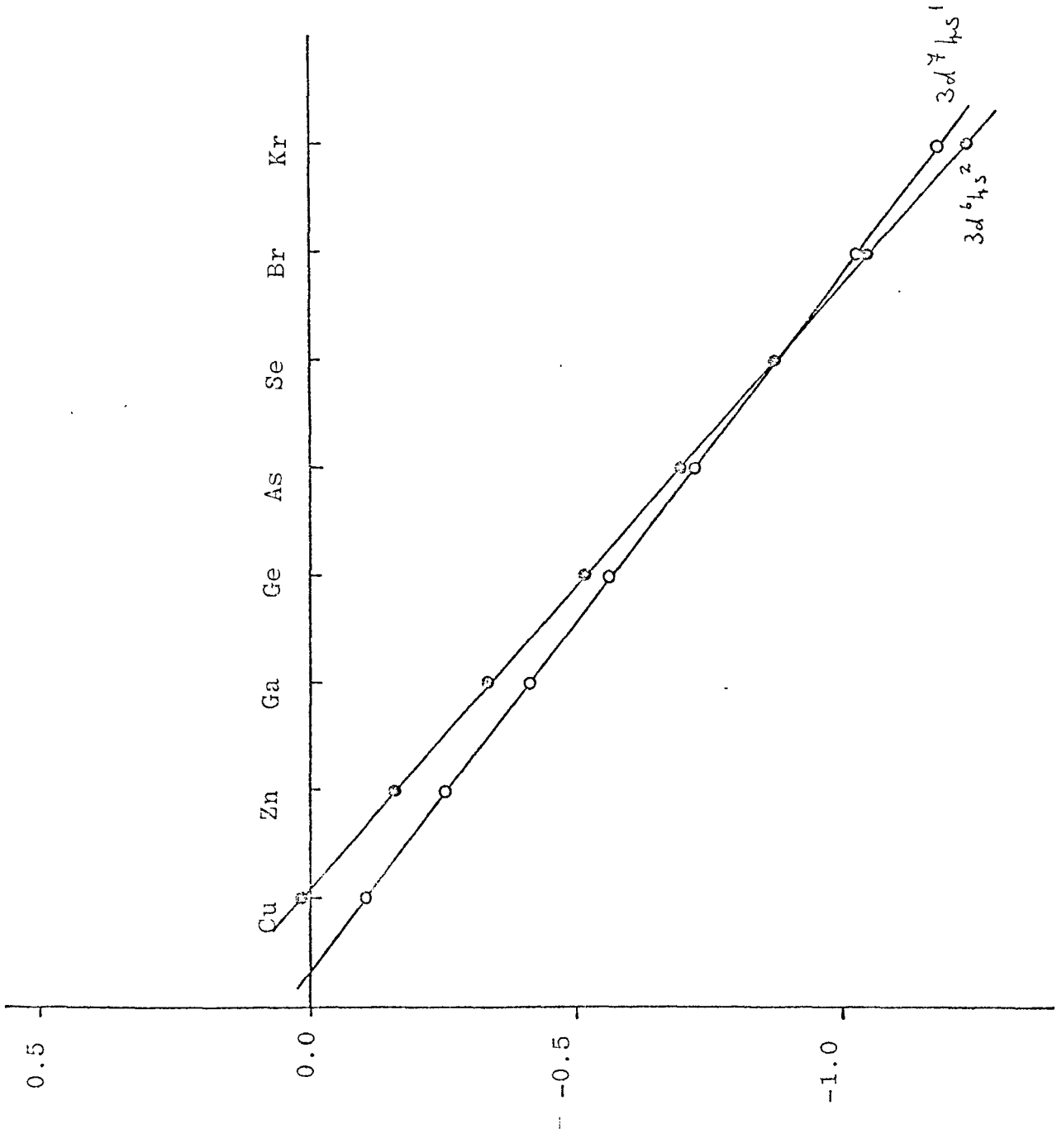

Figure 2.1 Slater potential (2.31) for non-transition element impurities in iron (e^2/a_o).

2.2.2 Model Density of States

In order to calculate the impurity hyperfine field we require the density of states $n(E)$ and its Hilbert transform $F(E)$. Unfortunately it is not possible to obtain $n(E)$ in analytic form even for the simplest three-dimensional case, namely the nearest neighbour, tight binding, simple cubic lattice with one s type orbital per atom. If the perturbation is strong however, as the calculations based on Slater's rules indicate for non-transition element impurities in iron, we would expect the $\phi_{\underset{\sim}{k}\sigma}(\underset{\sim}{r})$ to be strongly mixed so that the results would not depend strongly on the precise details of the density of states. It is reasonable, therefore, to use a relatively simple density of states whose Hilbert transform can be evaluated analytically. We have studied three such model densities of states.

(i) The Parabolic Density of States

$$n(E) = \frac{3}{4W}\left|1 - E^2/W^2\right| \qquad -W \leq E \leq W$$
$$= 0 \tag{2.32}$$

for which
$$F(E) = \frac{3}{4W}\left[2\left(\frac{E}{W}\right) + \left(\frac{E^2}{W^2} - 1\right)\ln\left|\frac{E-W}{E+W}\right|\right] \tag{2.33}$$

A bound state first occurs at the bottom of the band for a potential V_c given by

$$1 - V_c F(-W) = 0 \tag{2.34}$$

So for this density of state

$$V_c = \frac{-2W}{3} \tag{2.35}$$

(ii) The Triangular Density of States

$$n(E) = \frac{(1 + E/W)}{(1+\theta)W} \qquad -W \leq E \leq \theta W$$

$$= \frac{(1 - E/W)}{(1-\theta)W} \qquad \theta W \leq E \leq W \tag{2.36}$$

$$= 0$$

for which

$$F(E) = \frac{(1 + E/W)}{(1+\theta)W} \ln\left|\frac{E+W}{E-\theta W}\right| + \frac{(1 - E/W)}{(1-\theta)W} \ln\left|\frac{E-\theta W}{E-W}\right| \tag{2.37}$$

and $$V_c = \frac{(1-\theta)W}{2\ln\left(\frac{1+\theta}{2}\right)} \tag{2.38}$$

(iii) The Semi-Elliptical Density of States

$$n(E) = \frac{2}{\pi W}\left(1 - E^2/W^2\right)^{1/2} \qquad -W \leq E \leq W \tag{2.39}$$

$$= 0$$

for which

$$F(E) = \frac{2E}{W^2} \qquad -W \leq E \leq W$$

$$= \frac{2E}{W^2} + \frac{2}{W}\left[\left(E^2/W^2\right) - 1\right]^{1/2} \qquad E \leq -W \tag{2.40}$$

$$= \frac{2E}{W^2} - \frac{2}{W}\left[\left(E^2/W^2\right) - 1\right]^{1/2} \qquad E \geq W$$

and $$V_c = -\frac{W}{2} \tag{2.41}$$

2.3 Results

For the parabolic and triangular densities of states we evaluate the integrals involved in calculating the impurity hyperfine field by expanding to first order in Δ and evaluating the resulting integrals numerically. This is reasonable if the 4s polarisation is small in comparison with the bandwidth. Thus, using Leibnitz' theorem and (2.24) and (2.26), $(\alpha_{\uparrow}^{\text{Band}} - \alpha_{\downarrow}^{\text{Band}})$ is given by

$$\alpha_{\uparrow}^{\text{BAND}} - \alpha_{\downarrow}^{\text{BAND}} = \int_{-\omega}^{E_F+\Delta} \frac{n(\epsilon)\,d\epsilon}{[1-(V+\Delta)F(\epsilon)]^2 + [\pi(V+\Delta)n(\epsilon)]^2} - \int_{-\omega}^{E_F-\Delta} \frac{n(\epsilon)\,d\epsilon}{[1-(V-\Delta)F(\epsilon)]^2 + [\pi(V-\Delta)n(\epsilon)]^2} \tag{2.42}$$

$$\approx \frac{2\Delta\, n(E_F)}{[1-VF(E_F)]^2 + [\pi V n(E_F)]^2} + 4\Delta \int_{-\omega}^{E_F} \frac{n(\epsilon)F(\epsilon)\,d\epsilon}{\{[1-VF(\epsilon)]^2 + [\pi V n(\epsilon)]^2\}^2}$$

$$- 4\Delta V \int_{-\omega}^{E_F} \frac{n(\epsilon)\{F^2(\epsilon) + \pi^2 n^2(\epsilon)\}\,d\epsilon}{\{[1-VF(\epsilon)]^2 + [\pi V n(\epsilon)]^2\}^2}$$

whilst, from the completeness relation

$$\sum_{\text{ALL STATES}} c_{\sigma}^{*}(\underset{\sim}{k}, \underset{\sim}{R}_i)\, c_{\sigma}(\underset{\sim}{k}, \underset{\sim}{R}_j) = \delta_{ij} \tag{2.43}$$

we obtain for the total hyperfine field

$$\alpha_{\uparrow} - \alpha_{\downarrow} \approx \frac{2\Delta\, n(E_F)}{[1-VF(E_F)]^2 + [\pi V n(E_F)]^2} + 4\Delta \int_{E_F}^{\omega} \frac{\{Vn(\epsilon)[F^2(\epsilon) + \pi^2 n^2(\epsilon)] - n(\epsilon)F(\epsilon)\}\,d\epsilon}{\{[1-VF(\epsilon)]^2 + [\pi V n(\epsilon)]^2\}^2} \tag{2.44}$$

If the impurity potential V is strong it is more convenient from the point of view of numerical computation to use the expression (2.44) to evaluate the total hyperfine field rather than to evaluate the contribution of the band and bound states separately because of the resonance occuring in the integrals in (2.42) for attractive potentials if (2.14) is satisfied within the band.

If $V = 0$ (2.44) becomes

$$\begin{aligned} \alpha_\uparrow - \alpha_\downarrow &= 2\Delta\, n(E_F) - 4\Delta \int_{E_F}^{\omega} n(E)\,|F(E)|\,dE \\ &= 2\Delta\, n(E_F) + 4\Delta \int_{-\omega}^{E_F} n(E)\,|F(E)|\,dE \end{aligned} \tag{2.45}$$

since $$\int_{-\omega}^{\omega} n(E)\,F(E) = 0$$

equation (2.45) may be evaluated analytically for the parabolic and triangular densities of states, and for the parabolic density of states, for example, we obtain for $V = 0$

$$\begin{aligned} \alpha_\uparrow - \alpha_\downarrow = {} & \frac{3\Delta}{2}\left[1 - (E_F/\omega)^2\right] + \frac{9\Delta}{4\omega}\left[\left\{\frac{1}{5}\left(\frac{E_F}{\omega}\right)^5 - \frac{2}{3}\left(\frac{E_F}{\omega}\right)^3 \right.\right. \\ & \left.\left. + \frac{E_F}{\omega}\right\} \ln\left(\frac{1 + E_F/\omega}{1 - E_F/\omega}\right) + \frac{8}{15}\ln\left[1 - (E_F/\omega)^2\right]\right. \\ & \left. + \frac{8}{15}(E_F/\omega)^2 - \frac{2}{5}(E_F/\omega)^4 - \frac{16}{15}\ln 2 - \frac{2}{15}\right] \end{aligned} \tag{2.46}$$

The value of (2.46) is seen to depend quite strongly on the position of the Fermi level, that is, on the number of electrons per atom in the 4s band. This number has been a question of considerable controversy and does not, of course, admit a precise answer because of s-d hybridisation. Current opinion (e.g. Mott, 1964) favours a value of about 0.9 to 1.0 electrons per atom in the 4s band.

Figure 2.2 shows the contribution of the band and bound states to the impurity hyperfine field for the parabolic density of states (2.32) assuming one 4s electron per atom. The potential is measured in units of V_c, defined by (2.34), the potential at which a bound state first occurs at the bottom of the band. In the presence of a bound state the impurity hyperfine field is the sum of two contributions, a large positive one from the electrons in the band and a large negative one from the bound state.

Figure 2.3(a) shows the total impurity hyperfine field for the parabolic density of states and 0.9, 1.0 and 1.1 electrons per atom in the 4s band. Figures 2.3(b), (c) and (d) show the total impurity hyperfine field for the triangular density of states with Θ = -0.1, -0.2 and -0.3 respectively and 0.9, 1.0 and 1.1 electrons per atom in the 4s band. Θ was chosen slightly negative as this seems to be indicated in band structure calculations (e.g. Wood 1962, Tawil and Callaway 1973).

The semi-elliptical density of states is rather unrealistic because of the behaviour of the Hilbert transform within the band but has the advantage that (2.13) and (2.18) can be evaluated analytically.

With the substitution $E = -U\cos\Theta$

$$\int_{-W}^{W} \frac{n(E)\,dE}{[1-VF(E)]^2+[\pi V n(E)]^2} = \frac{2}{\pi}\int_0^{\pi} \frac{\sin^2\Theta\,d\Theta}{1+4U^2/W^2+4V/W\cos\Theta}$$

which may be evaluated by putting $Z = e^{i\Theta}$ and integrating around the unit circle in the Z plane. Cauchy's theorem then gives

$$\int_{-W}^{W} \frac{n(E)\,dE}{[1-VF(E)]^2+[\pi V n(E)]^2} = \begin{cases} 1 & \text{if } |V| < W/2 \\ \dfrac{W^2}{4U^2} & \text{if } V < -W/2 \end{cases} \qquad (2.47$$

But if the impurity potential is sufficiently attractive to form a bound state at the bottom of the band then the energy of the bound state is given by

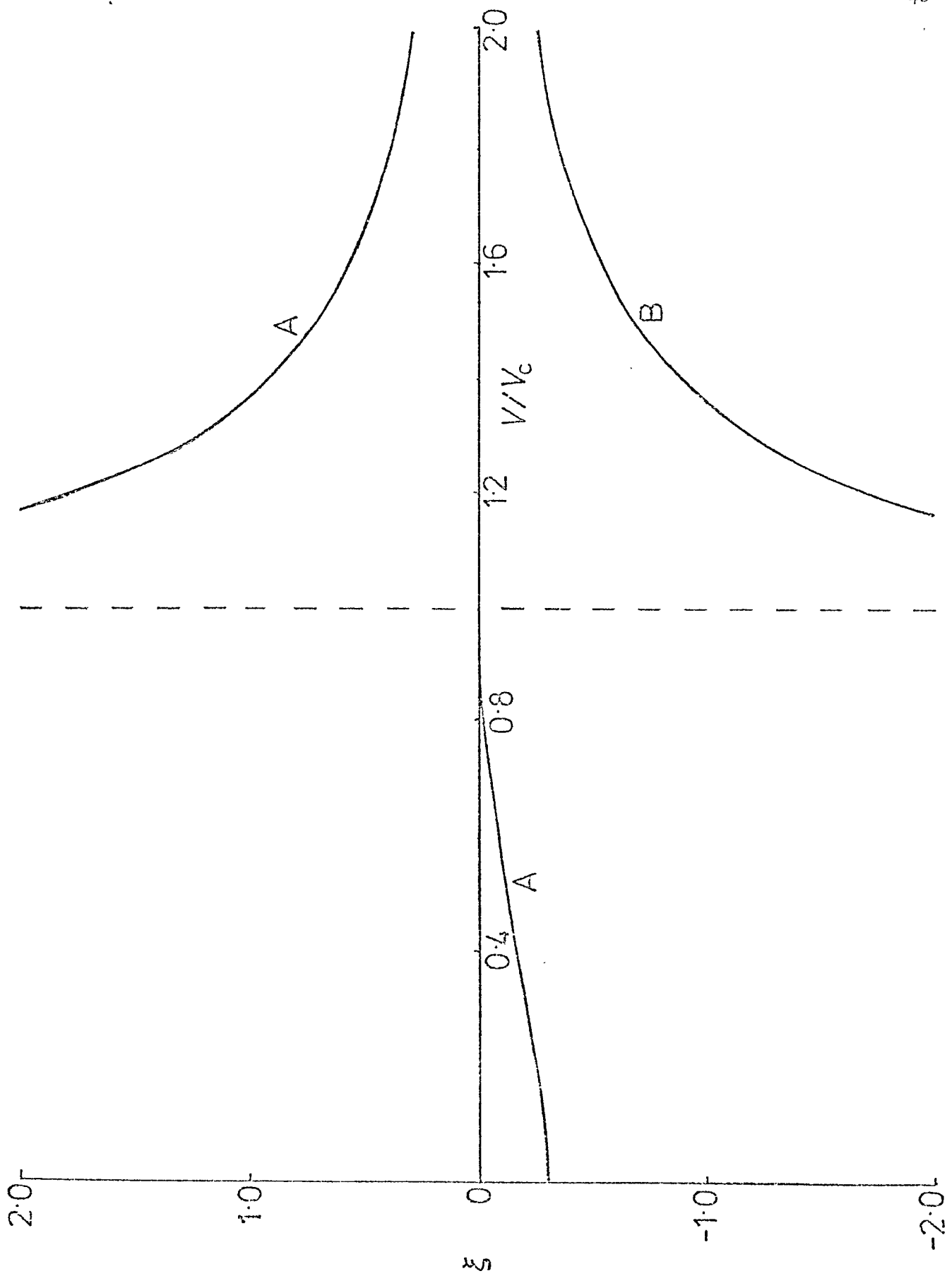

Figure 2.2 Contribution of band and bound states to the impurity hyperfine field for the parabolic density of states with 1el/atom in the 4s band. A, band states and B, bound state.

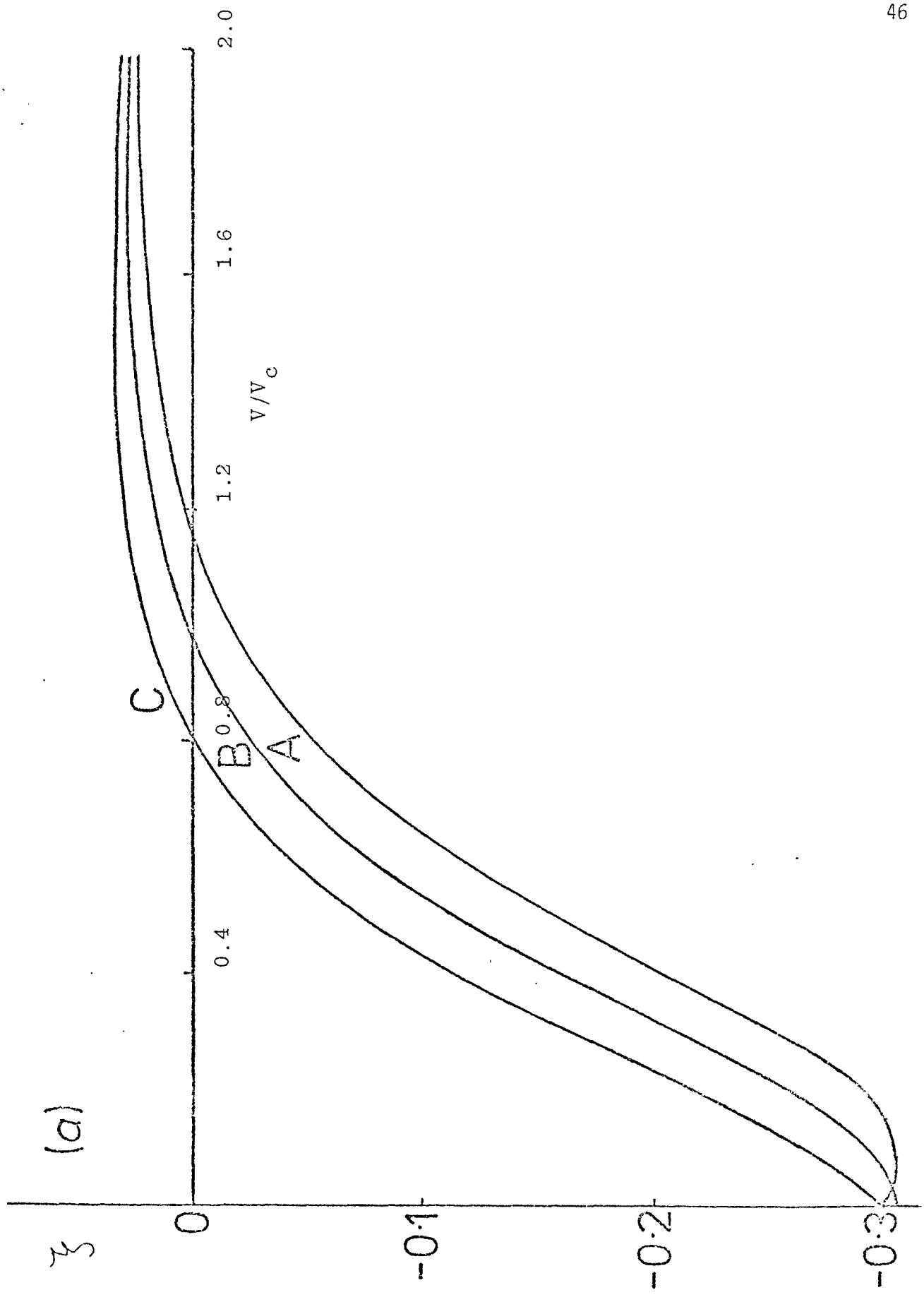

Figure 2.3. Total impurity hyperfine field for 0.9, 1.0 and 1.1 electrons/atom in the 4s band. (a), parabolic density of states; (b), triangular density of states with $\Theta = -0.1$; (c), $\Theta = -0.2$; (d), $\Theta = -0.3$ and (e), semi-elliptical density of states. A, $n_{4s} = 0.9$; B, $n_{4s} = 1.0$; C, $n_{4s} = 1.1$.

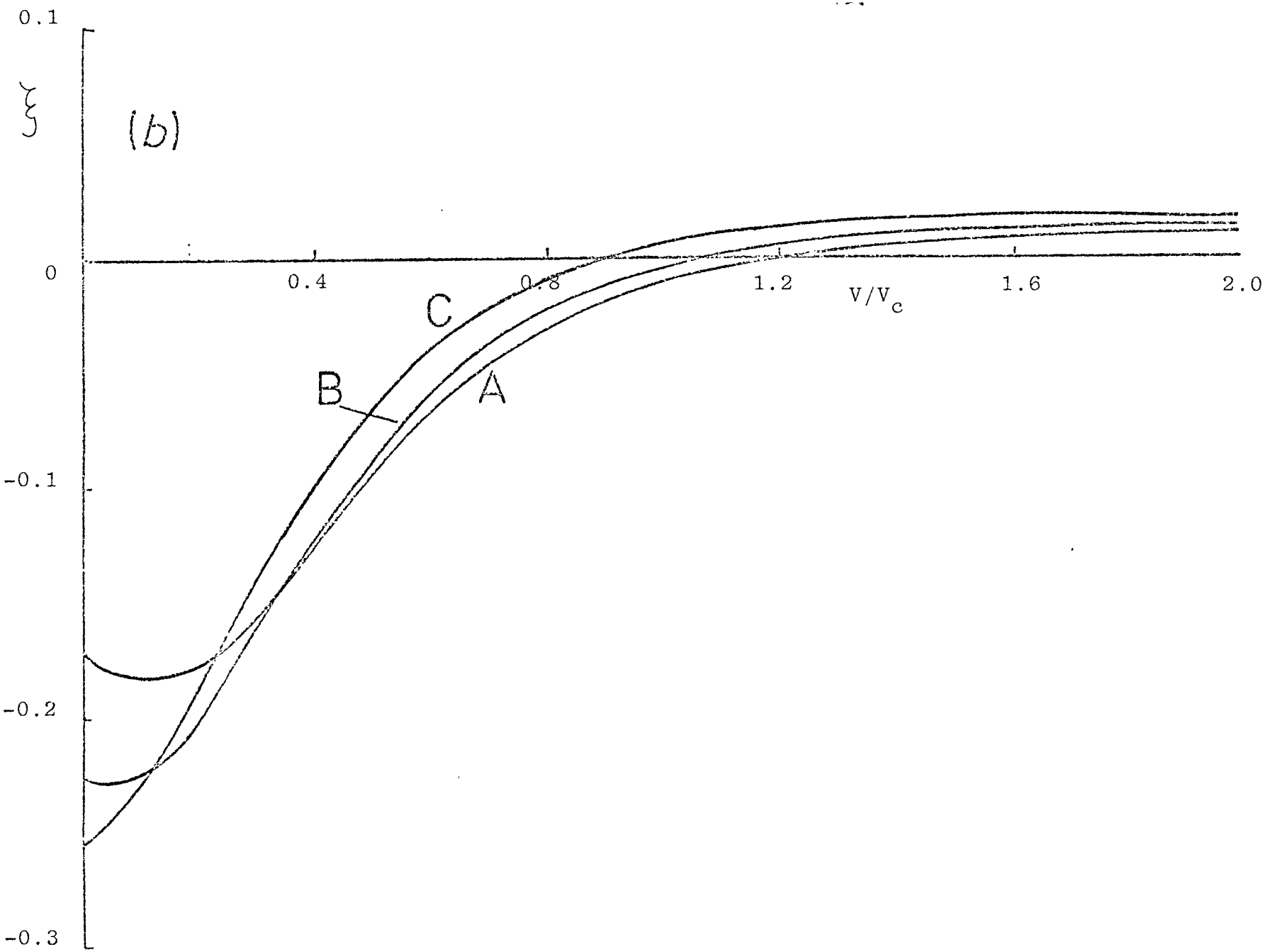
0.1
ξ
(b)
0
0.4
0.8
1.2
V/V_c
1.6
2.0
C
B
A
-0.1
-0.2
-0.3

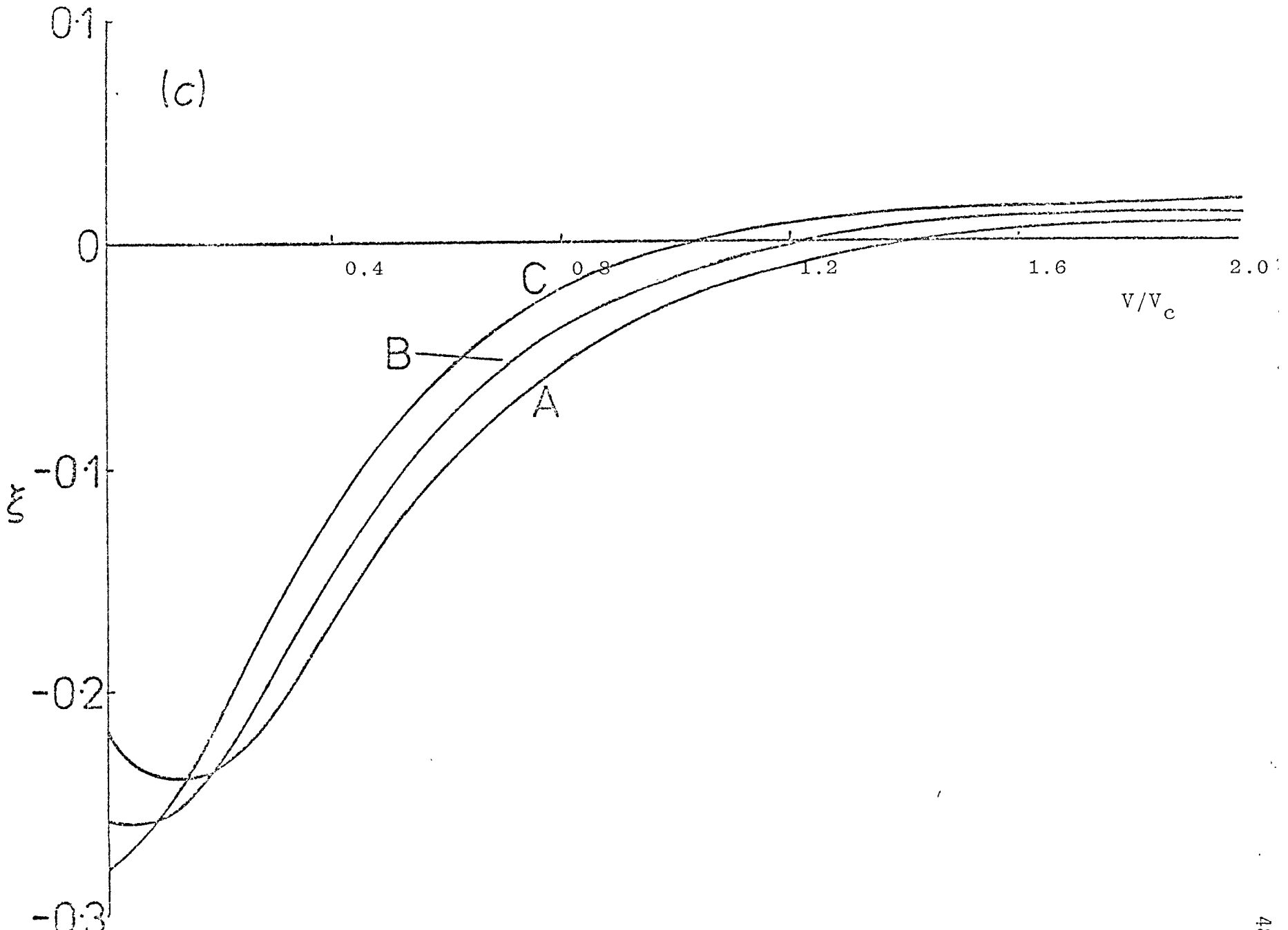
0·1
(c)
0
0.4
0.8
1.2
1.6
2.0
V/V_c
C
B
A
ξ
-0·1
-0·2
-0·3

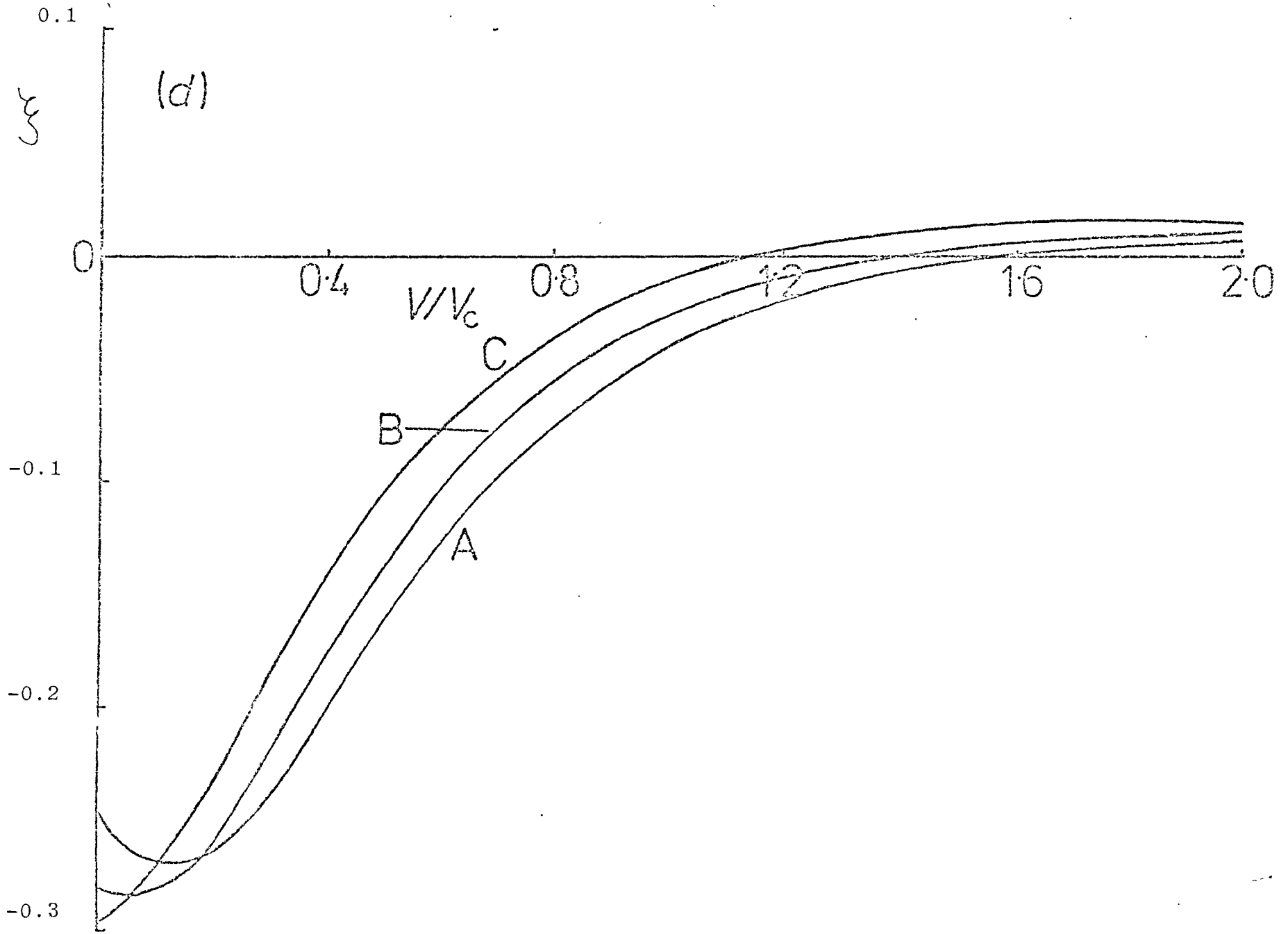
0.1
(d)
ξ
0
0·4
0·8
1·2
1·6
2·0
V/Vc
C
B
A
-0.1
-0.2
-0.3

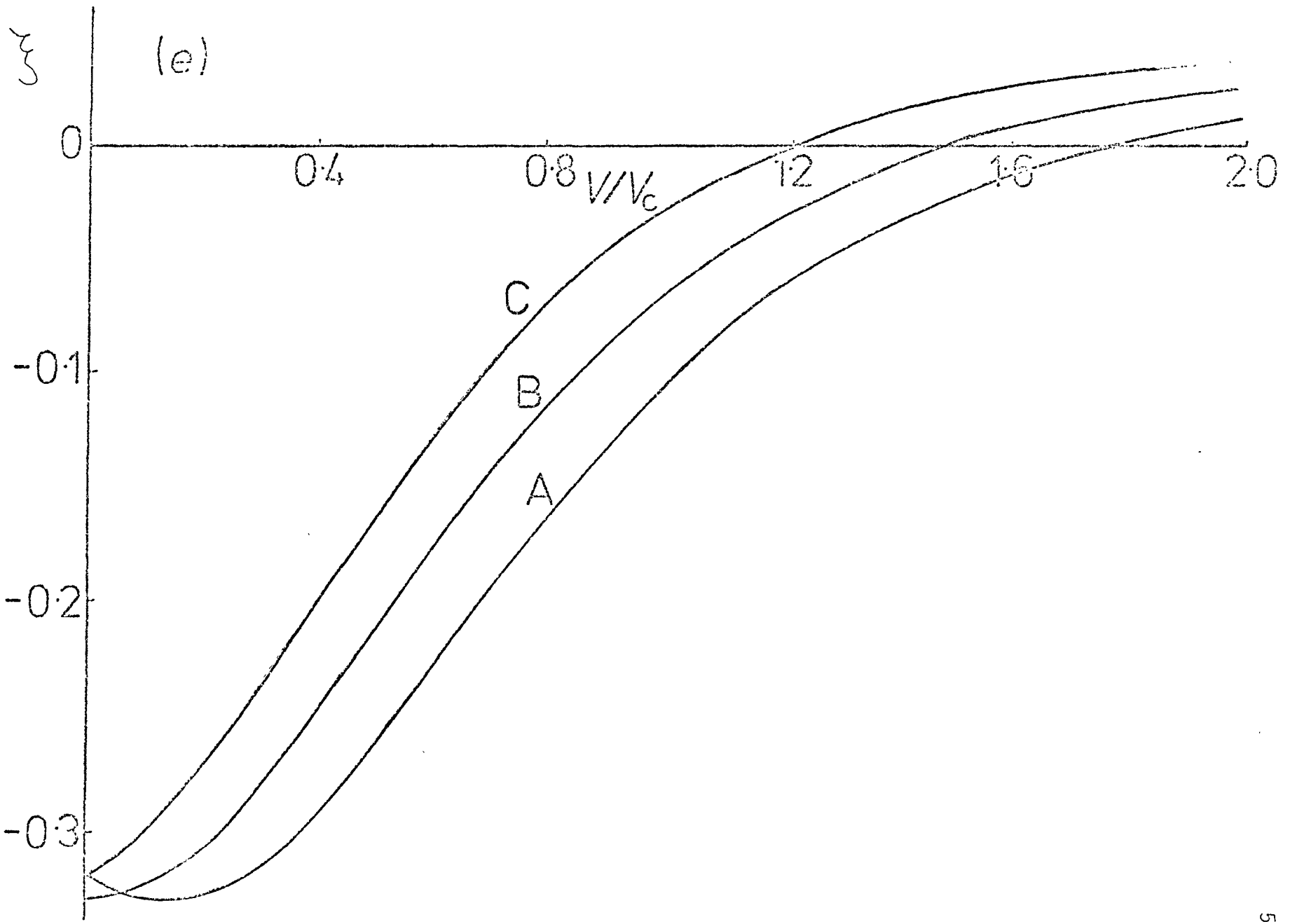
ξ
(e)
0
-0·1
-0·2
-0·3
0·4
0·8
V/Vc
1·2
1·6
2·0
C
B
A

$$E_0 = \frac{\omega^2}{4V} + V$$

giving $$F'(E_0) = \frac{4}{(\omega^2 - 4V^2)}$$

and consequently $$\left| \frac{F^2(E_0)}{F'(E_0)} \right| = 1 - \frac{\omega^2}{4V^2} \qquad (2.48)$$

adding (2.47) and (2.48) confirms (2.43) at the impurity site. With the assumption that only the Wannier function centred on the impurity site has amplitude at $\underset{\sim}{R}_0$, this is an illustration of the theorem (Bardasis et al. 1965, Campbell and Gomes 1967).

$$\int_{\text{BAND STATES}} dE \left[|\psi_{\underset{\sim}{k}\sigma}(\underset{\sim}{r})|^2 - |\phi_{\underset{\sim}{k}\sigma}(\underset{\sim}{r})|^2 \right] + \sum_{\text{BOUND STATES}} |\psi_{\underset{\sim}{k}\sigma}(\underset{\sim}{r})|^2 = 0 \qquad (2.49)$$

which demonstrates that the bound state wavefunction is closely related to the states in the continuum from which it is formed as the potential is increased.

For the semi-elliptical density of states we have to first order in Δ

$$\alpha_{\uparrow}^{\text{BAND}} - \alpha_{\downarrow}^{\text{BAND}} = \frac{4\Delta}{\pi\omega} \frac{(1 - E_F^2/\omega^2)^{1/2}}{(1 + 4V^2/\omega^2 - 4VE_F/\omega^2)} + \frac{16\Delta}{\pi\omega^2} \int_{-\omega}^{E_F} \frac{(E/\omega - 2V/\omega)(1 - E^2/\omega^2)^{1/2} dE}{(1 + 4V^2/\omega^2 - 4VE/\omega^2)^2} \qquad (2.50)$$

which gives

$$\alpha_{\uparrow}^{BAND} - \alpha_{\downarrow}^{BAND} = \frac{4\Delta}{\pi U} \frac{(E_F/\omega - 2V/\omega)(1 - E_F^2/\omega^2)^{1/2}}{(1 + 4V^2/\omega^2 - 4UE_F/\omega^2)}$$

$$+ \frac{2\omega\Delta}{\pi U^2}(1 - E_F^2/\omega^2)^{1/2} + \frac{4\Delta}{\pi\omega} \frac{(1 - E_F^2/\omega^2)^{1/2}}{(1 + 4V^2/\omega^2 - 4UE_F/\omega^2)} \qquad (2.51)$$

$$- \frac{\omega^2\Delta}{2\pi U^3} \sin^{-1}(E_F/\omega) - \frac{\omega^2\Delta}{4U^3} + \frac{\omega^2\Delta}{\pi U^3} \tan^{-1} \frac{(1 + 2V/\omega)}{(1 - 2V/\omega)}$$

$$+ \frac{\omega^2\Delta}{\pi U^3} \tan^{-1} \frac{[(1 + 4V^2/\omega^2)\tan(\tfrac{1}{2}\sin^{-1}E_F/\omega) - 4V/\omega]}{(1 - 4V^2/\omega^2)}$$

whilst if V is sufficiently strong to form a bound state at the bottom of the band

$$\alpha_{\uparrow}^{BOUND} - \alpha_{\downarrow}^{BOUND} = \frac{\omega^2\Delta}{U^3} \qquad (2.52)$$

In Figure 2.3(e) the total hyperfine field for the semi-elliptical density of states is plotted to first order in Δ for 0.9, 1.0 and 1.1 electrons per atom in the 4s band. Figure 2.4 shows the behaviour of (2.51) and (2.52) for one electron per atom in the 4s band. Assuming the 4s electrons in iron are positively polarised, as discussed earlier, the impurity hyperfine field is seen from Figure 2.3 to be negative for weak impurity potentials and to decrease in magnitude, finally becoming positive as the impurity becomes more attractive. The experimental values of the impurity hyperfine field show precisely this behaviour as may be seen in Figure 2.5, the data being taken from Shirley and Westenbarger (1965), Koster and Shirley (1971) and from a similar figure occuring in the review by Van der Woude

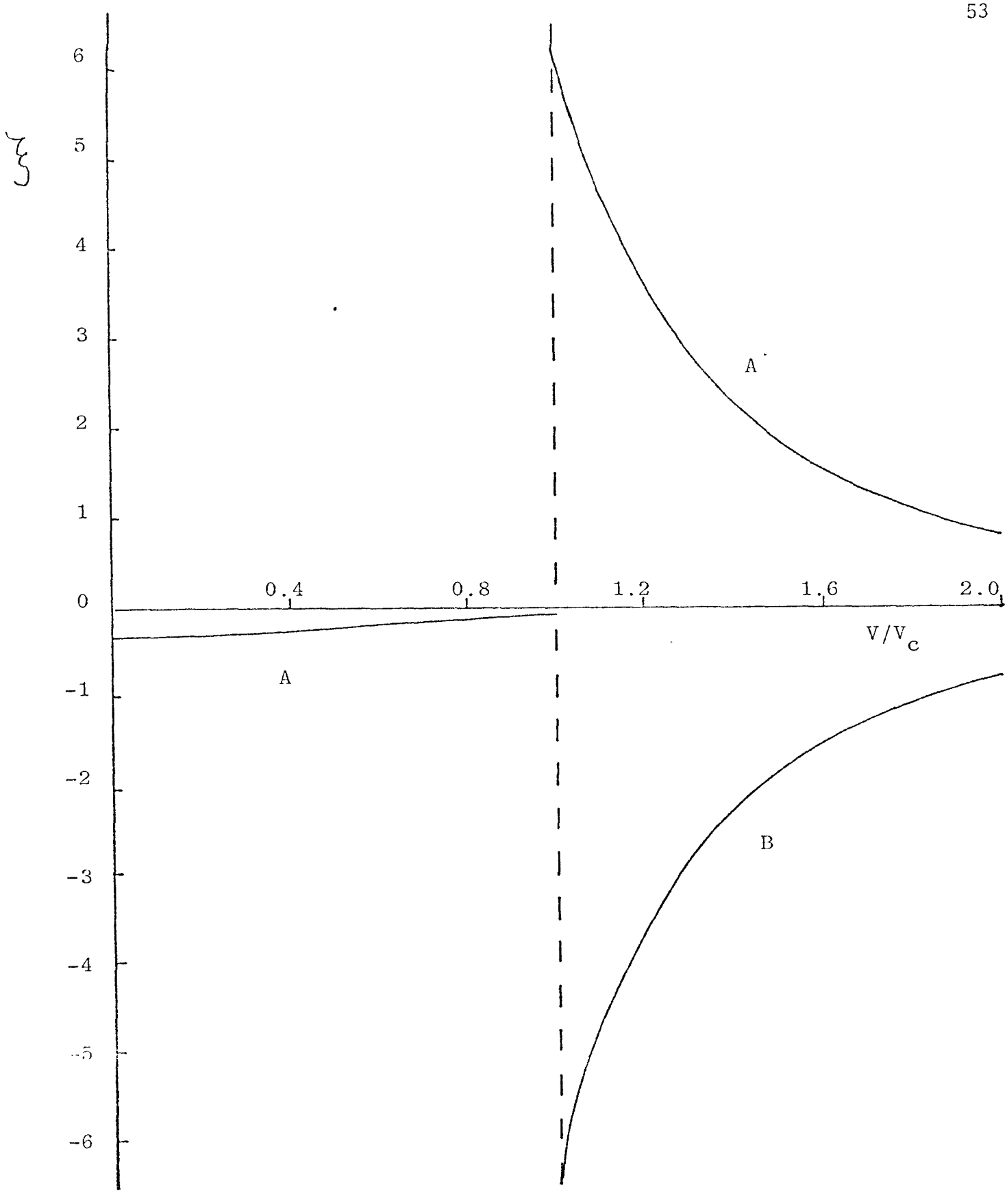

Figure 2.4. Contribution of band and bound states to the impurity hyperfine field for the semi-elliptical density of states with 1 electron/atom in the 4s band. A, band states and B, bound state

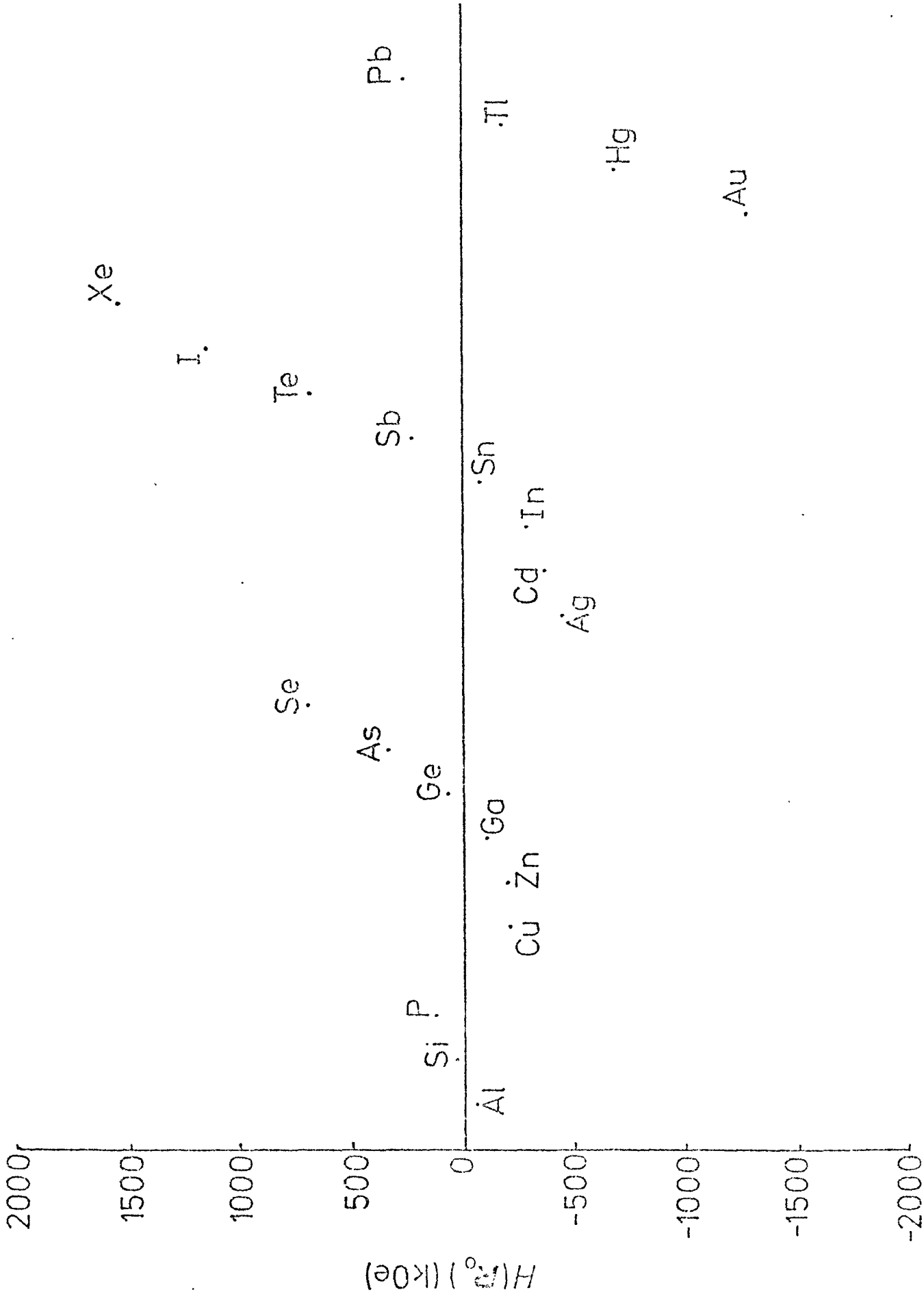

Figure 2.5. Hyperfine field measured at non-transition element impurity in iron. For references see text. H_{Ga} and H_{As} ; sign not measured, H_{Si} ; value in Fe_3Si.

and Sawatzky (1974). The change in sign expected from this simple model is seen to occur between Al and P in period 3, between Ga and Ge in period 4, between Sn and Sb in period 5, and between Tl and Pb in period 6. The hyperfine field at a Si nucleus in a dilute Fe Si allow has not been measured but in the ordered alloy Fe_3 Si is known to be +37 kOe (Kumagai et al. 1974). This is expected to be of the same sign but smaller in magnitude than the corresponding field in the dilute alloy, and so the change in sign in period 3 is expected to occur between Al and Si in iron. It is important to check this experimentally.

We see in Figure 2.3 that for about one 4s electron per atom in the pure matrix, the change in sign of the impurity hyperfine field occurs when the potential is strong enough to form a bound state on the impurity site. Recent measurements of the soft X-ray emission spectrum of an Fe 8 at % Al alloy (Sayers et al. 1975), to be discussed in Chapter 3, do indeed indicate the presence of a bound state on an Al impurity in iron, and since the hyperfine field on an Al nucleus in iron is negative (Kulkov 1972) the presence of a bound state on Al in iron favours slightly less than one 4s electron per atom, in agreement with current opinion.

We have discussed the difficulty of relating the Koster-Slater parameter V to the valence of the impurity. The simple discussion of the impurity potential based on Slater's rules indicate, however, that the potential represented by a Cu impurity in iron will be small and it is therefore easy in this case to obtain an estimate of the impurity hyperfine field. Taking V = 0 for Cu and the hyperfine field due to the 4s electrons at an iron nucleus in pure BCC iron to be +600 kOe as obtained by Stearns (Song et al. 1974) the hyperfine field obtained using the parabolic, triangular and semi-elliptical densities of states for 0.9, 1.0 and 1.1 electrons per atom in the 4s band are given in Table 2.2. These values compare

favourably with the measured value of -212.7 kOe (Shirley and Westenbarger 1965).

TABLE 2.2

Impurity Hyperfine Field (kOe) for V = 0

	Density of States				
n_{4s}	Parabolic	Triangular			Semi-elliptical
		Θ = -0.1	Θ = -0.2	Θ = -0.3	
0.9	-180.9	-104.1	-130.7	-148.9	-194.5
1.0	-185.4	-136.7	-155.9	-170.0	-200.0
1.1	-180.9	-153.1	-167.9	-179.1	-194.5

2.4 Discussion and Conclusions

We have presented a simple model of the screening of a non-transition element impurity in iron in which it is assumed that the 3d electrons are correlated and remain localised on the iron sites and only the 4s electrons contribute to the screening. Assuming a positive polarisation of the 4s electrons in the pure matrix, and about one 4s electron per atom, the hyperfine field was found to cross from negative to positive values as the potential becomes strong enough to form a bound state at the bottom of the band. The hyperfine field is indeed observed to change from negative to positive values as the valence within a given period is increased and in period 3, for example, this change in sign occurs between Al and Si in iron. We would therefore expect, on the basis of this model, that a bound state would first occur on either Al or Si in iron as the valence is increased in period 3 depending on the number of 4s electrons per atom in the pure matrix. We shall argue in Chapter 3, on the basis

of soft X-ray emission spectra of Al in Fe, that a bound state does indeed occur on Al in Fe favouring slightly less than 1.0 electrons per atom in the 4s band, in agreement with current opinion.

It is interesting to compare the results of § 2.3 with those of Daniel and Friedel (1964) who investigated the scattering of a spin polarised free electron gas with one electron per atom by a square well potential of depth $|V + \Delta|$ for majority spin electrons and depth $|V - \Delta|$ for minority spin electrons. Stoddart et al (1969) have discussed the spatial variation of the impurity potential implied by the Koster-Slater assumption (2.5). These authors find that the potential has a depth $|V_\sigma|$ at the origin, is a fairly flat-bottomed potential with a range of the order of the inter-atomic spacing and has oscillations as we go away from the origin which arise from the oscillations in the Wannier function. Thus the potential is rather like the square well potential of Daniel and Friedel. However, the results obtained by the two methods are quite different as may be seen by comparing Figures 2.2, 2.3 and 2.4 with Figure 3 of Daniel and Friedel (1964). In our model the impurity hyperfine field takes its maximum negative value at small values of the impurity potential, and decreases in magnitude as the impurity potential is made move attractive, becoming zero as a bound state first appears below the band, and crossing to positive values as the potential is increased still further. In the Daniel and Friedel model, however, the impurity hyperfine field increases in magnitude as the potential is increased from zero and takes its maximum negative value upon formation of an s bound state. The hyperfine field then decreases in magnitude as the potential is made more attractive finally changing sign to positive values. This difference arises because in our treatment we have considered the scattering of electrons in a tight binding band of finite width. This is particularly important when the impurity potential is strong enough to form a bound state as we may see from Equation (2.49).

CHAPTER III

X-Ray Emission Spectra of Alloys of Iron and Nickel with non-transition element impurities

3.1 Introduction

The calculation of the impurity hyperfine field presented in Chapter 2 gives results in good agreement with experiment, the impurity hyperfine field taking its maximum negative value for weak impurity potentials and decreasing in magnitude finally crossing to positive values as the impurity is made more attractive. This change in sign is found to occur as the impurity becomes strong enough to form a bound state at the bottom of the band and it is therefore of considerable interest to examine the electronic structure of those impurities in iron in the region of this cross-over, which occurs between Al and Si in the third period, between Ga and Ge in the fourth, between Sn and Sb in the fifth, and between Tl and Pb in the sixth. The bound state, if it exists, will lie at the bottom of the band for attractive potentials and will therefore have little effect on thermodynamic or transport properties. Thus the specific heat measurements of Beck and co-workers referred to in Chapter 1 show little change when Al, Si, Ge and Sb are added to iron. The presence of a bound or virtual bound state will, however, have important consequences for optical experiments. In soft X-ray emission spectroscopy (SXS) the solid is excited to a state in which a hole is produced in an atomic core state and the subsequent emission of soft X-radiation is studied. The core wavefunctions are well localised so only electrons in the immediate vicinity of the atom involved in the radiation process contribute to the spectrum. Consequently, SXS is particularly suitable for a study of the local electronic structure of an alloy. The soft X-ray emission intensity from a dilute binary alloy consists, therefore, of two sets

of bands, one arising from the excitation of a host metal atom, and one from excitation of the impurity. In addition, the symmetry of the electronic states can be investigated because of the selection rule governing the transition.

3.1.1 The Impurity Emission Spectrum

The impurity soft X-ray emission intensity arises from transitions to a vacant impurity core state, and if the concentration c of impurities is sufficiently small, the leading term will be c x the intensity emitted from an impurity in an otherwise perfect crystal. If the impurity potential is not strong enough to form a bound state the total intensity between E and $E + dE$ will be

$$I(E)dE = c\, n(E) \left\langle \left| \int d\underset{\sim}{r}\, \phi^{*}_{CORE}(\underset{\sim}{r})\, \nabla_{\underset{\sim}{r}}\, \psi(\underset{\sim}{r}) \right|^{2} dE \right\rangle \qquad (3.1)$$

where $n(E)$ is the density of states, $\nabla_{\underset{\sim}{r}}$ is the gradient operator accounting for dipole transitions only and $\left| \int d\underset{\sim}{r}\, \phi^{*}_{CORE}(\underset{\sim}{r})\, \nabla_{\underset{\sim}{r}}\, \psi(\underset{\sim}{r}) \right|^{2}$ is the transition probability from the state $\psi(\underset{\sim}{r})$ to the vacant core state $\phi_{CORE}(\underset{\sim}{r})$. The angular brackets indicate an average over the constant energy surface $E = E(k)$. For small c the alloy density of states differs from $n(E)$ by a term of $O(c)$. Thus the correction due to the change in the density of states is of $O(c^{2})$ for small c. If the potential is strong the energy dependence of (3.1) will be dominated by that of the transition probability. Assuming, as in Chapter 2, that the only Wannier function to have amplitude at $\underset{\sim}{R}_{0}$ is the one centred on the impurity site, we obtain from (3.1)

$$I(E)dE = c\, n(E) \left| C(\underset{\sim}{R}_{0}) \right|^{2} \int d\underset{\sim}{r}\, \phi^{*}_{CORE}(\underset{\sim}{r}-\underset{\sim}{R}_{0})\, \nabla_{\underset{\sim}{r}}\, \omega(\underset{\sim}{r}-\underset{\sim}{R}_{0}) \Big|^{2} \qquad (3.2)$$

where, from (2.8)

$$n(\epsilon)\,|c(\underset{\sim}{K}_0)|^2 = \frac{n(\epsilon)}{[1-VF(\epsilon)]^2 + [\pi V n(\epsilon)]^2} \tag{3.3}$$

The variation of (3.3) is illustrated in Figure 3.1 for the parabolic density of states (2.32) for various values of the impurity potential. A dramatic distortion is observed in the transition probability as the potential becomes more attractive, and for a critical value of the potential V_c defined by (2.34) a bound state first appears at the bottom of the band. When this occurs we have, in addition to (3.2), a contribution

$$I_{BOUND}(E) = c\,\delta(E-E_0)\left|\int d\underset{\sim}{r}\,\phi^*_{CORE}(\underset{\sim}{r})\,\nabla_{\underset{\sim}{r}}\,\psi_{BOUND}(\underset{\sim}{r})\right|^2 \tag{3.4}$$

from the bound state which, from (2.18) becomes

$$I_{BOUND}(E) = c\,\delta(E-E_0)\left|\frac{F^2(\epsilon)}{F'(E)}\right|\left|\int d\underset{\sim}{r}\,\phi^*_{CORE}(\underset{\sim}{r}-\underset{\sim}{R}_0)\,\nabla_{\underset{\sim}{r}}\,\omega(\underset{\sim}{r}-\underset{\sim}{R}_0)\right|^2 \tag{3.5}$$

The δ -function profile of the bound state contribution will, in practice, be broadened by

(i) Instrumental broadening.

(ii) Auger broadening due to radiationless transitions induced by electron-electron interactions.

(iii) Broadening due to the finite width of the core level involved in the transition.

The number of band electrons at the impurity site is given by

$$n_{IMP}^{BAND} = 2\int_{-\infty}^{E_F} \frac{n(\epsilon)\,d\epsilon}{[1-VF(\epsilon)]^2 + [\pi V n(\epsilon)]^2} \tag{3.6}$$

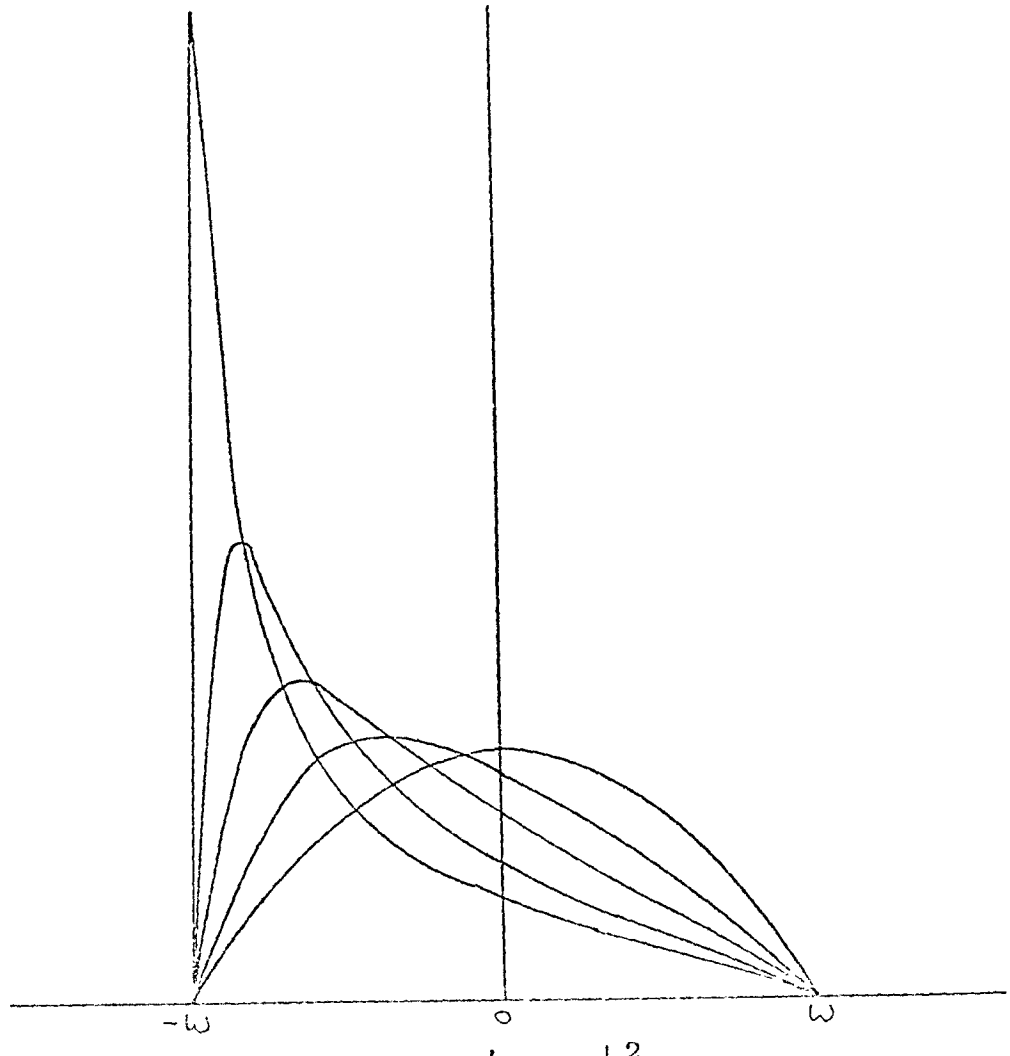

Figure 3.1. Variation of $n(E)\left| c(\underset{\sim}{R}_o)\right|^2$ given by (3.3) for the parabolic density of states (2.33) for various values of the impurity potential $Vn(E_F = 0) = 0.0, -0.1, -0.2, -0.3, -0.4$ for increasing distortion.

which is plotted in Figure 3.2 for the parabolic density of states (2.32) with one electron per atom in the band. The attractive impurity potential is seen to have a repulsive effect on the band states when a bound state is formed, $n_{Imp}^{Band} \to 0$ as $V \to -\infty$ Consequently, when a bound state is formed the emission due to band states at the impurity site is expected to be weak.

It is interesting to compare these results with those of Stott (1969) who calculated the energy dependence of the transition probability in (3.1) and (3.4) using well known expressions for the scattering of an electron gas by a square well potential, taking the core states involved in the transition to be the deep bound state in the potential well. This allows the transition probabilities to be calculated analytically with the following results. The K emission intensity, which results from a transition from a p state to the lowest core state of s symmetry, is in general smooth apart from the sharp cutoff at the Fermi energy and varies little as the impurity potential is changed. When the potential is such that a p state is nearly bound, however, there is a large distortion in the K intensity in the form of an intense peak on a smooth background. As the strength of the potential varies the peak moves to lower energy and becomes narrower and more intense until a bound state finally appears at the bottom of the band. The $L_{2,3}$ emission arises from transitions from s or d states to the lowest p type core state. The variation in intensity as a d state becomes bound is much the same as for a p state except that the peak is narrower and more intense. The distortion is found to have a different character when an s-bound state is found. In this case there is a build up of intensity at the bottom of the band, there being no sharp peak which moves to lower energies as in the case of p and d states.

In our treatment of the screening we assumed that the impurity potential extends only over the impurity site. Consequently, the only

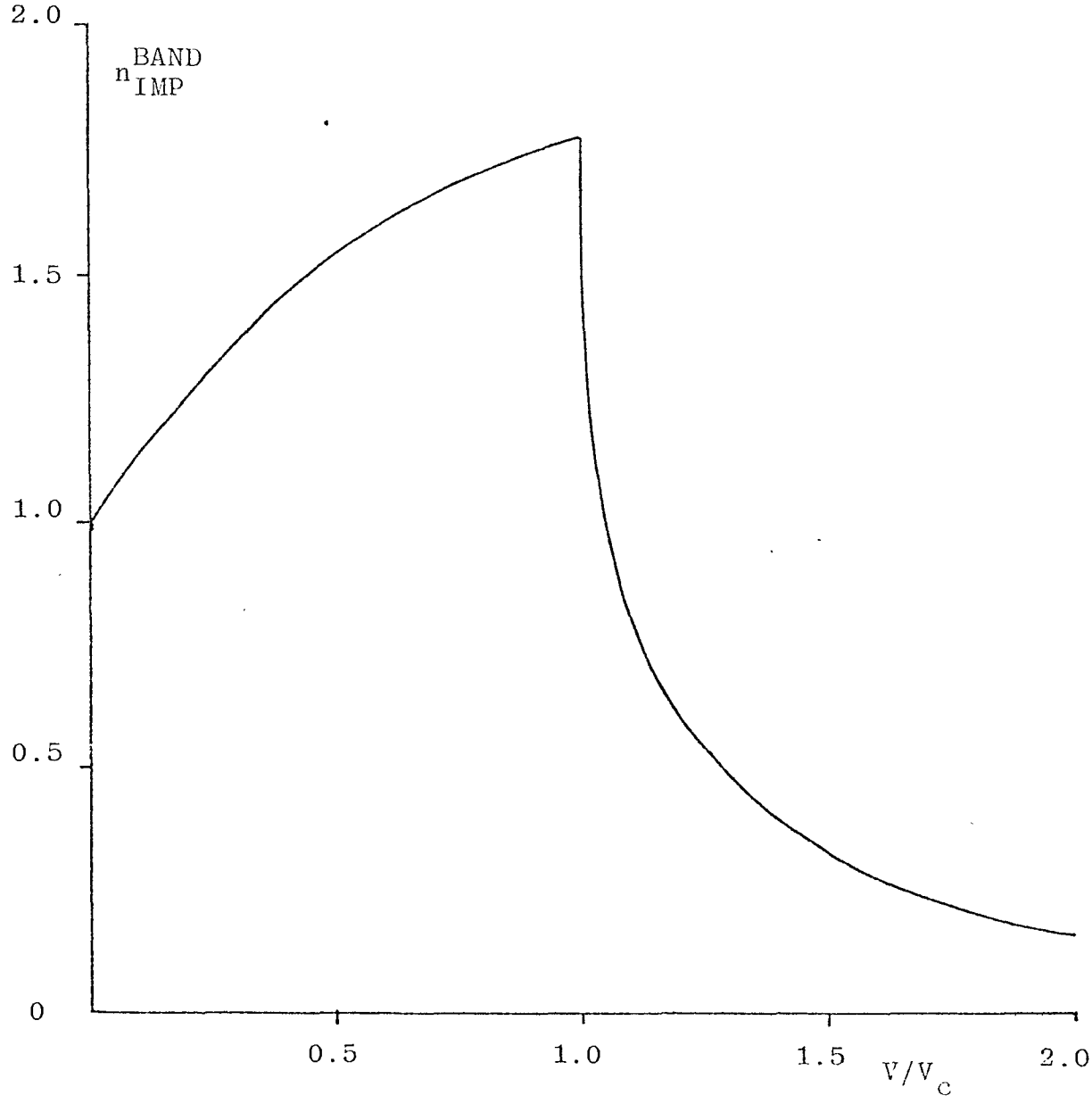

Figure 3.2. Number of band electrons at the impurity site, n_{IMP}^{BAND}, against the impurity potential V, for 1 el / at. in pure matrix.

bound state that can be found is one which is completely symmetric under the operations of the point group of the crystal, that is an s-state. In order to have bound states of higher symmetry we must allow the potential to extend over more lattice sites. It is reasonable to assume, however, that the first state to become bound is an s state since this is the only symmetry which allows a non-vanishing coefficient of the Wannier function at the impurity site where the perturbation is largest. The variation of the transition probability as such a state is formed is illustrated in Figure 3.1. Comparing this with the work of Stott we find much the same behaviour, but in this case the peak is seen to move to lower energies as the potential becomes more attractive.

In more concentrated alloys the situation is complicated by the overlap of impurity states, but a rough estimation of the perturbing effect of the impurity is provided by the differences between the valence of the impurity and the average valences of the alloy. We would therefore expect the impurity bound state to broaden due to overlap effects, and to move up in energy as the concentration is increased, finally becoming the valence band of the pure solute.

3.1.2 The Host Emission Spectrum

If the concentration of impurities in small and the impurity potential is weak the soft X-ray emission spectrum of the host atoms will be largely unaffected by the presence of the impurities. If, on the other hand, the impurity potential is sufficiently strong to form a bound state at the bottom of the band there will be a contribution to the host emission intensity due to the direct overlap of the impurity bound state onto neighbouring atoms and a contribution due to the covalent admixture between the impurity orbital and surrounding orbitals. Thus, for those impurities in iron in the region in which the hyperfine field changes sign we expect to observe a peak in the

host emission intensity at the bottom of the band since for these impurities the bound state is not strongly bound. As the valence of the impurity is increased further, however, the bound state will become more tightly bound around the impurity with a corresponding increase in its contribution to the impurity emission intensity and decrease in its contribution to the host emission intensity.

3.2 Interpretation of Measured Spectra

3.2.1. Iron aluminium alloys

Recently Dev, Fabian and Watson (Sayers et al. 1975) have measured the soft X-ray emission spectrum of an Fe 8 at % Al alloy, the measured spectrum being shown in Figure 3.3 where it is compared with the spectrum of pure iron. The striking feature is the peak at 45 eV in the alloy spectrum, absent in the pure iron spectrum, which is $\backsim$ 8 eV below the Fermi level, or near the bottom of the iron 3d 4s bands (Tawil and Callaway 1973). Figure 3.4 shows the soft X-ray emission spectra of the more concentrated alloys Fe_3Al, FeAl, $FeAl_3$ and of pure Al measured by Kapoor et al (1973). In particular no peak, but only a shoulder, occurs in the Fe_3Al spectrum at 45 eV. The peak observed in the Fe 8 at % Al alloy spectrum cannot, therefore, be attributed to the Al $L_1 - L_{2,3}$ transition at this energy since this involves a transition from a 2p to 2s state in the aluminium core. Thus, if the peak at 45 eV in the Fe 8 at % Al spectrum were due to the Al $L_1 - L_{2,3}$ transition the intensity of this peak, relative to that of the Fe $M_{2,3}$ emission intensity, would be expected to increase as the Al concentration is increased, in disagreement with the observed Fe_3Al spectrum. We therefore conclude, on the basis of Figure 3.3, that Al behaves as a strong perturbation in an Fe matrix giving rise to a bound or virtual bound s state at the bottom of the iron 3d 4s band. This is exactly what we would expect on the basis of the results

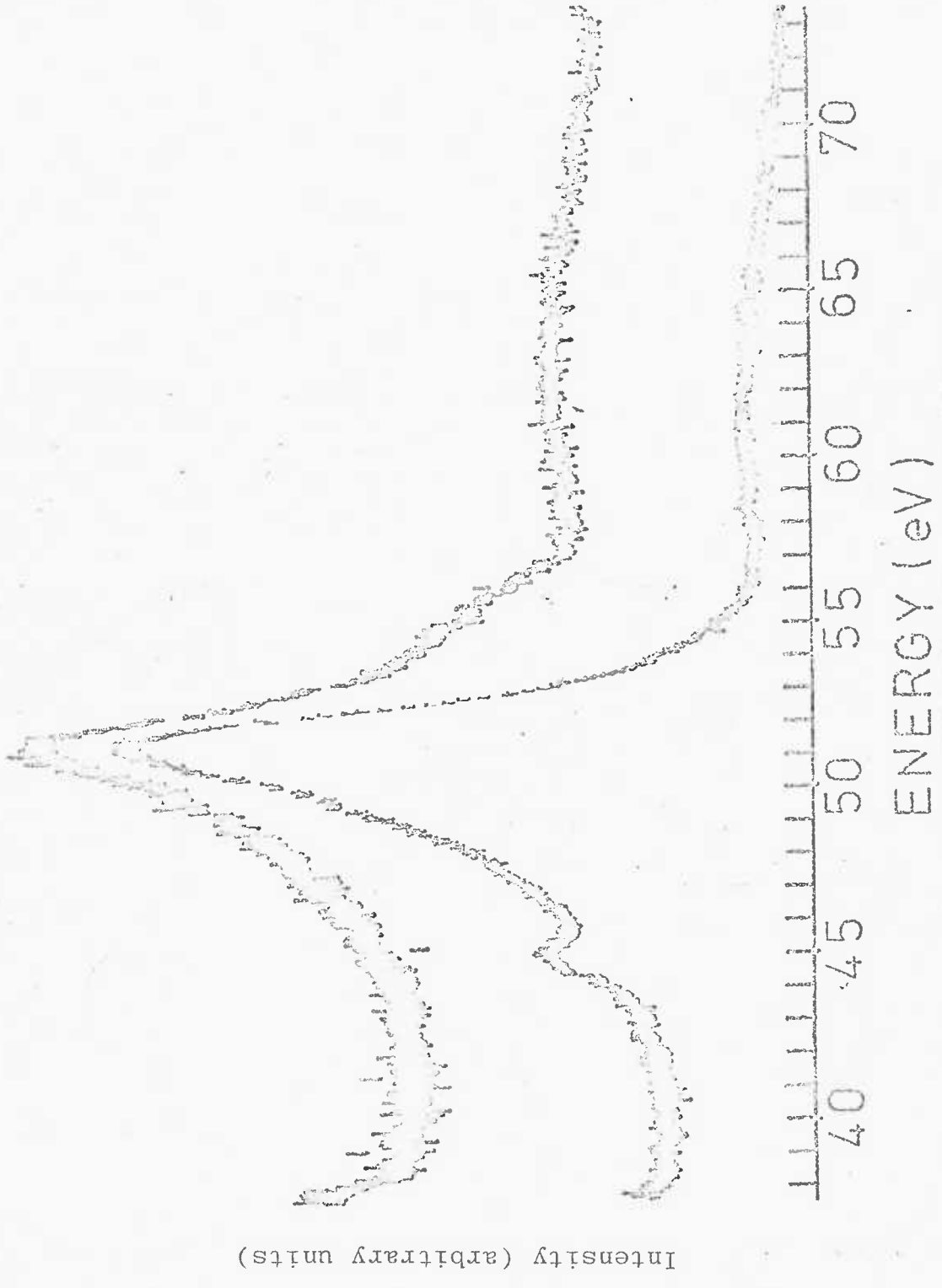

Figure 3.3. Soft x-ray emission spectra for Fe and alloy of Al in Fe; upper curve, $M_{2,3}$ emission from pure Fe; lower curve, emission in the region of the Al $L_{2,3}$ and Fe $M_{2,3}$ bands for an Fe 8 at%Al alloy. The weak Al $L_{2,3}$ band lies in the region 60-72 eV. (After Sayers et al. 1975)

presented in Chapter 2 which indicate that for about one electron per atom the hyperfine field changes sign upon formation of a bound state since the hyperfine field changes from negative to positive values between Al and Si in iron. Since the hyperfine field of Al in iron is negative (Kumagai et al. 1974) this favours slightly less than one electron per atom in the 4s band in agreement with current opinion. The decrease in intensity of the peak at 45 eV as the impurity concentration increases is precisely what we would expect if aluminium forms a bound state in iron. Thus as the impurity concentration increases the bound state will overlap and broaden giving a band as discussed in § 3.1.1. The peak at 45 eV would therefore be less intense in the more concentrated alloys because of the broadening which would occur. The formation of the Al valence band from the bound state, which exists in the impurities at low concentration, is clearly seen on the Al $L_{2,3}$ emission spectra in the region 60 - 75 eV as the Al concentration is increased. In further agreement with this interpretation is the weakness of the Al $L_{2,3}$ band in the Fe 8 at % Al spectrum. This indicates that the bound states overlap little at this concentration. We would however expect to observe a peak between 63 - 64 eV in the Al $L_{2,3}$ band corresponding to a transition from the impurity bound state to an Al 2p state but this energy lies close to the onset of Fe $M_{2,3}$ absorption (excitation of Fe 3p levels) as is seen in Figure 3.5 which shows the absorption spectrum of pure iron in the region 50 - 100 eV (Kunz, 1973) and would therefore not be seen at this concentration.

Terakura (1976) has presented a first principlescalculation of the electronic structure of non-transition element impurities in iron and finds a bound state of s symmetry on Al and Si in iron, the details being in very good agreement with the above interpretation of the Fe 8 at % Al spectrum. The bound state is found to have spectral weight within the impurity cell of 0.39, the rest spreading

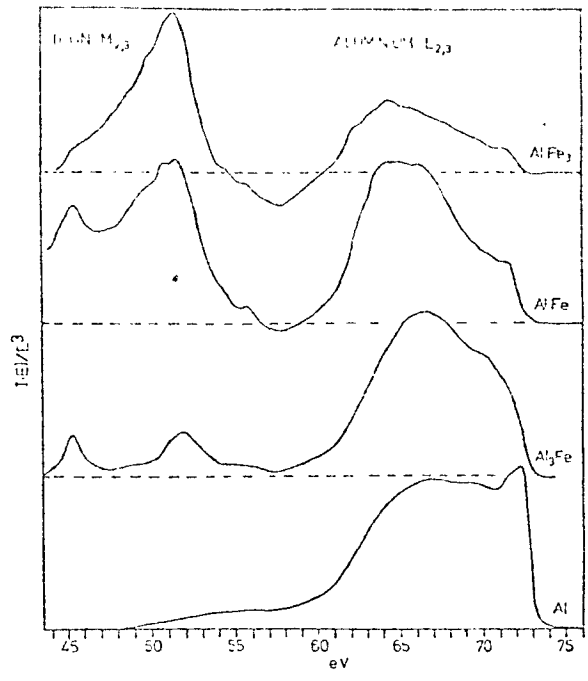

Figure 3.4. Aluminium $L_{2,3}$ and iron $M_{2,3}$ emission bands for Fe Al alloys taken from Kapoor et al. (1973).

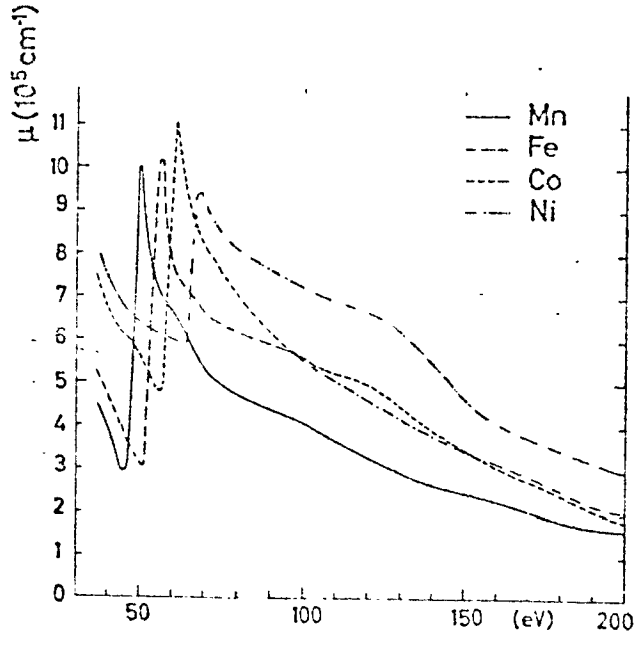

Figure 3.5. Photoabsorption coefficient of Mn, Fe, Co and Ni taken from Kunz (1973).

over neighbouring sites. This is consistent with the hyperfine field calculations presented in Chapter 2, the negative hyperfine field on Al in iron indicating that the bound state on Al will not be tightly bound, and with the bound state being seen in the Fe $M_{2,3}$ spectrum, corresponding to a transition to an Fe 2p state, and not in the Al $L_{2,3}$ spectrum.

3.2.2. Nickel aluminium alloys

Figure 3.6 shows the soft X-ray emission spectrum of alloys of nickel with aluminium (Cuthill et al. 1968). The Al $L_{2,3}$ and Ni $M_{2,3}$ emission spectra overlap extensively making the spectrum of such a system difficult to analyse. There is, however, no peak in the Ni $M_{2,3}$ spectrum corresponding to that observed in the Fe 8 at % Al alloy and in the Ni 8 at % Al alloy the Al $L_{2,3}$ spectrum is strong although there does appear to be a shift to lower energies as we would expect in the screening of a non-transition element impurity such as Al or Si. The apparent absence of a bound or virtual bound state on Al in nickel is in agreement with the behaviour of nickel as an itinerant ferromagnet and with the saturation magnetisation measurements of Crangle and Martin (1959) discussed in § 1.5 which indicate that the screening of a non-transition element impurity is dominated by the 3d electrons involving the high density of states at the Fermi level.

3.2.3. Iron germanium alloys

Figure 3.7 shows the soft X-ray emission intensity in the region of the iron K emission band for Fe Ge alloys (Nemoshkalenko et al. 1973). A peak occurs in the iron K emission at about 8 eV below the Fermi level and arises from a transition to the iron 1s state.

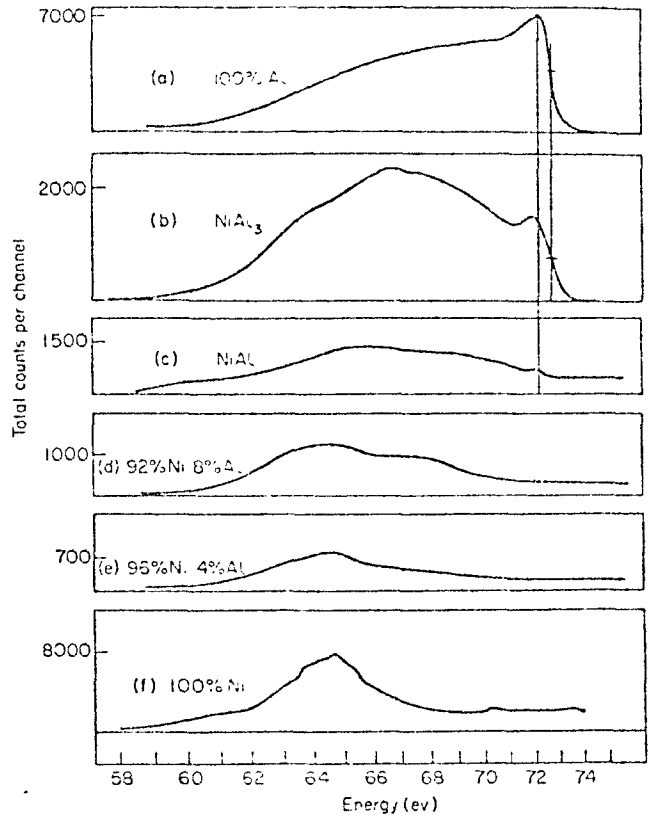

Figure 3.6. Soft x-ray emission spectrum of alloys of nickel with aluminium taken from Cuthill et al. (1968).

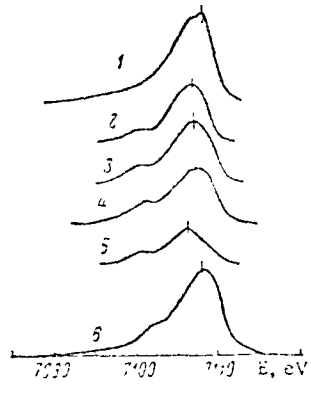

Figure 3.7. Soft x-ray emission intensity in the region of the iron K emission band for Fe Ge alloys taken from Nemoshkalenko et al. (1973).
1) Fe (pure metal); 2) $Fe_{3.25}Ge$; 3) Fe_3Ge; 4) Fe_2Ge;
5) Fe_4Ge_3; 6) FeGe.

This is similar to that observed in the Fe 8 at % Al iron $M_{2,3}$ band and is, we suggest, due to an admixture of an s band state on Ge overlapping with and mixing with the nearest neighbour iron 4p state. The presence of a bound or virtual bound state on Ge in iron is to be expected from the calculations of the hyperfine field presented in Chapter 2, the hyperfine field crossing from negative to positive values between Ga and Ge in iron.

3.2.4. Iron silicon alloys

A recent measurement of the soft X-ray emission spectrum of an Fe 4.13 at % alloy by Watson and Norris (Watson et al. to be published) indicates also the presence of a bound state on a Si impurity in iron. In this case the Fe $M_{2,3}$ absorption does not present a difficulty and a peak at 90 eV in the Si $L_{2,3}$ emission band (about 8 eV below the Fermi level) corresponding to a transition from the Si bound state to a Si 2p state is clearly seen. A small peak at 45 eV is also observable in the Fe $M_{2,3}$ spectrum corresponding to a transition from the impurity bound state to an Fe 3p state. This is weaker than the peak seen in the Fe 8 at % Al alloy because the concentration of impurities is smaller and because the Si atom represents a more attractive impurity potential than Al, the bound state being more localised on the impurity site. This is confirmed by the first principles calculation of Terakura (1976), the bound state having a spectral weight of 0.62 within the impurity Wigner-Seitz sphere.

3.3 Photoemission Experiments

Collins and Andrews (to be published in J.Phys.F.) have reported measurements of the photoemission spectrum of an Fe 8 at % Al alloy and do not observe a peak corresponding to that observed in the soft X-ray emission spectrum of Sayers et al (1975). These authors conclude from the absence of this peak that the peak observed in the soft X-ray

emission spectrum is actually due to the Al $L_1 - L_{2,3}$ emission discussed in § 3.2.1. We disagree with this conclusion as this would imply that the peak at 45 eV would increase in intensity relative to the Fe $M_{2,3}$ band with increasing Al concentration, in disagreement with the observed change on going from Fe 8 at % Al to Fe_3 Al. It is interesting to enquire therefore why no peak is seen in the photoemission spectrum. We would expect that since the peak is very narrow in energy only those impurities within a depth of the inelastic scattering length would contribute to such a peak in the XPS spectrum. In contrast, the Fe $M_{2,3}$ band is broad so most states would be expected to contribute in some way to this. This means there would be an effective concentration of impurities in XPS less than the mean concentration. In contrast SXS is ideally suited for an examination of localised states, the only complication being the soft absorption discussed in § 3.2.1. In addition, whilst the surface energy of Fe is 1790 erg/cm^2, that of Al is 1000 erg/cm^2. This would indicate that Fe would preferentially be found at the alloy surface again leading to the suggestion of a lower effective concentration of impurities in XPS than the mean concentration. A further important point is that because of the nature of the final state involved in the transition, SXS probes the electron distribution of a given symmetry local to the emitting atom whilst XPS measures the electron density averaged through a region of the emitting alloy and averaged over all symmetries with the appropriate weighting factor.

3.4 Photoabsorption Measurements

In photoabsorption spectroscopy a core electron is excited to an empty state above the Fermi level. Hagemann et al (1976) have studied the photoabsorption spectra of Fe-Al and Ni-Al alloys using synchrotron radiation in the energy range 30 to 150 eV. Table 3 gives the position of the onset of $M_{2,3}$ absorption, corresponding to

the excitation of transition metal 3p electrons, as measured by Hagemann et al.

TABLE 3.1

Position of Onset of $M_{2,3}$ Absorption of Fe-Al and Ni-Al Alloys

	Fe	Fe- 11% Al	FeAl	Ni	NiAl	$NiAl_3$
Position of onset of $M_{2,3}$ absorption (Ev)	52.0	52.0 $\pm$ 0.2	52.0	64.2	65.5	66.3

The onset of $M_{2,3}$ absorption is seen not to change in Fe based alloys upon increasing the Al concentration in agreement with the d electrons not participating in the screening which is localised on the impurity site. In contrast to Fe-Al alloys the Fermi level in Ni-Al alloys is seen to shift rapidly to higher energies indicating a filling of the Ni 3d band.

3.5 Further discussion of impurity hyperfine field and saturation magnetisation measurements.

The peak observed in the soft X-ray emission spectrum of the Fe 8 at % Al alloy of Sayers et al (1975) at 45 eV arises from a transition to a core p state on iron atoms neighbouring the impurity. This is consistent with the first principles calculations of Terakura which shows that the bound state on Al in iron has spectral weight of only 0.39 on the impurity site, the rest spreading over neighbouring sites, and with the hyperfine field calculation of Chapter 2 which indicates that a bound state is first formed on those impurities in iron for which the hyperfine field crosses from negative to positive values. According to Wenger et al (1971) the contribution of the 4s $\longrightarrow$ 2p transitions is two orders of magnitude smaller than that of the 3d $\longrightarrow$ 2p transitions so the intensity of the peak at 45 eV would appear to indicate a covalent admixture or hybridisation of the impurity

bound state with neighbouring d orbitals. Similarly, the peak occurring in the Fe K emission spectrum of Fe Ge alloys of Nemoshkalenko et al (1973) indicates a covalent admixture with neighbouring p states. This is in agreement with the model of Marshall referred to by Mott (1964) of the electron structure of an Al impurity in iron in which the Al 3s electrons are considered to form a localised state which mixes with neighbouring 3d orbitals.

The extent of this admixture depends sensitively on the exact form of the impurity orbital. This reveals a weakness in the Koster-Slater model since this is formulated in terms of the orthogonal Wannier functions of the 4s band. In the region of the impurity core the bound state would be expected to look rather like the outer s orbital of the free atom appropriately modified in the crystal, $\phi^{\sigma}_{IMP}(\underset{\sim}{r})$ say, than the Wannier function of the iron 4s band $\omega_{\sigma}(\underset{\sim}{r})$. This suggests that the treatment of the impurity hyperfine field presentation in Chapter 2 can be improved by replacing $\omega_{\sigma}(\underset{\sim}{r}-\underset{\sim}{R}_0)$ in (2.23) by $\phi^{\sigma}_{IMP}(\underset{\sim}{r}-\underset{\sim}{R}_0)$. To a first approximation $\phi^{\sigma}_{IMP}(\underset{\sim}{r}-\underset{\sim}{R}_0)$ will be spin independent since there is no moment on the impurity site and this is why the assumption $\omega_{\uparrow}(\underset{\sim}{r}-\underset{\sim}{R}_0)=\omega_{\downarrow}(\underset{\sim}{r}-\underset{\sim}{R}_0)$ made in § 2.2 yields reasonable agreement with the measured impurity hyperfine fields. The spin dependence of $\phi^{\sigma}_{IMP}(\underset{\sim}{r}-\underset{\sim}{R}_0)$ arises from the interaction between the impurity orbital and the magnetic 3d electrons. For a given group in the periodic table the amplitude of ϕ^{σ}_{IMP} at the impurity nucleus increases with increasing period since the outer s electrons see a greater positive charge at the nucleus as the period of the impurity increases. This leads to a periodic dependence of the impurity hyperfine field, the hyperfine field increasing in magnitude with the period of the impurity. This is seen in the hyperfine field data presented in Figure 2.5 and is particularly noticable for low valence impurities. Within a given period the amplitude of ϕ^{σ}_{IMP} at the impurity nucleus increases

rapidly with valence. This contributes to the very large positive fields measured at the nuclei of impurities in iron with large valence which are much larger than would be expected from the simple Koster-Slater model. A further contribution to these large positive fields comes from the covalent admixture of the impurity bound state with neighbouring 3d states. Since the 3d state involved in the bonding with the impurity state are spin polarised, there will be a greater admixture for $\downarrow$ spin states than for $\uparrow$ spin states because the $\uparrow$ spin 3d orbitals are more fully occupied. This will lead through the second term in Equation (2.23) with $\psi_\sigma(\underset{\sim}{r} - \underset{\sim}{R}_0)$ replaced by $\phi^\sigma_{IMP}(\underset{\sim}{r} - \underset{\sim}{R}_0)$ to a positive contribution to the hyperfine field when the bound state is established.

In § 1.5 we discussed the $d\bar{\mu}/dc$ measurements of Aldred (1968) on alloys of BCC iron with non-transition element impurities. Within a given period in groups 3 to 5 there is no valence dependence of the $d\bar{\mu}/dc$ values indicating that the magnetic 3d electrons do not contribute directly to the screening. The $d\bar{\mu}/dc$ values do however show a deviation from the simple dilution behaviour, $d\bar{\mu}/dc = -2.2\ \mu_B$, which increased with the period of the impurity. Vincze and Aldred (1974) suggested that it might be possible to understand this behaviour in terms of an increased admixture between the impurity bound state and neighbouring 3d states in Marshall's model as the period of the impurity increases. We shall now propose a mechanism by which the admixture of the impurity bound state with neighbouring 3d states can produce an increase in the moment on neighbouring iron atoms.

The s-like bound state on the impurity will transform under the irreducible representation A_{1g} of the O_h group relevant to a lattice of cubic symmetry. The effect of the cubic field is to remove the fivefold degeneracy of the 3d states and to split the levels into

a triply degenerate set labelled T_{2g} and a doubly degenerate set labelled E_g. In the body centred cubic lattice the T_{2g} orbitals are directed towards nearest neighbours whilst the E_g orbitals are directed towards next nearest neighbours. We shall assume that only σ bonding is operative and shall consider only the admixture of the s-like state on the impurity with the 3d states on nearest neighbours. Thus we only consider the bonding between the impurity bound state and the T_{2g} hybrid on nearest neighbours which is symmetric about the line joining the atom with the impurity. The method of molecular orbitals constructs solutions of the form

$$\psi_\sigma = a_\sigma \phi^\sigma_{imp} + b_\sigma \chi^\sigma_{3d} \tag{3.7}$$

where χ^σ_{3d} is the appropriate contribution of T_{2g} orbitals on nearest neighbours which transforms under the irreducible representation A_{1g} of the O_h group.

The mixing coefficients a_σ and b_σ can in principle be obtained from a variational calculation which would yield two solutions. The impurity bound state, if it exists, lies at the bottom of the band and so the state with lowest energy will be the one for which b_σ is small and will be doubly occupied. The antibonding state will have a small value of the coefficient a_σ and will be raised in energy giving a decrease in the occupancy of the T_{2g} orbitals involved in χ^σ_{3d}. This will be accompanied by a compensating increase in the E_g occupancy. The overlap of the E_g orbitals, which are directed towards next nearest neighbours in the body centred cubic lattice, is smaller than the overlap of the T_{2g} orbitals, which are directed towards nearest neighbours. Intra-atomic exchange will therefore be more effective in the E_g bands than in the T_{2g} bands of iron, and this is confirmed by the neutron diffraction studies of the 3d spin density in BCC iron (Shull and Yamada 1962, Shull 1963) which exhibit a non-spherical 3d spin

density distribution with favouritism towards the E_g symmetry configuration. Shull (1963) estimates that 53% of the 3d magnetisation arises from electrons with E_g symmetry and 47% with T_{2g} symmetry. This should be contrasted with the respective values of 40% and 60% to be expected for spherical symmetry. Since Hund's rule coupling or intra-atomic exchange is more effective in the E_g orbitals than in the T_{2g} orbitals the increase in the E_g occupancy, which occurs indirectly as a result of the covalent admixture of the impurity bound state with T_{2g} orbitals on neighbouring iron atoms, will result in an increase in the moment on iron atoms neighbouring the impurity. This increase is observed in the neutron diffraction experiments of Holden et al (1967) on iron based alloys. The increase in the moment on iron atoms neighbouring the impurity will increase as the admixture of the impurity bound state with neighbouring T_{2g} orbitals grows stronger and will therefore increase with the period of the impurity as suggested by Vincze and Aldred (1974) and in agreement with the saturation magnetisation measurements of Aldred (1968). Since the increase in moment on iron atoms neighbouring the impurity which is responsible for the observed departures from simple dilution is expected to occur mostly in the E_g orbitals this has interesting implications for neutron diffraction experiments on these alloys.

CHAPTER IV

Electron Correlations in the Cohesive properties of the transition metals

4.1 Introduction

In Chapter 2 we emphasised the localised or highly correlated nature of the 3d electrons in iron, treating only the part played by the 4s electrons in the screening of a non-transition element impurity. From the discussion in Chapter 1, however, it is clear that such a model would be inapplicable to nickel based alloys. Thus nickel behaves as an itinerant ferromagnet, the high 3d density of states playing an essential role in the screening of a non-transition element impurity. This difference in the electronic structure of iron and nickel is surprising because nickel has a greater nuclear charge than iron, so the 3d shell would be expected to be more tightly bound and we might therefore expect correlation effects to be more important in nickel than in iron. It is the purpose of this chapter to investigate the effects of electron interactions on the electronic structure by including intraatomic electron correlations which prevent electrons coming together on the same atom. We shall begin with a study of the one-band model and later discuss the applicability of the results to the transition metals.

Perhaps the most convincing illustration of the collective nature of the d electrons is provided by the cohesive energy of the transition metals shown in Figure 4.1 (Gschneider, 1964). The 4d and 5d transition metals are seen to have a large cohesive energy which varies in a regular way across the series, showing clearly that it must be related to the formation of a d-band as the atoms come together to form the solid. This was explained by Friedel (1964, 1969) using a simple band model which we shall describe in § 4.2. This model neglects the interaction energy associated with intra-atomic charge

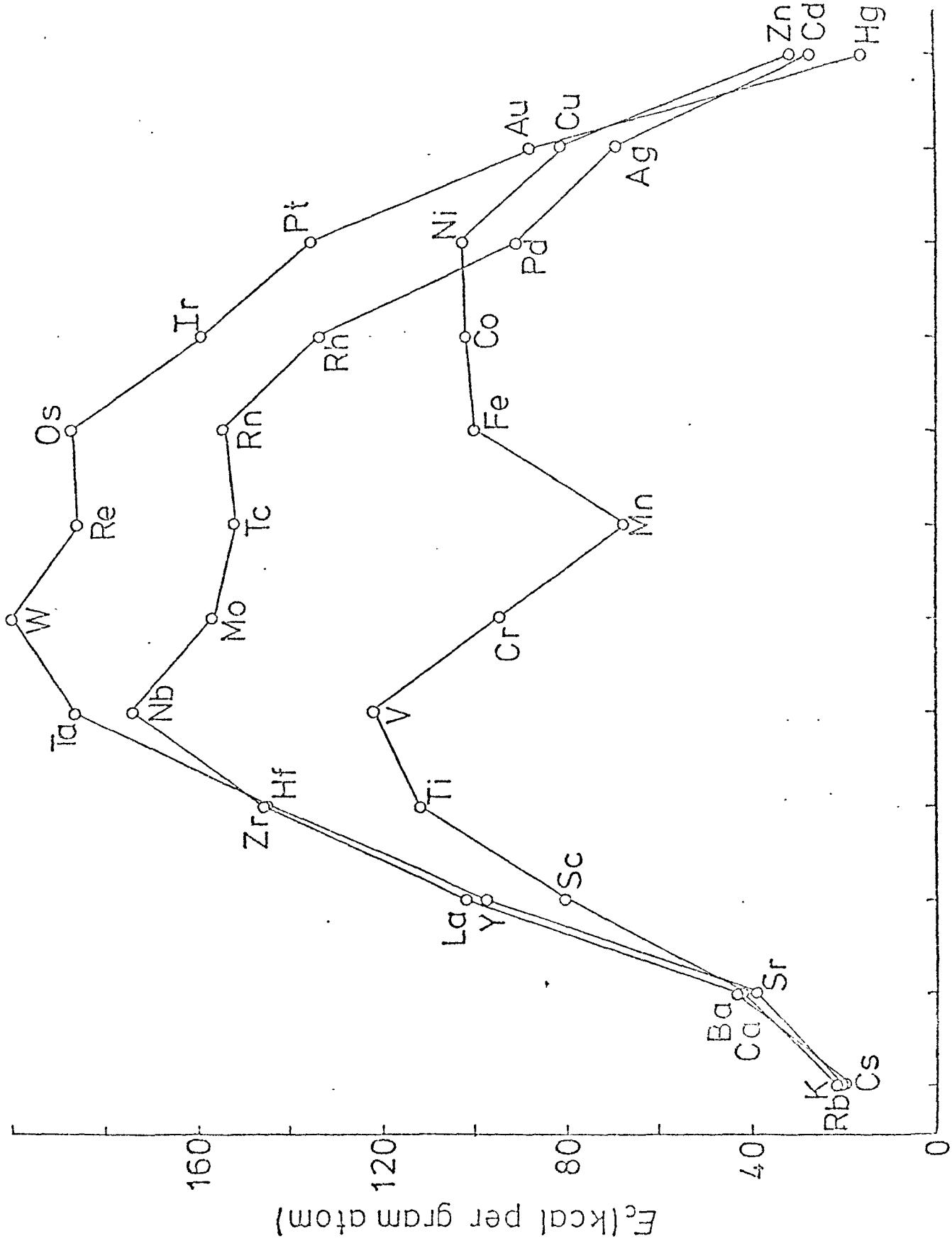

Figure 4.1. Cohesive energies of elements in the 3d, 4d and 5d transition metal series after Gschneider (1964).

fluctuations which are known to be of great importance in the 3d series, and a large difference in behaviour is seen between the cohesive energy of the 3d series on the one hand and that of the 4d and 5d series on the other. Thus manganese, iron and cobalt exhibit a lower cohesive energy than we would expect on the basis of Friedel's model, whilst nickel behaves very much like Pd and Pt in the 4d and 5d series, in agreement with its behaviour as an itinerant ferromagnet. We shall see in § 4.4 that this deviation in the middle of the 3d series comes in part from the well known stability of half-filled d shells in free atoms, but is is also found that a very similar behaviour occurs in the Young's modulus, shear modulus, bulk modulus, melting point and heat of fusion (Gschneider, 1964) which involve changes within condensed phases and not the ground state of the free atom.

It is particularly difficult to treat correlations in the 3d series because this lies between the strong correlation limit corresponding to the more localised f states in the rare earth metals, and the wide band limit of the simple metals and perhaps of the 4d and 5d series. Thus the ground state is determined by the balance between the interaction energy, which would be lowest if charge fluctuations were completely supressed, and the kinetic energy, which would be lowest if the electrons were unrestricted in their motion. The conventional approach to this problem has centred around model Hamiltonians, the most popular being that of Hubbard (1963, 1964). Hubbard used a Green's function decoupling procedure, and whilst this approximation is reasonable for the insulating phase it does not properly describe the Fermi surface, as was emphasised by Herring (1966) and by Edwards and Hewson (1965). This is particularly serious in the transition metals where the Fermi surface has been well investigated and is described well by the band structure calculations of Callaway and co-workers (Tawil and Callaway 1973, Wang and Callaway

1974) as emphasised in Chapter 1. On the other hand, Kanamori (1963) has applied Brueckner's theory of nuclear matter (Brueckner 1955, Wada and Brueckner 1958) to the problem of correlations in the transition metals which is known to be exact in the limit of low particle density (Galitski, 1958). This ladder approximation is not applicable to the 3d series however except perhaps for Ni with 0.6 holes per atom in the 3d band.

A method is required therefore to treat electron interactions over the range of densities found in the 3d series, whilst preserving the features of the Fermi surface which is well described by band theory. Perhaps the most promising such method is that of Gutzwiller (1963, 1965) who proposed a variational wavefunction for the ground state. The philosophy of this approach is rather similar to the treatment of correlation effects in the hydrogen molecule presented in § 1.4 and is ideally suited for a treatment of the balance between the kinetic and interaction energies which is so important in the 3d series. This method will be used to discuss cohesion in the one band model in § 4.3 and the applicability of the results to the transition metals will be discussed in § 4.4.

4.2 Friedel's model of cohesion in the transition metals

Consider n electrons (or n holes if the band is more than half filled) m of which have spin ↑ and μ have spin ↓ in a lattice of N sites with $n \leq N$. In the single band model the ground state wavefunction is the conventional Bloch state

$$\Phi_{K\uparrow K\downarrow} = \prod_{K\uparrow K\downarrow} a^{\dagger}_{\underset{\sim}{k}\sigma} |0\rangle \tag{4.1}$$

where $K\uparrow = \{\underset{\sim}{k}_1, \ldots, \underset{\sim}{k}_{m\uparrow}\}$ and $K\downarrow = \{\underset{\sim}{k}_1 \ldots \underset{\sim}{k}_{\mu\downarrow}\}$

is the occupied region of $\underset{\sim}{k}$ space.

The operator $a^{\dagger}_{\underset{\sim}{k}\sigma}$ creates a spin σ electron in the single particle state $\phi_{\underset{\sim}{k}\sigma}(\underset{\sim}{r})$ with energy $\epsilon_{\underset{\sim}{k}}$ determined by the crystal potential $V(r)$

$$\left[-\frac{\hbar^2}{2m} \nabla^2 + V(\underset{\sim}{r}) \right] \phi_{\underset{\sim}{k}\sigma}(\underset{\sim}{r}) = \epsilon_{\underset{\sim}{k}} \phi_{\underset{\sim}{k}\sigma}(\underset{\sim}{r}) \tag{4.2}$$

which may be expressed as a sum over potentials $V_g(\underset{\sim}{r} - g)$ centred on lattice sites g

$$V(\underset{\sim}{r}) = \sum_g V_g(\underset{\sim}{r} - g) \tag{4.3}$$

In principle $V(\underset{\sim}{r})$ should be determined self-consistently and the V_g would be dependent upon the lattice spacing. In practice the V_g are usually taken as atomic potentials as in the Wigner-Seitz scheme. Thus the interaction of electrons on different sites is effectively included since atoms surrounding the one under consideration are made neutral, but, owing to the cancellation of the self-Coulomb and the self-exchange term in the Hartree-Fock equations, the potential of the atom upon which the electron sits is that of the positive ion. Thus the energy cost of intra-atomic charge fluctuations is neglected. The reason for this procedure is, of course, that when an electron is on a particular atom, correlation effects act to prevent another electron hopping onto the same site. The method does, however, neglect the increase in kinetic energy which would occur as a result of the correlation. The advantage of the method is that the same potentials are used in both the solid and the system of free atoms, allowing one to compare directly the energy in the two cases (Friedel 1964, 1969) and so compute the cohesive energy.

Thus, following Friedel and neglecting the energy cost of intra-atomic charge fluctuations, the energy is just

$$E_{K\uparrow K\downarrow} = \sum_{K\uparrow K\downarrow} \epsilon_{\underline{k}} \tag{4.4}$$

with the cohesive energy given by

$$E_c = -\frac{1}{N} \sum_{K\uparrow K\downarrow} \epsilon_{\underline{k}} + \frac{(m+\mu)}{N} E_0 \tag{4.5}$$

where E_0 is the energy of the isolated atomic d state. Thus, if $n(E)$ is the density of states per atom, then in the non-magnetic state discussed by Friedel

$$E_c = 2 \int^{E_F} (E_0 - E)\, n(E)\, dE \tag{4.6}$$

which, for the rectangular density of states

$$n(E) = \frac{1}{2\omega} \qquad E_0 - \omega - s < E < E_0 + \omega - s \tag{4.7}$$

$$= 0 \quad \text{otherwise}$$

shifted from E_0 by an amount s, gives the parabolic behaviour

$$E_c = \frac{\omega n}{2} (2 - n) + ns \tag{4.8}$$

upon filling the band. In the transition metals the crystal field splitting is small in comparison with the bandwidth (Friedel 1969) and tight binding computations suggest that in cubic crystals the E_g and T_{2g} parts of the density of states are fairly uniformly distributed over the d band with only the top and bottom of the band having a definite E_g or T_{2g} character. Thus, assuming five identical

subbands, the cohesive energy due to the d electrons is

$$E_c = \frac{\omega p}{10}(10-p) + ps \qquad (4.9)$$

where $p = 5n$ is the number of electrons per atom in the d band, as obtained by Friedel (1964, 1969) who demonstrated that for a given bandwidth the behaviour of the cohesive energy is not very sensitive to the details of $n(E)$. This explained why E_c varies fairly smoothly through a series, though there are differences in lattice structure between one element and the next. Equation (4.9) is seen to offer a good description of the cohesive energy in the 4d and 5d series displayed in Figure 4.1 with reasonable values of ω and s, but there is a large departure from this behaviour in the 3d series. The cohesive energy is not, however, necessarily a good indication of the strength of cohesion in the metal because it involves the ground state of the free atom and we shall see in § 4.4 that the deviation arises in part from the well known stability of half filled d shells in atoms. A more reliable estimate of the bonding strength is given by properties involving changes within condensed phases such as the elastic moduli, the melting point and the heat of fusion. In the 4d and 5d series these vary in much the same way as the cohesive energy with a maximum corresponding to a half filled d band, in accordance with Friedel's model. It is found, however, that in the middle right of the 3d series, the Young's modulus, shear modulus, bulk modulus, melting point and heat of fusion (Gschneider, 1964) are much smaller than we would expect on the basis of the simple model of binding presented by Friedel. This behaviour indicates that in the middle of the 3d series the d electrons are unable to participate fully in the binding, and is, we propose, due to electron interactions not included in the simple Wigner-Seitz approximation to the correlations.

4.3 Correlations in the single band model

In order to investigate the effect of electron interactions on the ability of electrons to participate in the bonding, we define Wannier functions

$$w(\underline{r}-\underline{g}) = \frac{1}{\sqrt{N}} \sum_{\underline{k}} e^{-i\underline{k}\cdot\underline{g}} \phi_{\underline{k}}(\underline{r}) \tag{4.10}$$

for the band under consideration, and express the Bloch state (4.1) in terms of configuration states $\Phi_{G\uparrow G\downarrow}$ as

$$\Phi_{K\uparrow K\downarrow} = \sum_{G\uparrow G\downarrow} A_{G\uparrow G\downarrow} \Phi_{G\uparrow G\downarrow} \tag{4.11}$$

where

$$\Phi_{G\uparrow G\downarrow} = \prod_{G\uparrow G\downarrow} a^{\dagger}_{g\sigma} |0\rangle \tag{4.12}$$

$G\uparrow = \{g_{1\uparrow} \cdots g_{m\uparrow}\}$ $\quad G\downarrow = \{g_{1\downarrow} \cdots g_{\mu\downarrow}\}$ being the sets of lattice sites occupied by the $m\uparrow$ spin and $\mu\downarrow$ spin electrons.

The coefficient $A_{G\uparrow G\downarrow}$ is given by

$$A_{G\uparrow G\downarrow} = \left(\frac{1}{\sqrt{N}} e^{ik_{\uparrow}g} \,\middle|\, \begin{matrix} k_{1\uparrow} \cdots k_{m\uparrow} \\ g_{1\uparrow} \cdots g_{m\uparrow} \end{matrix}\right)\left(\frac{1}{\sqrt{N}} e^{ik_{\downarrow}g} \,\middle|\, \begin{matrix} k_{1\downarrow} \cdots k_{\mu\downarrow} \\ g_{1\downarrow} \cdots g_{\mu\downarrow} \end{matrix}\right) \tag{4.13}$$

using an obvious notation for determinants.

As was pointed out by Van Vleck (1953) the Bloch wavefunction (4.11) with coefficients (4.13) contains too many configurations $\Phi_{G\uparrow G\downarrow}$ with large polarity, that is it allows too many doubly occupied sites in the presence of electron interactions.

Gutzwiller (1963, 1965) constructed a local wavefunction for the ground state by starting with the conventional Bloch state (4.11) for

the non-interacting ground state and reducing the amplitude of all configurations in which ν atoms are doubly occupied by an amount η^{ν} where $0 \leq \eta \leq 1$ is a variational parameter. Thus Gutzwiller proposed the variational wavefunction

$$\Psi_c = \sum_{G\uparrow G\downarrow} \eta^{\nu} B_{G\uparrow G\downarrow} A_{G\uparrow G\downarrow} \Phi_{G\uparrow G\downarrow} \tag{4.14}$$

where the $B_{G\uparrow G\downarrow}$ are introduced to account for the less important inter-atomic interactions. The uncorrelated wavefunction is obtained by setting $B = \eta = 1$. By letting B differ from one, the diagonal and off-diagonal elements of the n'th order density matrix ρ_n can be given certain simple properties which may not follow from setting $B = 1$.

Using this wavefunction Gutzwiller (1965) calculated the first and second order density matrices within the quasi-chemical approximation in which the electrons of one spin are considered fixed for the purpose of calculating the kinetic energy of electrons of the opposite spin. This is a reasonable assumption when dealing with electrons in narrow bands as in the transition metals. Within this approximation the calculation of the density matrices reduce to a sum over configuration, the details being given in Appendix B. Thus, from Appendix B, the first order density matrix is given by

$$\begin{aligned} \rho_{1\uparrow}(g_{1\uparrow} | g_{2\uparrow}) &= p_{\uparrow}(g_{1\uparrow} - g_{2\uparrow}) \quad \text{if } g_{1\uparrow} = g_{2\uparrow} \\ &= q_{\uparrow} p_{\uparrow}(g_{1\uparrow} - g_{2\uparrow}) \quad \text{if } g_{1\uparrow} \neq g_{2\uparrow} \end{aligned} \tag{4.15}$$

where $$p_{\uparrow}(g_{1\uparrow} - g_{2\uparrow}) = \frac{1}{N} \sum_{k\uparrow} e^{ik(g_{1\uparrow} - g_{2\uparrow})} \tag{4.16}$$

and

$$q_\uparrow = \frac{1}{m(N-m)}\left[(N-m-\mu+\nu_0)^{1/2}(m-\nu_0)^{1/2} + (\mu-\nu_0)^{1/2}\nu_0^{1/2}\right]^2 \tag{4.17}$$

with similar expressions for $\downarrow$ spin electrons. Here ν_0 is the number of doubly occupied atoms in the ground state and is related to the parameter η in (4.14) by

$$\frac{(m-\nu_0)(\mu-\nu_0)}{\nu_0(N-m-\mu+\nu_0)}\,\eta^2 = 1 \tag{4.18}$$

We now write the energy in density functional language as

$$E[\rho_\uparrow,\rho_\downarrow] = T[\rho_\uparrow] + T[\rho_\downarrow] + \int d\underline{r}\, V(\underline{r})\left[\rho_\uparrow(\underline{r}) + \rho_\downarrow(\underline{r})\right] + E_I[\rho_\uparrow,\rho_\downarrow] \tag{4.19}$$

where $E_I[\rho_\uparrow,\rho_\downarrow]$ describes the intra atomic electron interactions not included in $V(\underline{r})$, the lattice potential used to calculate the $\phi_{\underline{k}\sigma}(\underline{r})$ in (4.2). We approximate $E_I[\rho_\uparrow,\rho_\downarrow]$ by

$$E_I[\rho_\uparrow,\rho_\downarrow] = C\nu_0 \tag{4.20}$$

where C is the intra atomic interaction energy. Now

$$n_{\underline{k}\sigma} = \frac{1}{N}\sum_{g_1 g_2} e^{i\underline{k}(g_1-g_2)} \langle \Psi | a^\dagger_{g_1} a_{g_2} | \Psi \rangle$$

$$= q + (1-q)\frac{n_\sigma}{N} \quad \text{if } \underline{k}\sigma \in K\sigma$$

$$= (1-q)\frac{n_\sigma}{N} \quad \text{if } \underline{k}\sigma \notin K\sigma \tag{4.21}$$

using the single particle density matrix (4.15) derived by Gutzwiller, where n_σ is the number of electrons with spin σ and K_σ is the occupied region of k space in the Bloch state (4.1). We have therefore a piecewise constant occupaction probability in reciprocal space, the discontinuity at the Fermi surface being given by q_σ. $n_{\underline{k}}$ is seen to consist of two parts : a scaled Fermi distribution function corresponding to the correlation reduced electron hopping, and a constant throughout the band representing the localised property of the electrons in the presence of correlations. Thus within a framework in which the Fermi surface is built in from the start we have the possibility of both itinerant and localised behaviour without the need of postulating that some of the electrons are localised.

The energy of the electron gas is then

$$E(V_0) = m\, q_\uparrow\, \bar{\epsilon}_\uparrow + \mu\, q_\downarrow\, \bar{\epsilon}_\downarrow + C V_0 \qquad (4.22$$

where we have normalised $\sum_{BAND} \epsilon_k = 0$ such that $\bar{\epsilon}_\uparrow = \frac{1}{m} \sum_{K\uparrow} \epsilon_k$ and $\bar{\epsilon}_\downarrow = \frac{1}{\mu} \sum_{K\downarrow} \epsilon_k$ are negative.

The ground state energy is then obtained by minimisation of (4.22) by varying V_0. This determines V_0 as a function of C.

If $n > N$ then with m and μ now being the number of $\uparrow$ and $\downarrow$ spin holes and V_0 the number of empty lattice sites, the interaction energy will be $C(N - m - \mu + V_0)$ giving the same expression as before for V_0 upon minimisation of the energy. In the atomic limit $U \to 0, V_0 \to 0$ so with the normalisation $\sum_{Band} \epsilon_{\underline{k}} = 0$ the energy will be zero if $n \leq N$ and $C(n-N)$ if $n > N$. Thus ignoring the small shift s in (4.8) the cohesive energy/atom in the solid is

$$E_C = -\bar{m}\, q_\uparrow\, \bar{\epsilon}_\uparrow - \bar{\mu}\, q_\downarrow\, \bar{\epsilon}_\downarrow - C \bar{V}_0 \qquad (4.23$$

where $\bar{m} = m/N$, $\bar{\mu} = \mu/N$ and $\bar{\nu}_0 = \nu_0/N$ and for $n \leq N$ m and μ are the number of $\uparrow$ and $\downarrow$ spin electrons and ν_0 is the number of doubly occupied sites in the ground state, whilst for $n > N$, m and μ are the number of $\uparrow$ and $\downarrow$ spin holes and ν_0 is the number of empty lattice sites.

For the case of one electron per atom considered by Brinkman and Rice (1970) the energy (4.22) is just

$$\frac{E}{N} = 16\bar{\epsilon}\,\bar{\nu}_0\left(\tfrac{1}{2} - \bar{\nu}_0\right) + C\,\bar{\nu}_0 \tag{4.24}$$

Minimising with respect to $\bar{\nu}_0$ gives

$$\bar{\nu}_0 = \frac{1}{4}\left(1 + \frac{C}{8\bar{\epsilon}}\right) \tag{4.25}$$

giving $$\frac{E}{N} = \bar{\epsilon}\left(1 + \frac{C}{8\bar{\epsilon}}\right)^2 \tag{4.26}$$

So at a critical value of the interaction strength

$$C = -8\bar{\epsilon} \tag{4.27}$$

the system undergoes a metal insulator transition with the number of doubly occupied sites and the ground state energy going to zero.

We shall consider the case $m = \mu$, $m + \mu = n$ where n is not necessarily equal to the number of lattice sites (Sayers, 1976). If $C = 0$ the Hartree-Fock result $\bar{\nu}_0 = \bar{m}^2$ is obtained. If C is small we expand in powers of δ defined by

$$\nu_0 = \frac{n^2}{4} - \delta \tag{4.28}$$

with δ small. Thus, from (4.17)

$$q \approx 1 - \frac{2\delta^2}{n^3(1-n/2)^3} + O(\delta^3) \tag{4.29}$$

$$\Rightarrow E(\delta) \approx \left[1 - \frac{2\delta^2}{n^3(1-n/2)^3}\right] n\bar{\epsilon} + C\left(\frac{n^2}{4} - \delta\right) \tag{4.30}$$

Minimising with respect to δ gives

$$\delta = -\frac{C n^3 (1-n/2)^3}{4 n \bar{\epsilon}} \tag{4.31}$$

$$\Rightarrow E = n\bar{\epsilon} + \frac{Cn^2}{4} + n^2(1-n/2)^3 \frac{C^2}{8\bar{\epsilon}} + O(C^3) \tag{4.32}$$

Equation (4.31) gives the reduction ($\bar{\epsilon}$ is negative) in the number of doubly occupied (empty) sites due to correlation effects to first order in C. For small c the first order correction to the energy is seen from (4.32) to be just the Hartree-Fock interaction energy $Cn^2/4$. The effect of correlations is seen to be of order C^2 for small c and is seen to reduce the interaction energy from the Hartree-Fock value by allowing electrons to avoid coming together on the same atom.

For the general case C is not small and for $m = \mu$ the equation for ν_0 obtained upon minimising the energy is

$$\left[\frac{(m-\nu_0)^2}{\nu_0(N-2m+\nu_0)} - 1\right](N-2m) = -\frac{(N-m)C}{2\bar{\epsilon}}\left[2(N-4m+4\nu) - \frac{(N-m)C}{2\bar{\epsilon}}\right] \tag{4.33}$$

which may be written in the form

$$8(1-\bar{m})\frac{c}{2\bar{\epsilon}}\bar{V}_0^3 - (1-\bar{m})\left[(1-\bar{m})\frac{c}{2\bar{\epsilon}} - (10-24\bar{m})\right]\frac{c}{2\bar{\epsilon}}\bar{V}_0^2$$

$$-(1-2\bar{m})\left[(1-\bar{m})^2\frac{c^2}{4\bar{\epsilon}^2} - 2(1-\bar{m})(1-4\bar{m})\frac{c}{2\bar{\epsilon}} + (1-2\bar{m})\right]\bar{V}_0 \qquad (4.34)$$

$$+ \bar{m}^2(1-2\bar{m})^2 = 0$$

As $c \to 0$, $\bar{V}_0 \to \bar{m}^2$ the Hartree-Fock result, whilst as

$$\bar{m} \to 1/2, \quad \bar{V}_0 \to \frac{1}{4}\left(1 + \frac{c}{8\bar{\epsilon}}\right)$$

Dividing through by $8(1-\bar{m})\frac{c}{2\bar{\epsilon}}$ and making the substitution

$$\bar{V}_0 = x + \frac{1}{24}\left[(1-\bar{m})\frac{c}{2\bar{\epsilon}} - (10-24\bar{m})\right] \qquad (4.35)$$

gives the reduced equation

$$x^3 + px + q = 0 \qquad (4.36)$$

with solutions

$$x_1 = u + v$$

$$x_2 = -\frac{u+v}{2} + \frac{u-v}{2}i\sqrt{3} \qquad (4.37)$$

$$x_3 = -\frac{u+v}{2} - \frac{u-v}{2}i\sqrt{3}$$

where

$$u = \left[-\frac{q}{2} + \left\{ \left(\frac{q}{2}\right)^2 + \left(\frac{p}{3}\right)^3 \right\}^{1/2} \right]^{1/3}$$

$$v = \left[-\frac{q}{2} - \left\{ \left(\frac{q}{2}\right)^2 + \left(\frac{p}{3}\right)^3 \right\}^{1/2} \right]^{1/3} \qquad (4.38)$$

Clearly with $D \equiv (q/2)^2 + (p/3)^3$ if

$D > 0$ there is one real root and two conjugate complex roots

$D = 0$ there are three real roots of which at least two are equal

$D < 0$ there are three real roots

In the last case we must find the cube roots of a complex quantity the solutions being

$$x_1 = 2\sqrt{\frac{|p|}{3}} \cos \frac{\phi}{3}$$

$$x_2 = -2\sqrt{\frac{|p|}{3}} \cos (\phi - \pi)/3 \qquad (4.39$$

$$x_3 = -2\sqrt{\frac{|p|}{3}} \cos (\phi + \pi)/3$$

where ϕ is the solution of $\cos\phi = \dfrac{-q/2}{\left[\left(\frac{|p|}{3}\right)^3\right]^{1/2}}$

although the above represents an analytic solution of (4.34), with the coefficients in (4.34), D is a rather complicated function of $c/2\epsilon$ and $\bar{m}$ and may vary between negative and positive values as these parameters change. In order to display the behaviour of

the solutions of (4.34) it is necessary therefore to follow the roots numerically.

We have solved (4.34) for several model densities of states. For the rectangular density of states (4.7), for example, neglecting the small shift s

$$\bar{\epsilon} = \frac{U}{2}\left(\bar{n} - 2\right) \tag{4.40}$$

Figure 4.2 illustrates the variation of $\bar{\nu}_0$ for various values of $C/2U$ as the band is filled for this density of states. Figure 4.3 shows the variation of the cohesive energy defined by Equation (4.23). For one electron per atom a metal-insulator transition occurs for $C/2U = 2$. This corresponds to the situation discussed by Brinkman and Rice (1970). For any other number of electrons per atom the Gutzwiller ground state is always metallic.

The inclusion of intra-atomic electron interactions gives a lower cohesive energy than the parabolic variation (4.8) obtained by Friedel (1964, 1969) using the Wigner-Seitz approximation to the correlations, the reduction in the cohesive energy being the greatest for a half-filled band. If n is the number of electrons (holes) per atom in the band, then if $C/2U$ is small we see from Figure 4.2 that the number of doubly occupied (empty) lattice sites ν_0 increases monotonically as $\bar{n} \to 1$. Hence the interaction energy is greatest for $\bar{n} = 1$. If $C/2U$ is large, η is small and since the number of configurations in (4.14) affected by η is greatest for a half filled band, the increase in kinetic energy is greatest for that case. This is further enhanced by the fact that for a given value of $C/2U$, η is smallest for a half filled band. Thus from (4.34) and (4.18) we find

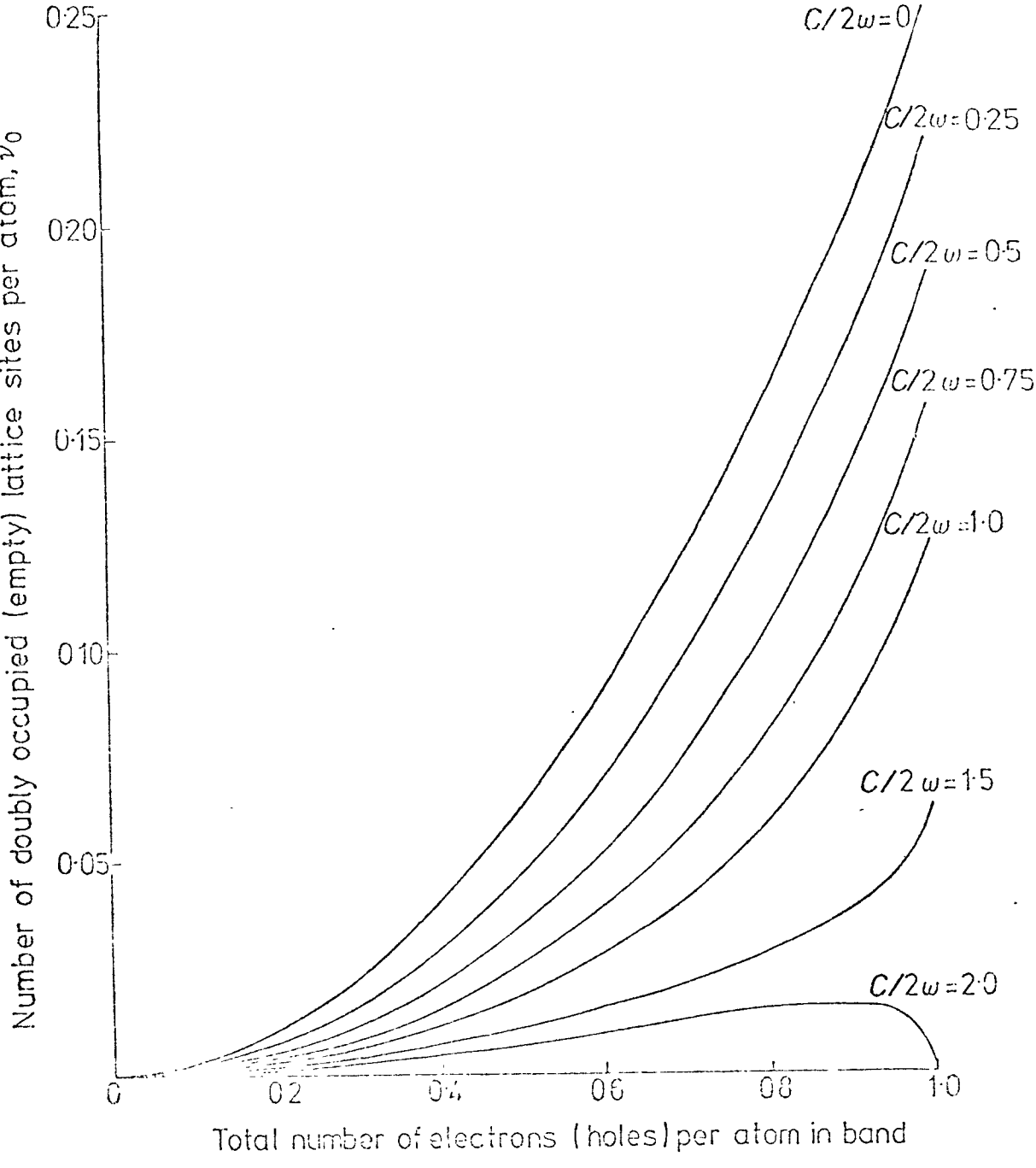

Figure 4.2. Variation of the number of doubly occupied (empty) lattice sites $\bar{\nu}_0$ for the constant density of states (4.7) as the number electrons (holes) in the band is increased for $n \leqslant N (n \geqslant N)$ for various values of C/2W.

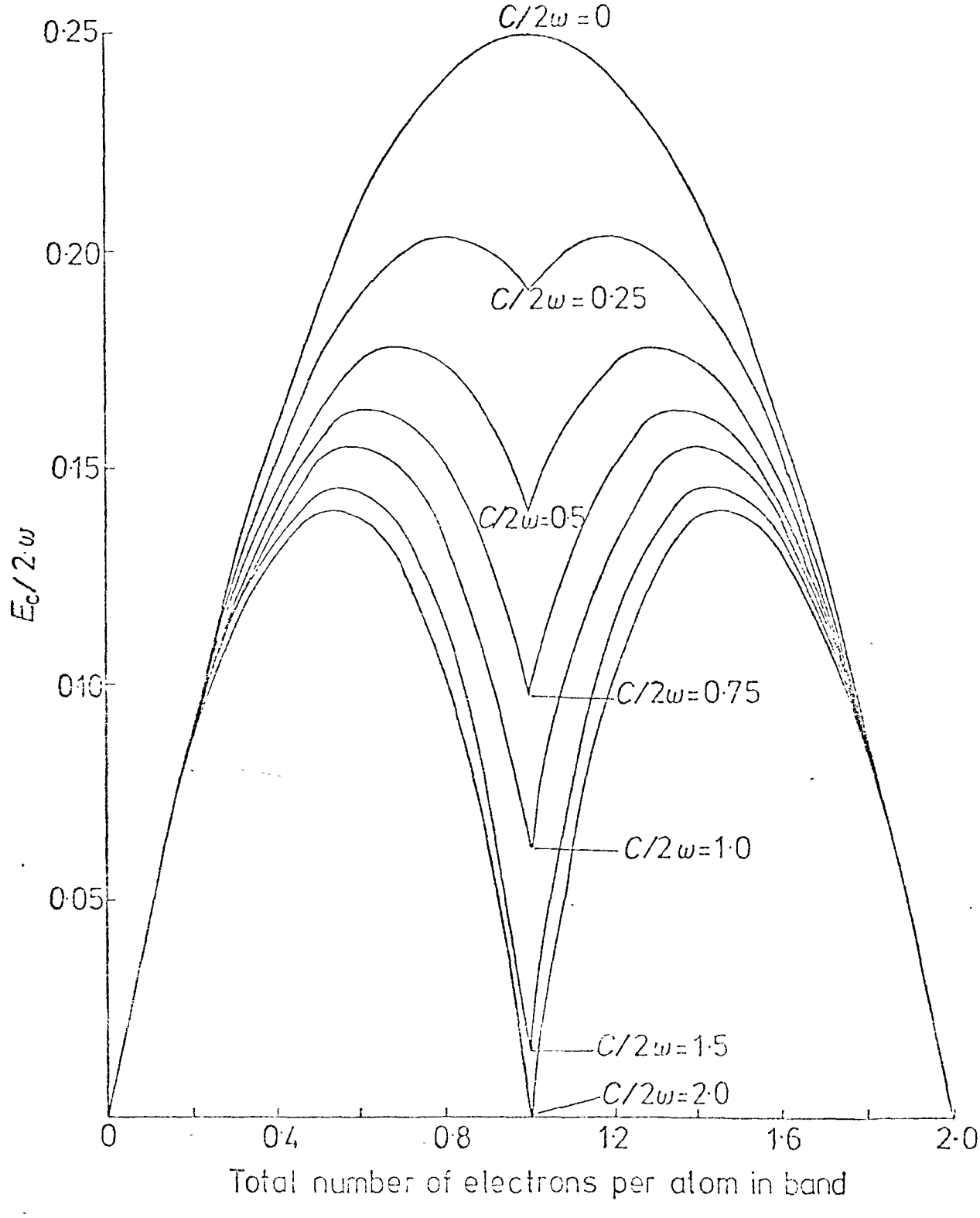

Figure 4.3. Variation of the cohesive energy defined by (4.23) of a single non-magnetic band as the band is filled for various values of C/2W for the constant density of states (4.7). The case of C/2W = 0 corresponds to the case studied by Friedel (1964,1969) .

$$\eta \rightarrow \frac{1}{(1 + C/2\omega)} \quad \text{as} \quad \bar{n} \rightarrow 0$$
$$\rightarrow \frac{(1 - C/4\omega)}{(1 + C/4\omega)} \quad \text{as} \quad \bar{n} \rightarrow 1 \qquad (4.41)$$

for a symmetric band with lower limit at $-\omega$ and upper limit at ω. Figure 4.4 shows the variation of η given by (4.18) for the rectangular density of states using the calculated values of $\bar{V}_0$ presented in Figure 4.2 for several values of $C/2\omega$

For a small number of electrons per atom in the band the probability of two electrons coming together on the same atom is small and the interaction energy is low. For a nearly full band fluctuations are, of course, limited by the exclusion principle. Thus for a small number of electrons or holes in the band the number of configurations in (4.14) affected by η is small and the wavefunction resembles the Bloch state (4.1). For a half filled band, however, a large proportion of the configurations in (4.14) are affected, and for large $C/2\omega$ the itinerancy of the electrons, and hence their ability to participate in the bonding, is greatly reduced. This is illustrated by the quantity q in (4.21) which gives the discontinuity at the Fermi surface. For $m = \mu$

$$q \rightarrow \frac{(1 - \bar{n})}{(1 - \bar{n}/2)} \quad \text{as} \quad C \rightarrow \infty \qquad (4.42)$$

which $\rightarrow 1$ as $\bar{n} \rightarrow 0$ and $\rightarrow 0$ as $\bar{n} \rightarrow 1$. For other values of $C/2\omega$ the quantity q is plotted in Figure 4.5 for the rectangular density of states, using the values of $\bar{V}_0$ presented in Figure 4.2

If we consider only the frequency dependence of the self energy, the effective mass m^*/m is given by the reciprocal of the discontinuity at the Fermi surface, q^{-1}. Thus the value of q may be determined by de Haas van Alphen effect measurements. It is found

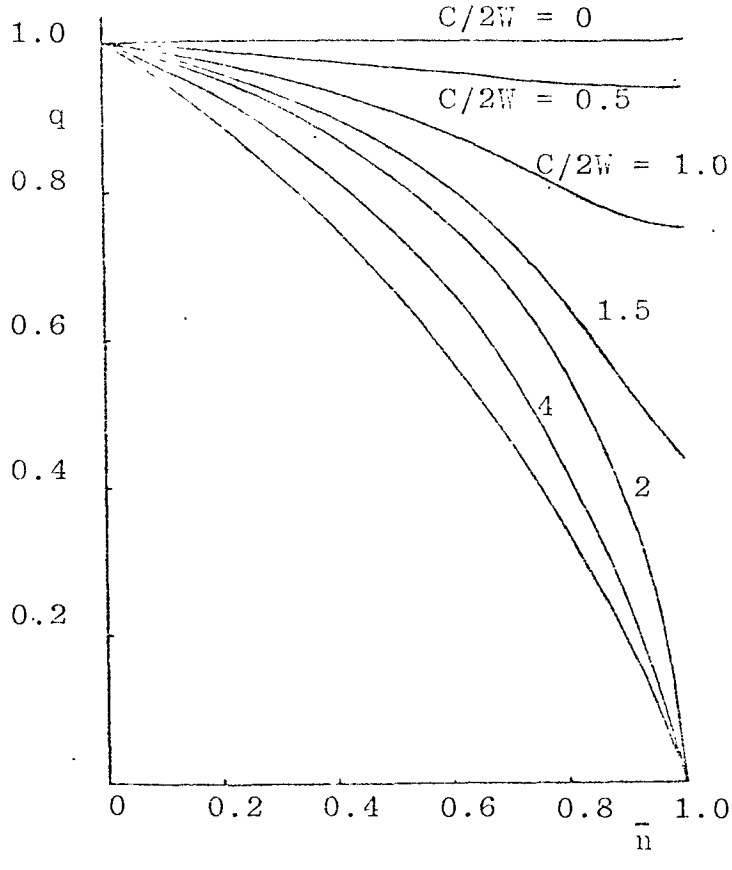

Figure 4.5. Variation of the discontinuity at the Fermi surface q given by (4.17), for $m = \mu$, with $\bar{n}$, evaluated for the rectangular density of states.

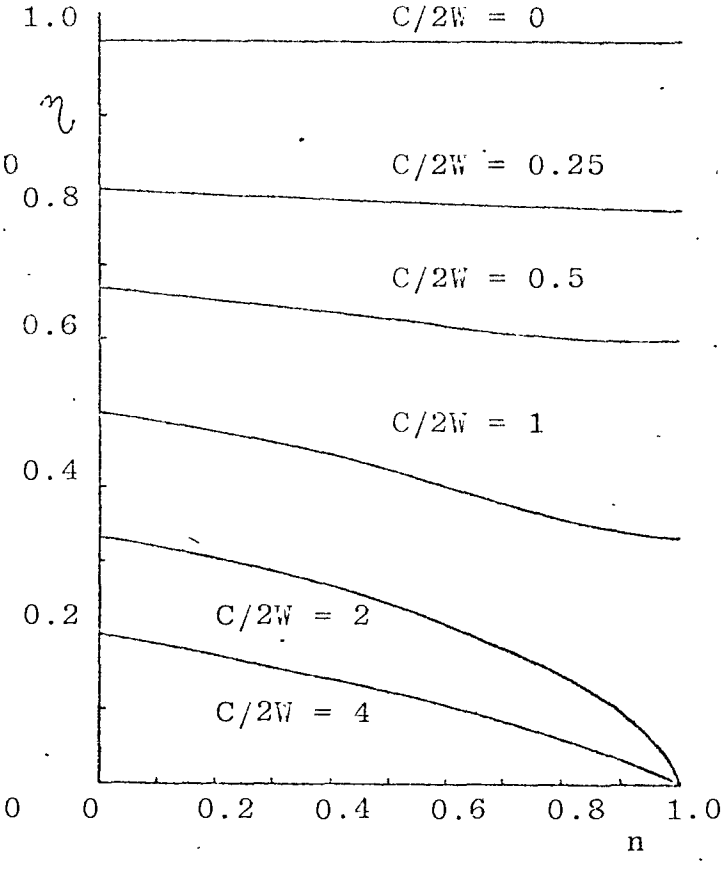

Figure 4.4. Variation of η given by (4.18), for $m = \mu$, with $\bar{n}$, evaluated for the rectangular density of states.

(Gold et al. 1971) that the oscillations arising from the minority spin sheets in iron are typically four orders of magnitude weaker than those arising from corresponding external orbits around the similarly shaped Fermi surfaces of Mo and W, indicating a large effective mass and small q .

In the middle of the 3d, 4d and 5d series the body centred cubic structure usually has the lowest energy. This is due to the band being subdivided in the BCC structure into a bonding and anti-bonding part connected by a region of low density of states as a result of there being two sublattices, all the nearest neighbours of an atom on one sublattice being on the other sublattice. In order to include this possibility we have studied the cohesive energy for the double triangular density of states

$$
\begin{aligned}
n(E) &= \frac{2}{\omega}\left(1+\frac{E}{\omega}\right) && -\omega \le E \le -\omega/2 \\
&= -\frac{2E}{\omega^2} && -\omega/2 \le E \le 0 \\
&= \frac{2E}{\omega^2} && 0 \le E \le \omega/2 \\
&= \frac{2}{\omega}\left(1-\frac{E}{\omega}\right) && \omega/2 < E < \omega
\end{aligned}
\qquad (4.43)
$$

intended to represent crudely this behaviour, for which

$$
\begin{aligned}
\bar{\epsilon} &= \frac{\omega}{3}\left[(2\bar{n})^{1/2} - 3\right] && -\omega \le E_F \le -\omega/2 \\
&= \frac{\omega}{6\bar{n}}\left[2\sqrt{2}\,(1-\bar{n})^{3/2} - 3\right] && -\omega/2 \le E_F \le 0
\end{aligned}
\qquad (4.44)
$$

Figures 4.6 and 4.7 show the variation of $\bar{V}_0$ and the energy difference between the band and atomic limit E_c as the band is filled for this density of states. The behaviour is seen to be rather similar to that found for the rectangular density of states.

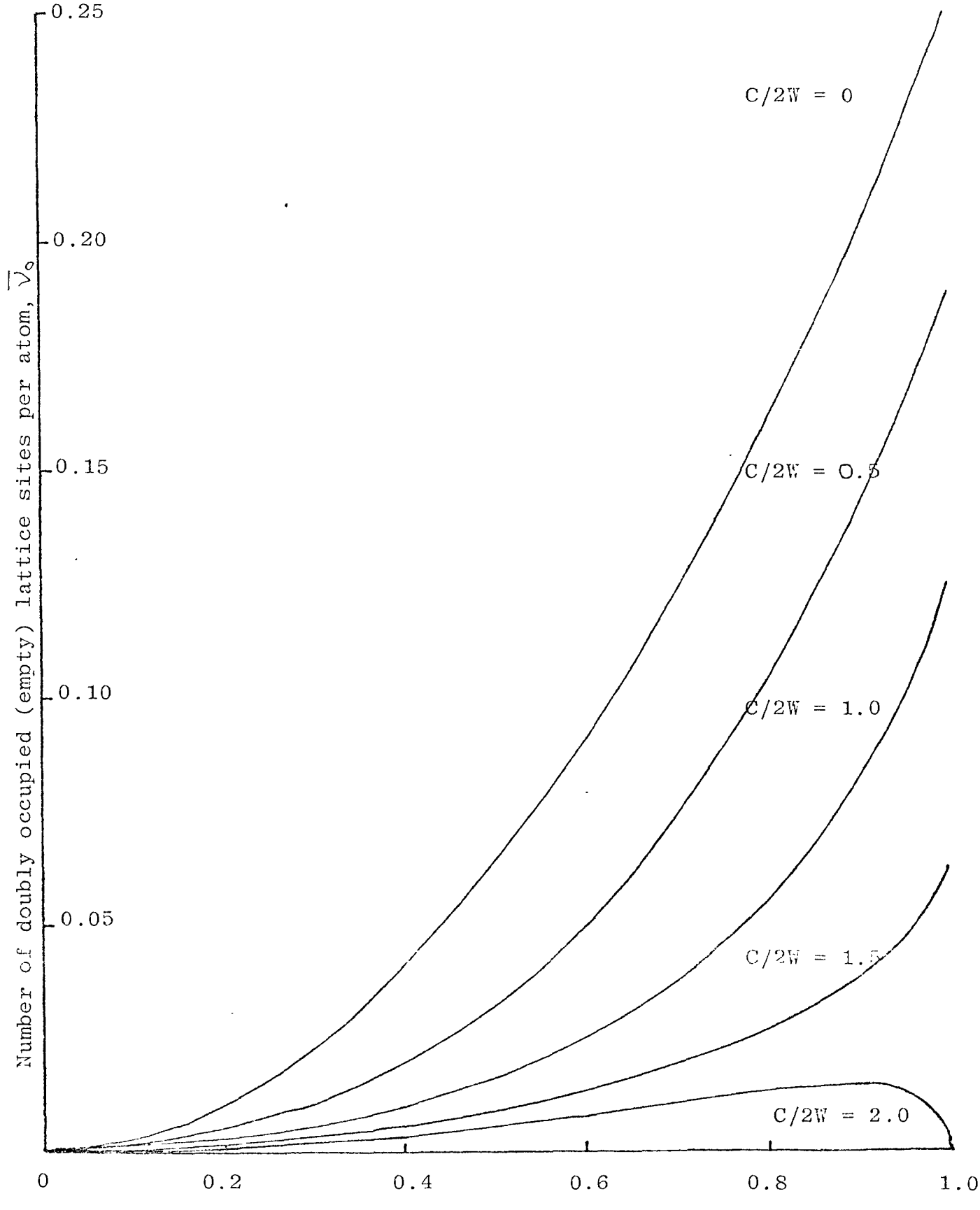

Figure 4.6. Variation of the number of doubly occupied (empty) lattice sites $\overline{\nu}_o$ for the density of states (4.43) as the number of electrons (holes) in the band is increased for $n \leqslant N (n \geqslant N)$ for various values of C/2W.

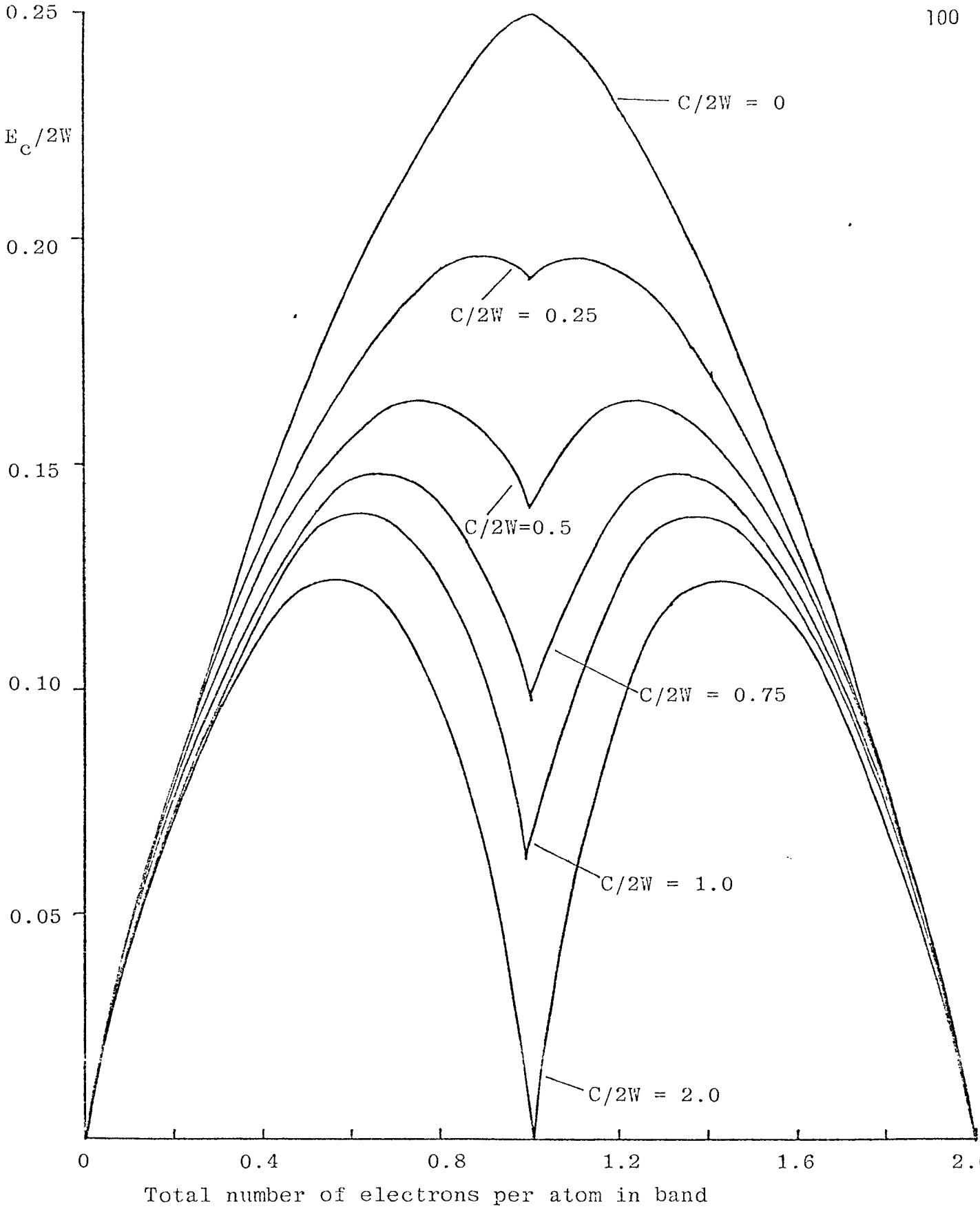

Figure 4.7. Cohesive energy defined by (4.23) of the density of states (4.43) as the band is filled for various values of C/2W.

4.4 Application to the Transition Metals

The cohesive energy does not give a reliable indication of of the binding strength in the transition metals since it involves the ground state of the free atom, and more can be learnt about the nature of bonding from properties involving changes within condensed phases such as the elastic moduli, melting point and heat of fusion (for values see Gschneider, 1964). In the 4d and 5d series these properties behave in much the same way as the cohesive energy, peaking to a maximum at a point corresponding approximately to a half-filled band. In the middle of the 3d series, however, the Young's modulus, shear modulus, bulk modulus, melting point and heat of fusion are much smaller than we would expect on the basis of Friedel's model. This departure from the roughly parabolic variation observed in the 4d and 5d series begins at Cr, is greatest for Mn, and decreases in magnitude as the band is filled further, Ni having properties similar to those of Pd and Pt. In particular, the properties of Mn seem closer to those of Cu in the same period with a full d band, in which the d electrons only contribute to the cohesion through s-d hybridisation, than to those of T_c and R_e in the same group, where strong bonding is indicated in accordance with Friedel's model. In the middle right of the 3d series, therefore, the d electrons seem to be prevented from participating fully in the bonding. Further support for this conclusion comes from the variation of atomic volume in the solid, which would be expected to decrease with increasing binding strength. In the 4d and 5d series (Gschneider, 1964) the atomic volume decreases smoothly as the band becomes half filled, and then increases as the band is filled further, in agreement with Friedel's model. In the 3d series however, Fe and Co have an atomic volume larger than that of Ni, in contrast to the behaviour in the 4d and 5d series.

This behaviour can be understood in terms of the results of

§ 4.3 which show that the effect of electron interactions on the itinerancy of the wavefunction is greatest for a half-filled band. Indeed we can extend Gutzwiller's method to deal with correlation effects in the d band by introducing variational parameters η_n, which determine the optimum concentration C_n of atoms with n electrons in the presence of electron interactions. Assuming, for simplicity, that the d band consists of five identical sublevels, the concentration C_n in the absence of correlations is just

$$C_n = \frac{10!}{n!(10-n)!}\left(1-\frac{p}{10}\right)^{10-n}\left(\frac{p}{10}\right)^{n} \qquad (4.45)$$

where p is the average number of electrons per atom in the d-band. In Ni, with p = 9.4, screening by the 0.6 electrons per atom in the 4s band will greatly reduce the energy difference between the $3d^9$ and $3d^{10}$ configurations, whilst fluctuations to states with more d electrons are, of course, suppressed by the exclusion principle. With less electrons per atom in the d band, however, fluctuations to states with large interaction energy become possible, the number of configurations in the Bloch wavefunction with large interaction energy being greatest for a half-filled band. Thus in iron, with p = 7.1, screening by the 0.9 electrons per atom in the 4s band will reduce the energy of forming a $3d^8$ configuration, but the cost of a $3d^9$ or $3d^{10}$ configuration, which have appreciable probability according to (4.45), will remain prohibitive, as was pointed out by Edwards (1970). In the ground state the probability of such configurations will therefore be considerably reduced, to an extent determined by the balance between the kinetic energy, which would be lowest if the electrons were unrestricted in their motion, and the interaction energy. In the middle of the 3d series, where the number of configurations with high interaction energy in the Bloch state is large, there will therefore be a considerable reduction in

the i inerancy of the wavefunction leading to the anomalous behaviour of the cohesive properties seen in the middle of the 3d series. This is in contrast to the 4d and 5d series where the bandwidth is large and correlation effects may be included by analogy with Equation (4.32), the first order term in the interaction energy being the Hartree-Fock term.

The importance of correlation effects in the middle of the 3d series is well illustrated by the difference in electronic structure of iron and nickel emphasised throughout this thesis, nickel behaving in a way characteristic of an itinerant ferromagnet whilst iron has many of the properties of a system of localisted spins, the behaviour being as if there are two spins per atom, coupled ferromagnetically by Hund's rule exchange. The spin coupling in iron is made effective by the reduced probability of an atom being in a $3d^9$ or $3d^{10}$ state and these spins remain aligned at temperatures well above the Curie point (Hofmann et al 1956, Mott and Stevens 1957) despite becoming decoupled from neighbouring moments.

In the 4d and 5d series where the average Coulomb interaction between two electrons on the same atom U is small in comparison to the bandwidth we may neglect correlation effects to first order in U, the interaction energy per atom in the solid being

$$\sum_{n=0}^{10} \frac{1}{2} n(n-1) U \frac{10!}{n!\,(10-n)!} \left(1 - \frac{p}{10}\right)^{10-n} \left(\frac{p}{10}\right)^{n} = \frac{9 U p^2}{20} \qquad (4.46$$

where p is the number of electrons per atom. If $l \leq p \leq l+1$ where l is an integer and J is the average intra-atomic exchange integral the energy in the atomic limit will be

$$\frac{1}{2}p(p-1)(U-J) + \frac{1}{2}c(1-c)(U-J) \quad \text{if } p \leq 5$$

$$\frac{1}{2}p(p-1)U + \frac{1}{2}c(1-c)U - \frac{1}{2}J(10-p)(9-p)J - \frac{1}{2}Jc(1-c) \quad \text{if } p \geq 5 \tag{4.47}$$

thus, for the rectangular density of states (4.7) neglecting the small shift s the cohesive energy is

$$\frac{E_c}{2\omega} = \frac{p}{20}(10-p)(1-U/2\omega) - \frac{1}{2}p(p-1)\frac{J}{2\omega} + \frac{1}{2}c(1-c)\frac{(U-J)}{2\omega} \qquad p \leq 5$$

$$= \frac{p}{20}(10-p)(1-U/2\omega) - \frac{1}{2}(10-p)(9-p)J/2\omega \tag{4.48}$$

$$+ \frac{1}{2}c(1-c)(U-J)/2\omega \qquad p \geq 5$$

where c is the atomic concentration of atoms with $(\ell + 1)$ electrons. The effect of U is seen to reduce the amplitude of the cohesive energy curve from that obtained by Friedel, the reduction in the cohesive energy being greatest in the middle of the series. In addition we obtain a dip in the middle of the series due to the intra-atomic exchange coupling J. This arises from the well known stability of half filled d shells in atoms. It is important to note in (4.48) that although J is usually much smaller than U, its effect in the middle of the series is of the same order of magnitude as that of U. For an almost full or empty band, however, the effect of J is negligible.

The first order correction to the cohesive energy due to Coulomb correlations will be

$$E_{CORR} = \frac{25}{D}\left[\frac{p}{10}\left(1-\frac{p}{10}\right)U\right]^2 \qquad (4.49)$$

by analogy with (4.32) where the denominator D is of the order of the bandwidth. This can be understood in second order perturbation theory (Friedel and Sayers, 1976) as due to the virtual excitation of the P/10 electrons per atoms in a given spin orbital to the five empty portions (1 - P/10) of orbitals with the same spin. The matrix element of each excitation is $\frac{p}{10}\left(1-\frac{p}{10}\right)U$. The number of excitations is 10 x 5 and the energy denominator is of the order of the bandwidth $2W$. We note that for small U the corrections to E_c of order U and U^2 can be considered as the first terms of a development of an "effective" Hartree-Fock correction $-\frac{p}{20}(10-p)\,U_{EFF}$ with

$$U_{EFF} = U - \frac{p}{10}(10-p)\frac{U^2}{2W} \approx \frac{U}{1+\frac{p}{10}(10-p)\frac{U}{2W}} \qquad (4.50)$$

which is reminiscent of Kanamori's formula (Kanamori, 1963) to be discussed in Chapter 5.

A further correction to the cohesive energy, important in the 5d series, is the spin orbit coupling which we shall introduce only to first order in the perturbation. In that case spin orbit coupling is important in the free atoms, but not in the solid where the orbital moment is quenched to first order. Thus the correction to the cohesive energy due to spin orbit coupling will be $-\lambda$ LS where

$$L = \frac{1}{2} p (5 - p) \qquad \text{for } p \leq 5$$

$$2S = p \qquad (4.51)$$

$$L = \frac{1}{2} (10 - p)(p - 5) \qquad \text{for } p > 5$$

$$2S = (10 - p)$$

(Friedel and Sayers, 1976).

4.5 Conclusion

The cohesive energy and properties reflecting the strength of binding in the solid such as the Young's modulus, shear modulus, bulk modulus, meling point, heat of fusion and atomic valence vary in a regular way across the 4d and 5d series and indicate a maximum cohesion from a half filled band. This shows clearly that in the 4d and 5d series the d electrons are collective and Friedel (1964, 1969) explained this behaviour on the basis of a simple band model in which the energy cost of charge fluctuations are neglected, correlation effects being treated in the Wigner-Seitz scheme. In the 3d series, however, it is known that electron interactions are crucially important in determining the ground state and result, for example, in the occurrence of magnetism within this series. Thus a large deviation in the above properties is observed in the 3d series from the behaviour in the 4d and 5d series indicating, for those elements in the middle right of the 3d series, a much weaker bonding than is expected on the basis of Friedel's model. The effect of electron interactions on the electronic structure and cohesion in the single band model was investigated using Gutzwiller's method, the

principal results being shown in Figures 4.2 to 4.5 for the rectangular band considered by Friedel. The effect of electron interactions is to decrease the number of doubly occupied sites $\bar{\nu}_0$ in the ground state as is seen in Figure 4.2 For small c, $\bar{\nu}_0$ increases monotonically as the number of electron (holes) per atom $\bar{n} \to 1$ and consequently the reduction in the cohesive energy due to electron interactions is greatest for a half filled band. If the interaction energy C is large the parameter η in (4.14) is small and since the number of configurations in (4.14) affected by η is greatest for a half filled band, the increase in kinetic energy due to correlation effects is greatest for that core. For a small number of electrons in the band, however, electrons rarely come together on the same atom and the number of configurations affected by η is small. Similarly, for a nearly full band, fluctuations are limited by the exclusion principle. Thus for a small number of electrons or holes in the band the wavefunction resembles the Bloch state obtained in normal band structure calculations. For a half-filled band, however, a large number of configurations in the Bloch state are projected out of the wavefunction and the itineracy of the electrons is severely reduced. These conclusions are seen to extend qualitatively to the 3d series where, in the middle right of the series, there is a much weaker cohesion that is expected on the basif of Friedel's model. Correlation effects are not important for elements at the beginning of the series where the nuclear charge is small, but as the band becomes filled the bandwidth decreases and correlation effects become more important. In nickel the energy cost of forming the $3d^{10}$ configuration will be much reduced by s-electron screening and fluctuations to states with large interaction energy are prevented by the exclusion principle. Thus, for Ni, relatively few configurations will be projected from the wavefunction in the ground state and band structure calculations are appropriate for treating the electronic structure. In the case

of iron, on the other hand, with 2.9 holes per atom in the d band, there is a large probability of having $3d^9$ and $3d^{10}$ configurations in the Bloch wavefunction , the energy cost of which will be largely unaffected by s electron screening. The probability of such configurations would therefore be greatly reduced in the ground state by the admixture of antibonding wavefunctions into the wavefunction with a corresponding decrease in the itineracy of the ground state.

These conclusions, derived from the cohesive properties of the transition metals, are in good agreement with the difference in the magnetic properties of iron and nickel discussed in Chapter 1. Thus, whilst nickel behaves in a way characteristic of an itinerant ferromagnet being adequately described by Stoner theory, iron has many of the properties of a system of localised spins, the behaviour being as if there are two spins per atom, coupled ferromagnetically by Hund's rule exchange. This coupling is made effective by the reduced probability of an atom being in a $3d^9$ or $3d^{10}$ configuration in the ground state. These spins remain aligned at temperatures well above the Curie point (Hofmann et al 1956, Mott and Stevens 1957) despite becoming decoupled from neighbouring moments.

4.6 Surface Properties of Transition Metals

It is interesting to consider the implications of the present work for the behaviour of the d electrons at the surface of a transition metal in view of the importance of this in a number of important processes including chemisorption and catalysis. Because of the reduced opportunities for hopping at the surface, correlation effects are expected to be of particular importance here. As has been pointed out by Cyrot-Lackmann (1969) and by Brown and March (1976) the behaviour of the surface tension of liquid transition metals behaves in much the same way as the cohesive energy in the transition metals. Unfortunately, there are to date rather few results for the

solid phase. Cyrot-Lackmann (1967, 1969) has calculated the behaviour of the surface tension in the absence of correlations using the tight binding approximation and finds that it varies parabolically with the filling of the band as does the cohesive energy. Experimentally the surface tension γ behaves in this way for the 5d series but for the 3d series there is a considerable deviation as we would expect from our discussion. Assuming that the average number of electrons per atom near the surface remains very close to that in the bulk (Friedel, 1976) we obtain from (4.46) to (4.49) to 2nd order in U

$$\gamma \approx \left\{ \frac{p(10-p)}{20} W - \frac{25}{W} \left[\frac{p}{10} \left(1 - \frac{p}{10} \right) U \right]^2 \right\} \alpha \frac{\delta z}{z} \qquad (4.5$$

(Friedel 1976, Friedel and Sayers 1976) where z is the number of nearest neighbours in the bulk and δz the decrease in the number of neighbours for surface atoms. α is a numerical coefficient arising from the local d band width at the surface being $W - \delta W \approx (z - \delta z)^{\alpha} W$. $\alpha = 1$ corresponds to simple hopping whilst $\alpha = 1/2$ is obtained by deducing the band width from the second moment of the density of states.

The Coulomb correlation to 2nd order in U is seen to produce a central dip in the otherwise parabolic variation of the surface tension. Higher order terms are seen from § 4.3 to reduce the amplitude of this dip without altering its shape.

Chapter V

Ferromagnetism in the one-band Gutzwiller Model

5.1 Introduction

If we neglect correlations between electrons of opposite spin the number of doubly occupied atoms is $m\mu/N$ for all values of C, the energy of the Bloch wave-function (4.1) therefore being

$$E_{HF} = m\bar{\epsilon}_{\uparrow} + \mu\bar{\epsilon}_{\downarrow} + \frac{Cm\mu}{N} \tag{5.1}$$

where $\bar{\epsilon}_{\uparrow} = \frac{1}{m}\sum_{K\uparrow}\epsilon_k$ and $\bar{\epsilon}_{\downarrow} = \frac{1}{\mu}\sum_{K\downarrow}\epsilon_k$ are negative

with the normalisation $\sum_k \epsilon_k = 0$.

Defining $n\zeta$ by

$$n\zeta = m-\mu \tag{5.2}$$

Where $n = m+\mu$ is the number of electrons, we have

$$m = \frac{n}{2}(1+\zeta) \qquad \mu = \frac{n}{2}(1-\zeta) \tag{5.3}$$

and expanding in small ζ^2 gives

$$m\bar{\epsilon}_{\uparrow} + \mu\bar{\epsilon}_{\downarrow} = n\bar{\epsilon} + \frac{h^2\zeta^2}{4n(E_F)} \tag{5.4}$$

where $\frac{n\zeta}{2} = \frac{1}{2}(m-\mu)$ is the number of spins turned round and $\frac{1}{2}\frac{n\zeta}{n(E_f)} = \frac{1}{2}\frac{(m-\mu)}{n(E_f)}$ is the average increase in energy when a spin is reversed, $n(E_f)$ being the density of states at the Fermi level. Thus for small ζ^2 the difference in energy between the magnetic and non-magnetic state is just

$$E_{\zeta^2} - E_0 = \frac{h^2\zeta^2}{4Nn(E_F)}\left[1 - Cn(E_F)\right] \tag{5.5}$$

Magnetisation will therefore lead to a lower energy if the Stoner criterion

$$Cn(E_f) > 1 \qquad (5.6)$$

is satisfied.

The Stoner criterion clearly overemphasises the tendency to ferromagnetism since, as we have seen in Chapter 4, when C is large the number of doubly occupied atoms ν_o in the ground state is substantially reduced below the Hartree-Fock value $m\mu/N$. The interaction energy in the ground state is therefore greatly reduced below the value $Cm\mu/N$ in (5.1) and to compensate for the effects of correlation C is often replaced by an effective parameter C_{eff} in the Stoner criterion which becomes

$$C_{eff}n(E_f) > 1 \qquad (5.7)$$

We shall evaluate C_{eff} in Gutzwiller's model in §5.2, the results being valid for arbitary number of electrons (holes) per atom $\bar{n}$ in the band. This extends the work of Brinkman and Rice (1970) who obtained the Stoner parameter for the case of one electron per atom in the band. In §5.4 the results are compared with those of Kanamori (1963) in the limit $\bar{n} \to 0$. Gutzwiller (1965) compared the energy in the non-magnetic state $m=\mu$ in the limit $C \to \infty$ with that in the state in which all the spins are aligned parallel and thereby obtained a criterion for complete ferromagnetism, but did not consider the possibility of a partially aligned state. We find in §5.2 that even when the ferromagnetic state is of higher energy than the non-magnetic state, a partially aligned state may have the lowest energy. In §5.3 we discuss the dependence of the energy on the magnetisation and illustrate this for a model density of states and the case of one electron per atom in the band.

Before proceeding to calculate the Stoner parameter in Gutzwiller's theory we can estimate the effect of electron correlation on the effective interaction between electrons by finding the value of C_{HF} which, when substituted for C in (5.1), gives the same energy as that of the non-magnetic ground state in Gutzwiller's model corresponding to the bare interaction C. C_{HF} so defined is then given by

$$C_{HF} = \frac{N}{m^2}\left[2m\bar{\epsilon}(q-1) + C\nu_o\right] \qquad (5.8)$$

where, in the non-magnetic case $m=\mu$

$$q = \frac{(m-\nu_o)}{m(N-m)}\left[(N-2m+\nu_o)^{\frac{1}{2}} + \nu_o^{\frac{1}{2}}\right]^2 \qquad (5.9)$$

$$\text{Thus } C_{HF} \to \frac{-2\bar{\epsilon}}{(1-\bar{m})} \quad \text{as } C \to \infty \qquad (5.10)$$

that is, C_{HF} tends to a finite limit of the order of the bandwidth as $C \to \infty$. This occurs because when the electron interaction is strong electrons will avoid coming together on the same atom by sacrificing a one-electron energy of the order of the bandwidth. This increase in the kinetic energy then corresponds to the effective magnitude of the interaction, a point first emphasised by Kanamori (1963).

In the case of the rectangular density of states

$$n(E) = \frac{1}{2W} \qquad -W<E<W \qquad (5.11)$$

$$= 0 \qquad \text{otherwise}$$

for which $\bar{\epsilon} = W(\bar{m}-1)$ we find that $C_{HF}/2W \to 1$ as $C \to \infty$.

We can evaluate C_{HF} defined by (5.8) as a function of C using the results for ν_o obtained in Chapter 4. C_{HF} is plotted against C in figure 5.1 for this density of states.

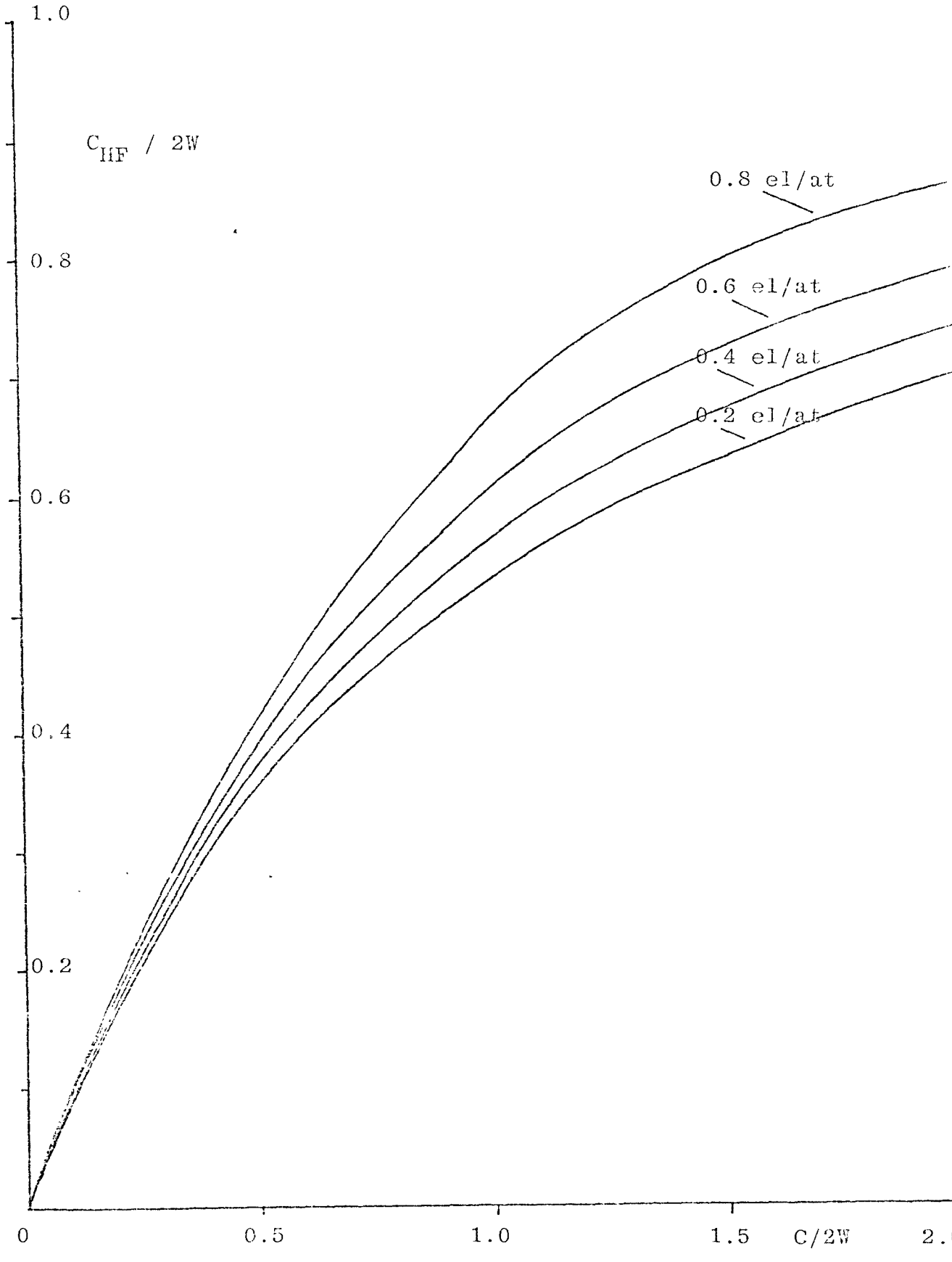

Figure 5.1. Variation of the effective interaction C_{HF} with the bare interaction C for the density of states (5.11).

5.2 Stoner parameter in Gutzwiller's theory

For small $n\zeta = m-\mu$ the exchange splitting is given by

$$\Delta = \frac{n\zeta}{2} \times \frac{1}{n(E_f)} \tag{5.12}$$

where $\frac{n\zeta}{2}$ is the number of reversed spins, giving

$$m\bar{\epsilon}_\uparrow = \int_{-\omega}^{E_F+\Delta} E n(E)\,dE = \frac{n\bar{\epsilon}}{2} + \frac{E_F n\zeta}{2} + \frac{n^2\zeta^2}{8n(E_F)}$$

$$\mu\bar{\epsilon}_\downarrow = \int_{-\omega}^{E_F-\Delta} E n(E)\,dE = \frac{n\bar{\epsilon}}{2} - \frac{E_F n\zeta}{2} + \frac{n^2\zeta^2}{8n(E_F)} \tag{5.13}$$

Now for small

$$q_\uparrow \approx \frac{(n/2-v)}{m(N-m)}\left\{(N-n)\left[1+\frac{n\zeta}{2(n/2-v)} - \frac{n^3\zeta^3}{64(n/2-v)^3} + \frac{n^4\zeta^4}{1024(n/2-v)^4}\right]\right.$$
$$+ 2v\left[1+\frac{n^4\zeta^4}{1024(n/2-v)^4}\right] \tag{5.14}$$
$$\left. + 2(N-n+v)^{1/2}v^{1/2}\left[1-\frac{n^2\zeta^2}{8(n/2-v)^2} + \frac{n^4\zeta^4}{1024(n/2-v)^4}\right]\right\}$$

$$\mu(N-\mu)m\bar{\epsilon}_\uparrow \approx \frac{n}{2}\left[\frac{n\bar{\epsilon}}{2} + \frac{E_F n\zeta}{2} + \frac{n^2\zeta^2}{8n(E_F)}\right]\left[(N-n/2) - (N-n)\zeta - \frac{n\zeta^2}{2}\right] \tag{5.15}$$

with similar expressions for $q_\downarrow$ and for $m(N-m)\mu\bar{\epsilon}_\downarrow$ obtained by reversing the sign of ζ and changing m for μ. Thus, neglecting terms in ζ^4 and higher orders and using the expansion

$$\frac{1}{m\mu(N-m)(N-\mu)} \approx \left[1+\zeta^2+\frac{n^2\zeta^2}{4(N-n/2)^2}\right] \Big/ \frac{n^2}{4}\left(N-\frac{n}{2}\right)^2 \tag{5.16}$$

we obtain for the energy per atom

$$E(\bar{\nu}) = \frac{(\bar{n}/2 - \bar{\nu})}{(1-\bar{n}/2)}\left[(1-\bar{n}+\bar{\nu})^{1/2} + \bar{\nu}^{1/2}\right]^2 2\bar{\epsilon} \tag{5.17}$$

$$+ \frac{(\bar{n}/2 - \bar{\nu})}{(1-\bar{n}/2)}\left[(1-\bar{n}+\bar{\nu})^{1/2} + \bar{\nu}^{1/2}\right]^2 \frac{\bar{n}\,\zeta^2}{2n(\epsilon_F)}\left\{1 - n(\epsilon_F)\left[\frac{\bar{n}\bar{\epsilon}}{2(\bar{n}/2-\bar{\nu})^2} - \frac{\bar{n}\,\bar{\epsilon}}{(1-\bar{n}/2)^2}\right.\right.$$

$$+ \frac{\bar{n}^2\bar{\epsilon}}{2(1-\bar{n}/2)(\bar{n}/2-\bar{\nu})\left[(1-\bar{n}+\bar{\nu})^{1/2}+\bar{\nu}^{1/2}\right]^2} - \frac{\bar{n}\bar{\epsilon}}{2(\bar{n}/2-\bar{\nu})^2\left[(1-\bar{n}+\bar{\nu})^{1/2}+\bar{\nu}^{1/2}\right]^2}$$

$$\left.\left. + \frac{2(1-\bar{n})(\bar{\epsilon}-\epsilon_F)}{(\bar{n}/2-\bar{\nu})\left[(1-\bar{n}+\bar{\nu})^{1/2}+\bar{\nu}^{1/2}\right]^2} - \frac{4(1-\bar{n})(\bar{\epsilon}-\epsilon_F)}{\bar{n}(1-\bar{n}/2)}\right]\right\}$$

which has the following asymptotic behaviour

(i) If $\zeta^2 = 0$, $E(\bar{\nu}) = \dfrac{2(\bar{n}/2-\bar{\nu})\bar{\epsilon}\left[(1-\bar{n}+\bar{\nu})^{1/2}+\bar{\nu}^{1/2}\right]^2}{(1-\bar{n}/2)}$ (5.18)

(ii) If $\bar{n} = 1$, $E(\bar{\nu}) = 16\bar{\nu}(1/2-\bar{\nu})\bar{\epsilon}$

$$+ \frac{4\bar{\nu}(1/2-\bar{\nu})\zeta^2}{n(\epsilon_F)}\left[1 + \frac{n(\epsilon_F)\bar{\epsilon}(3-16\bar{\nu}+16\bar{\nu})^2}{4(1/2-\bar{\nu})^2}\right] + C\bar{\nu} \tag{5.19}$$

(iii) If $\bar{\nu} = 0$, $E(\bar{\nu}) = \bar{n}\bar{\epsilon}\dfrac{(1-\bar{n})}{(1-\bar{n}/2)}$ (5.20)

$$+ \frac{\bar{n}^2(1-\bar{n})\zeta^2}{4(1-\bar{n}/2)n(\epsilon_F)}\left\{1 + n(\epsilon_F)\left[\frac{n\bar{\epsilon}}{(1-\bar{n}/2)^2} + \frac{2\epsilon_F}{(1-\bar{n}/2)}\right]\right\}$$

The non-magnetic state will be unstable against spin alignment if

$$\left.\frac{dE}{d\zeta^2}\right|_{GS} = \left.\frac{\partial E}{\partial \zeta^2}\right|_{GS} + \left.\frac{\partial E}{\partial \nu}\frac{d\nu}{d\zeta^2}\right|_{GS} \tag{5.21}$$

is negative, where GS is the non-magnetic ground state. The non-magnetic gound state energy must have a minimum at the optimum number of doubly occupied atoms ν_o. The non-magnetic state is therefore unstable against ferromagnetic spin alignment if

$$1 + n(E_F)\left[\frac{\bar{n}\,\bar{\epsilon}}{(1-\bar{n}/2)^2} - \frac{\bar{n}\,\bar{\epsilon}}{2(\bar{n}/2-\bar{\nu}_o)^2} + \frac{\bar{n}\,\bar{\epsilon}}{2(\bar{n}/2-\bar{\nu}_o)^2\left[(1-\bar{n}+\bar{\nu}_o)^{1/2}+\bar{\nu}_o^{1/2}\right]^2}\right.$$

$$-\frac{\bar{n}^2\,\bar{\epsilon}}{2(1-\bar{n}/2)(\bar{n}/2-\bar{\nu}_o)\left[(1-\bar{n}+\bar{\nu}_o)^{1/2}+\bar{\nu}_o^{1/2}\right]^2} + \frac{4(1-\bar{n})(\bar{\epsilon}-E_F)}{\bar{n}(1-\bar{n}/2)}$$

$$\left.-\frac{2(1-\bar{n})(\bar{\epsilon}-E_F)}{(\bar{n}/2-\bar{\nu}_o)\left[(1-\bar{n}+\bar{\nu}_o)^{1/2}+\bar{\nu}_o^{1/2}\right]^2}\right] < 0 \qquad (5.22)$$

the Stoner parameter C_{eff} then has the following behaviour

(i) If $\bar{\nu}_o = \frac{\bar{n}^2}{4}$ corresponding to C=0 then $C_{eff} = 0$.

(ii) If $\bar{\nu}_o = 0$ corresponding to $C \to \infty$ and $\bar{n} \neq 1$ then

$$C_{eff} = \frac{-1}{(1-\bar{n}/2)^2}\left[\bar{n}\bar{\epsilon} + 2E_f(1-\bar{n}/2)\right] \qquad (5.23)$$

(iii) If $\bar{n} = 1$

$$C_{eff} = \frac{-\bar{\epsilon}}{4(\frac{1}{2}-\bar{\nu}_o)^2}\left[3-16\bar{\nu}_o + 16\bar{\nu}_o^2\right] \qquad (5.24)$$

In this case $\bar{\nu}_o = \frac{1}{4}\left(1 + \frac{C}{8\bar{\epsilon}}\right)$, (5.24) becoming

$$C_{eff} = \frac{C(1 - C/16\bar{\epsilon})}{(1 - C/8\bar{\epsilon})^2} \qquad (5.25)$$

in agreement with the result obtained by Brinkman and Rice (1970) who investigated the susceptibility enhancement in Gutzwiller's model for one electron per atom. This result may also be obtained as follows. For one electron per atom we have to first order in ζ^2.

$$E(\bar{\nu}) = 16\left[\bar{\epsilon} + \zeta^2/4n(\epsilon_F)\right]\left[\left(\frac{1}{2}-\bar{\nu}\right)\bar{\nu}(1+\zeta^2) - \frac{\bar{\nu}\zeta^2}{16(\frac{1}{2}-\bar{\nu})}\right] + C\bar{\nu} \qquad (5.26)$$

The condition for $\bar{\nu}_0$ then being

$$16\left[\bar{\epsilon} + \zeta^2/4n(\epsilon_F)\right]\left[\left(\frac{1}{2}-2\bar{\nu}_0\right)(1-\zeta^2) - \frac{\zeta^2}{32(\frac{1}{2}-\bar{\nu}_0)^2}\right] + C = 0 \qquad (5.27)$$

If the correlation is strong such that $\bar{\nu}_0 \ll 1$ then

$$\bar{\nu}_0 \approx \frac{1}{4}\left(1+\frac{C}{8\bar{\epsilon}}\right) - \frac{\zeta^2}{4}\frac{C}{8\bar{\epsilon}}\left[1+\frac{1}{4\bar{\epsilon}n(\epsilon_F)}\right] - \frac{\zeta^2}{4}\left(\frac{1}{2}+\frac{C}{32\bar{\epsilon}}\right) \qquad (5.28)$$

In general we look for a solution $\bar{\nu}_0 = A+B\zeta^2$. Substituting into (5.27) for small ζ^2 and equating powers of ζ^2 gives

$$\bar{\nu}_0 = \frac{1}{4}\left(1+\frac{C}{8\bar{\epsilon}}\right) - \frac{\zeta^2}{4}\left(1-\frac{C}{8\bar{\epsilon}}\right)^{-2} - \frac{\zeta^2}{4}\frac{C}{8\bar{\epsilon}}\left[1+\frac{1}{4\bar{\epsilon}n(\epsilon_F)}\right] \qquad (5.29)$$

which is seen to reduce to (5.28) when $1+\frac{C}{8\bar{\epsilon}} \ll 1$, that is near the metal insulator transition.

Substituting (5.29) into (5.26) then gives

$$E(\bar{\nu}_0) = \bar{\epsilon}\left(1+\frac{C}{8\bar{\epsilon}}\right)^2 + \frac{\zeta^2\left(1-C^2/64\bar{\epsilon}^2\right)}{4n(\epsilon_F)}\left[1-Cn(\epsilon_F)\left\{\frac{(1-C/16\bar{\epsilon})}{(1-C/8\bar{\epsilon})^2}\right\}\right] \qquad (5.30)$$

in agreement with (5.25).

Gutzwiller (1965) obtained a criterion for strong ferromagnetism by comparing the energy of the completely aligned state with that of the non-magnetic state in the limit $C \to \infty$. In the non-magnetic state

$$E_{NM} = nq\bar{\epsilon} + C\nu_o \qquad (5.31)$$

with q given by (5.9). As $C \to \infty$, $E_{NM} \to \frac{(N-n)}{(N-n/2)} n\bar{\epsilon}$

so if $\bar{\epsilon}_f$ is the average energy of the n electrons if they all have the same spin, complete ferromagnetism will be possible for sufficiently large C if

$$\frac{\bar{\epsilon}_f}{\bar{\epsilon}} > \frac{(N-n)}{(N-n/2)} \qquad (5.32)$$

We shall illustrate the behaviour of the Stoner parameter C_{eff} in Gutzwiller's model by considering several model densities of states.

1. Rectangular Density of States

For this density of states given by (5.10)

$$E_f = W(n-1)$$

$$n\bar{\epsilon} = \frac{Wn}{2}(n-2) \qquad (5.33)$$

The Stoner parameter C_{eff} is given from (5.22) by

$$C_{EFF} = \frac{n\bar{\epsilon}}{2(\bar{n}/2-\bar{\nu}_0)^2} - \frac{\bar{n}\,\bar{\epsilon}}{(1-\bar{n}/2)^2} + \frac{\bar{n}^2\,\bar{\epsilon}}{2(1-\bar{n}/2)(\bar{n}/2-\bar{\nu}_0)\left[(1-\bar{n}+\bar{\nu}_0)^{1/2}+\bar{\nu}_0^{1/2}\right]^2}$$

$$- \frac{n\,\bar{\epsilon}}{2(\bar{n}/2-\bar{\nu}_0)^2\left[(1-\bar{n}+\bar{\nu}_0)^{1/2}+\bar{\nu}_0^{1/2}\right]^2} + \frac{2(1-\bar{n})(\bar{\epsilon}-\epsilon_F)}{(\bar{n}/2-\bar{\nu}_0)\left[(1-\bar{n}+\bar{\nu}_0)^{1/2}+\bar{\nu}_0^{1/2}\right]^2}$$

$$- \frac{4(1-\bar{n})(\bar{\epsilon}-\epsilon_F)}{\bar{n}(1-\bar{n}/2)} \qquad (5.34)$$

and is plotted in figure 5.2 using the results for $\bar{\nu}_o$ obtained in Chapter 4 for this density of states. As $C \to \infty$

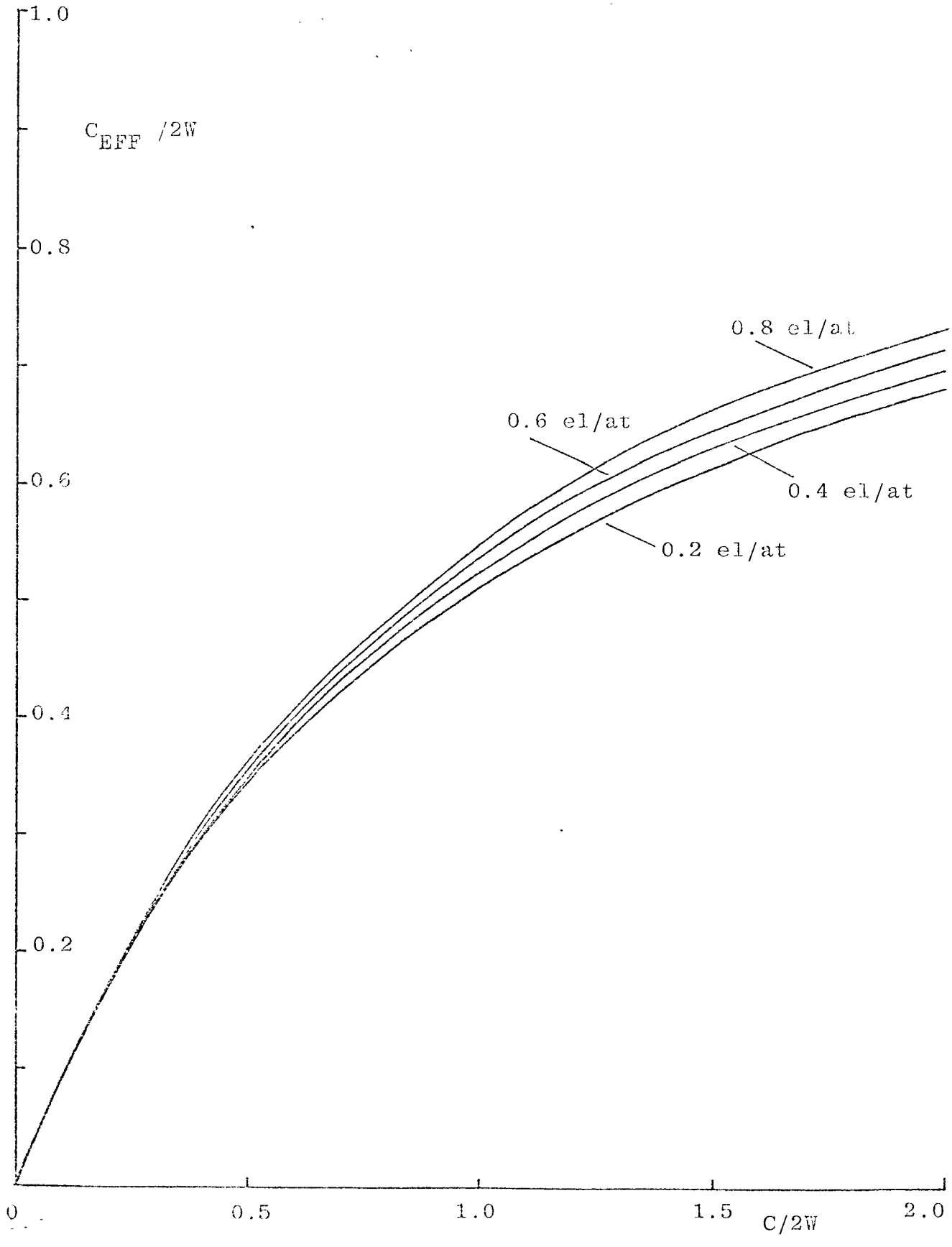

Figure 5.2. Variation of the Stoner parameter C_{EFF} (5.34) with C for the rectangular density of states (5.10) .

$$C_{EFF} \rightarrow -\frac{1}{(1-\bar{n}/2)^2}\left[\bar{n}\,\bar{\epsilon} + 2(1-\bar{n}/2)E_F\right] \qquad (5.35)$$

and it is clear that the Stoner criterion (5.7) is not satisfied with E_f and $n\bar{\epsilon}$ given by (5.33) and $n(E_f)$ given by (5.10). Thus C_{eff} is never large enough to cause a ferromagnetic transition for this density of states. For small $\bar{n}$ the variation of C_{eff} is seen to be close to that of C_{HF} defined in §5.1. In this limit this supports Kanamori (1963) who took the Stoner parameter C_{eff} to be given approximately by the effective interaction between electrons of opposite spin in the non-magnetic state. As $\bar{n} \to 1$, however, $C_{HF} - C_{eff}$ is seen to increase and we therefore expect that Kanamori's theory would overestimate the tendency to ferromagnetism. This is seen to be the case in § 5.4.

For this density of states the average energy in the completely aligned state is $\bar{\epsilon}_f = W(n-1)$ and it is seen that Gutzwiller's criterion (5.32) for complete ferromagnetism is also not satisfied for this density of states for any value of C.

2. Triangular density of states

$$\begin{aligned} h(E) &= \frac{1}{(1+\theta)\omega}\left[1 + \frac{\theta}{3} + \frac{E}{\omega}\right] && -\omega\left(1+\frac{\theta}{3}\right) < E < \frac{2}{3}\omega\theta \\ &= \frac{1}{(1-\theta)\omega}\left[1 - \frac{\theta}{3} - \frac{E}{\omega}\right] && \frac{2}{3}\omega\theta < E < \omega\left(1-\frac{\theta}{3}\right) \\ &= 0 && \text{otherwise} \end{aligned} \qquad (5.36)$$

which is positioned such that $\sum_{\text{ALL } \underline{k}} \epsilon_{\underline{k}} = 0$

Consider the case in which the Fermi level lies in the lower part of the band. We then have

$$E_F = U\left[(1+\theta)^{1/2} n^{1/2} - 1\right] - \frac{U\theta}{3}$$

$$n\bar{\epsilon} = \frac{U}{3}\left[2(1+\theta)^{1/2} n^{3/2} - 3n\right] - \frac{U\theta n}{3} \qquad (5.37)$$

with $n \leqslant (1+\theta)$.

Figure 5.3 shows the variation of C_{eff} with C for the case $\theta = 0$ for several values of $\bar{n}$, whilst figure 5.4 shows the variation of $1-n(E_f)C_{eff}$ with C where

$$n(E_f) = \frac{n^{\frac{1}{2}}}{(1+\theta)^{\frac{1}{2}}W} \qquad (5.38)$$

from which the value of C at which the non-magnetic state first becomes unstable with respect of spin alignment is easily deduced. Again, for large C, the effective interaction between the electrons is very much reduced by correlation effects.

As $C \to \infty$

$$C_{eff} \to \frac{U}{(1-n/2)^2}\left[\frac{1}{3}(1+\theta)^{1/2} n^{3/2} - 2(1+\theta)^{1/2} n^{1/2} + 2 + \frac{2\theta}{3}\right] \qquad (5.39)$$

so from (5.38) the non-magnetic state is unstable against ferromagnetic spin alignment for sufficiently large C if

$$\frac{2n^{1/2}}{\left(1+n-\frac{n^2}{12}\right)} > \frac{(1+\theta)^{1/2}}{(1+\theta/3)} \qquad (5.40)$$

which is only satisfied if the Fermi level lies close to the peak in the density of states. Thus if $\theta=0$, for example, the non-magnetic state will be unstable against spin alignment for sufficiently large C if $n \gtrsim 0.66$ electrons

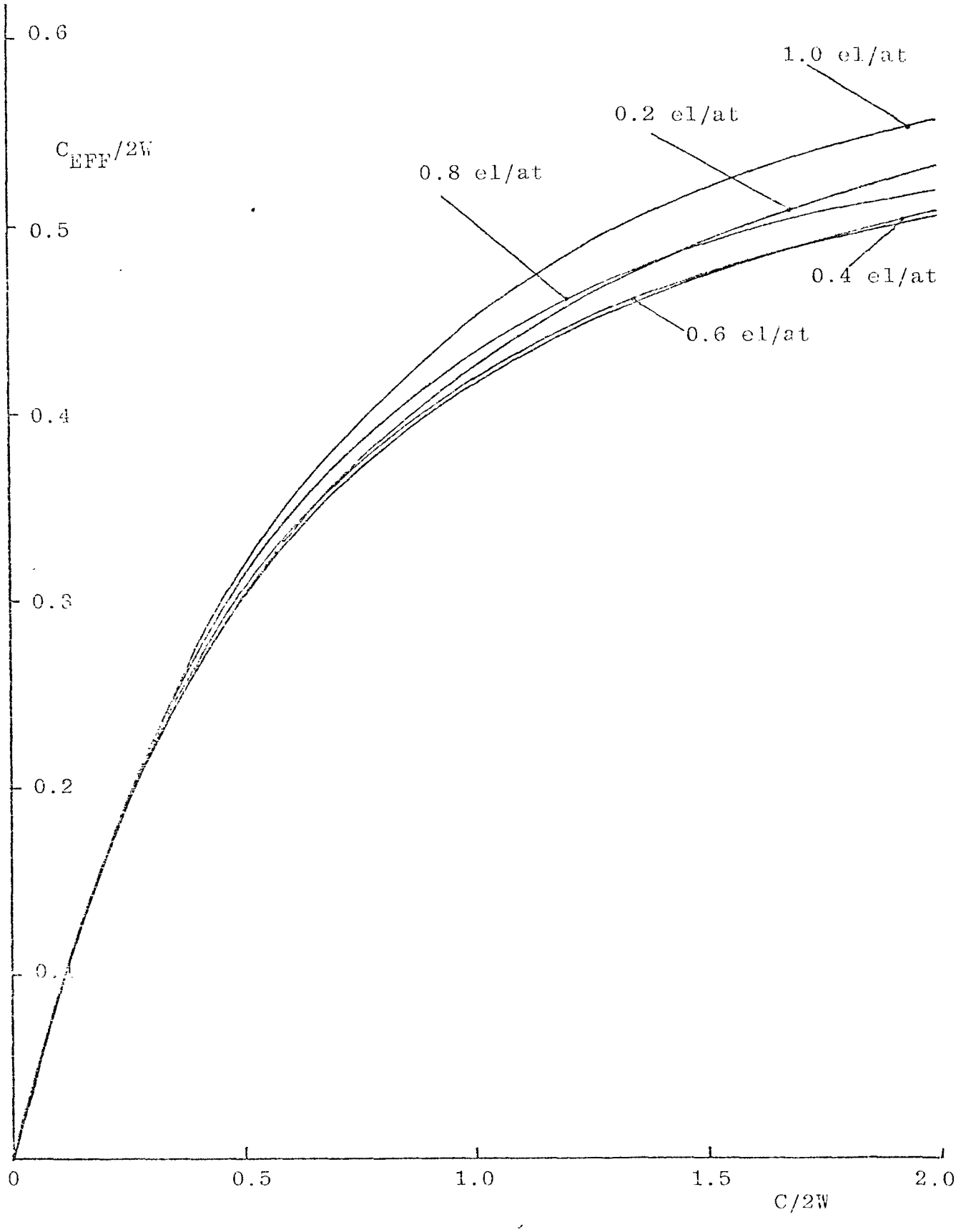

Figure 5.3. Variation of the Stoner parameter C_{EFF} (5.34) with C for the triangular density of states (5.36).

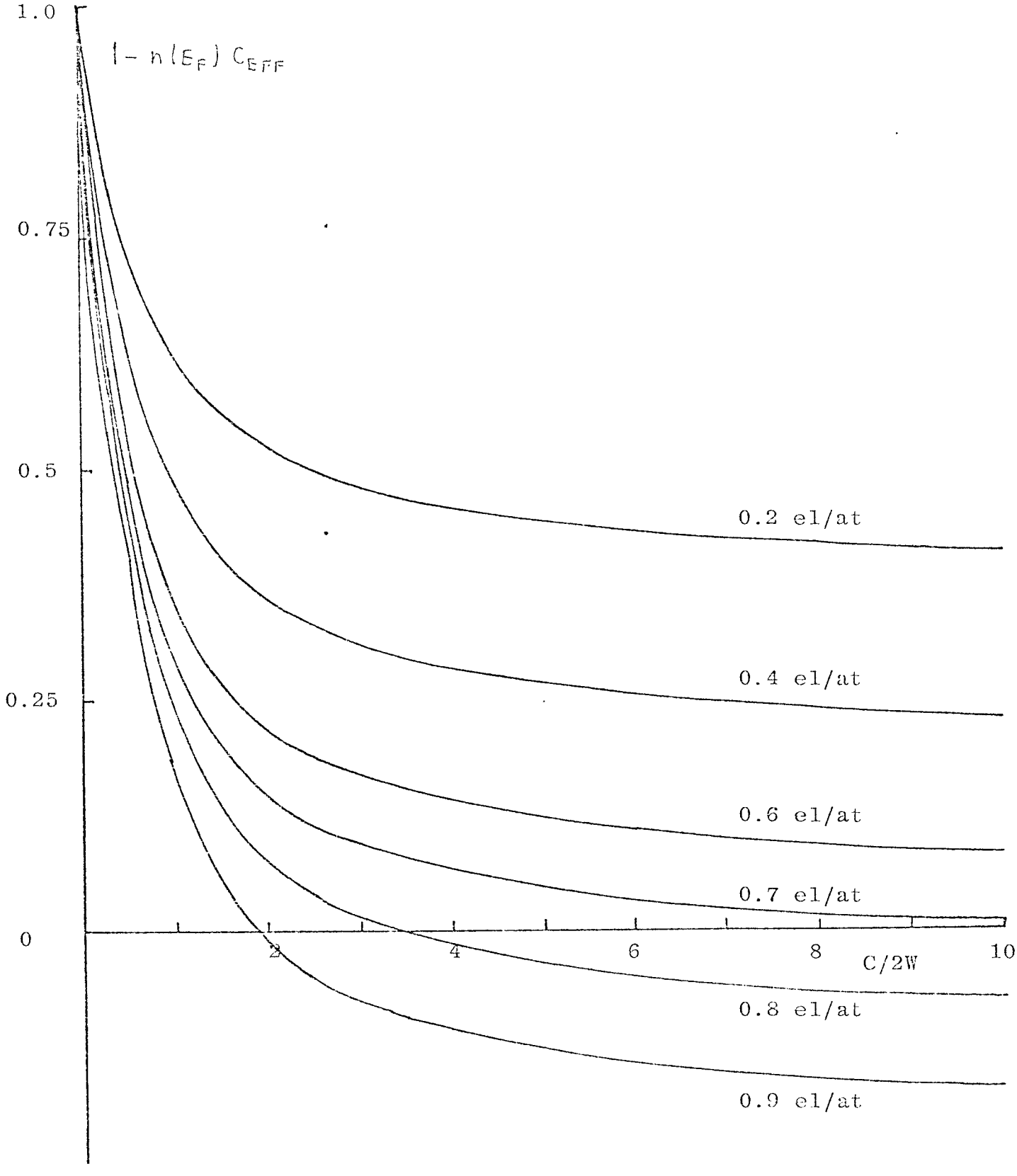

Figure 5.4. $1-n(E_f)C_{eff}$ versus C for the triangular density of states (5.36).

per atom in the band. Table 5.1 gives the maximum value of θ, θ_{MAX} , for which a ferromagnetic transition is possible for a given number of electrons per atom in the band.

Table 5.1 Values of θ_{MAX}

$\bar{n}$	0.1	0.2	0.3	0.4	0.5
θ_{MAX}	-0.83	-0.66	-0.50	-0.35	-0.21
$\bar{n}$	0.6	0.7	0.8	0.9	1.0
θ_{MAX}	-0.07	0.05	0.17	0.29	0.39

3. Double Triangular density of states

For this density of states given by (4.43),

$$E_f = W\left[\left(\frac{n}{2}\right)^{\frac{1}{2}} - 1\right] \qquad (5.41)$$

$$\bar{\epsilon} = \frac{W}{3}\left[(2n)^{\frac{1}{2}} - 3\right]$$

if $0 \leq \bar{n} \leq \frac{1}{2}$, whilst if $\frac{1}{2} \leq \bar{n} \leq 1$

$$E_F = -\frac{\upsilon}{\sqrt{2}}(1-n)^{1/2} \qquad (5.42)$$

$$\bar{\epsilon} = \frac{\upsilon}{6n}\left[2\sqrt{2}(1-n)^{3/2} - 3\right]$$

Thus, as $C \to \infty$

$$C_{EFF} \to \frac{-1}{(1-\bar{n}/2)^2}\left[\bar{n}\bar{\epsilon} + 2E_F(1-\bar{n}/2)\right] \qquad (5.43)$$

$$= \frac{\upsilon}{6(1-\bar{n}/2)^2}\left[\sqrt{2}\,n^{3/2} - 6\sqrt{2}\,n^{1/2} + 12\right] \quad 0 \leq \bar{n} \leq 1/2$$

$$= \frac{\upsilon}{6(1-\bar{n}/2)^2}\left[4\sqrt{2}(1-n)^{3/2} + 3\sqrt{2}\,\bar{n}(1-\bar{n})^{1/2} + 3\right] \quad \frac{1}{2} \leq \bar{n} \leq 1$$

So the non-magnetic state is unstable against spin alignment for sufficiently large C if

$$12\left(\frac{n}{2}\right)^{1/2} > 3 + 3n - \frac{n^2}{4} \qquad 0 \leq \bar{n} \leq \frac{1}{2}$$
$$3\left(\frac{1-n}{2}\right)^{1/2} > -1 + 2n - \frac{n^2}{4} \qquad \frac{1}{2} \leq \bar{n} \leq 1 \qquad (5.44)$$

that is, if $0.171 \lesssim \bar{n} \lesssim 0.915$. Thus ferromagnetism occurs for sufficiently large C if the Fermi level lies sufficiently close to the peak in the density of states.

4. Parabolic Density of States

For this density of states given by (2.32)

$$n = 2\int_{-\omega}^{E_F} n(E)\,dE = 1 + \frac{3E_F}{2\omega} - \frac{E_F^3}{2\omega^3}$$
$$n\bar{E} = 2\int_{-\omega}^{E_F} E\,n(E)\,dE = -\frac{3}{8\omega^2}\left(E_F^2 - \omega^2\right)^2 \qquad (5.45)$$

So the non-magnetic state is unstable against spin alignment for sufficiently large C if

$$-1 + 9\frac{E_F^2}{\omega^2} - 16\frac{E_F^3}{\omega^3} + 9\frac{E_F^4}{\omega^4} - \frac{E_F^6}{\omega^6} < 0 \qquad (5.46)$$

which is satisfied for $\frac{E_f}{W} \gtrsim -0.268$

Again, ferromagnetism is only possible when the Fermi level lies in the region of the maximum in the density of states.

It is clear from these examples that in order for the non-magnetic state to be unstable against ferromagnetic spin alignment for sufficiently large C a high density of states is required at the Fermi level. For the examples given however, the critical value of C at which ferromagnetism occurs is rather large as may be illustrated for the case of one electron per atom in the band. In this

case a transition to ferromagnetism will occur if

$$1 - Cn(E_f)\left[\frac{(1 - C/16\bar{\epsilon})}{(1 - C/8\bar{\epsilon})^2}\right] < 0 \qquad (5.47)$$

as may be seen from (5.30), from which it follows that the critical value of C, C_{CRIT}, at which a transition to ferromagnetism first occurs is given by

$$C_{CRIT} = 8\bar{\epsilon}\left[1 - \sqrt{\frac{4\bar{\epsilon}\, n(\epsilon_F)}{1 + 4\bar{\epsilon}\, n(\epsilon_F)}}\right] \qquad (5.48)$$

This is clearly not satisfied for real C for the rectangular density of states (5.10), whilst for the parabolic density of states (2.32) and the triangular density of states with $\theta = 0$, $C_{CRIT} = 6W$ and $^{8W}/_{3}$ respectively. On the other hand, a metal insulator transition occurs for $C = 3W$ for the parabolic density of states and for $C = {}^{8W}/_{3}$ for the triangular density of states with $\theta = 0$ for one electron per atom, and it is clear that for a transition to ferromagnetism to be possible before the metal insulator transition occurs a rather larger density of states is required at the Fermi level.

Consider, for example, the following density of states

$$n(E) = \begin{cases} \dfrac{y}{\omega}\dfrac{(1-\alpha)}{(2y-\alpha)} & -\omega < E < -\dfrac{\omega\alpha}{2y} \\ \dfrac{y}{\omega} & -\dfrac{\omega\alpha}{2y} < E < \dfrac{\omega\alpha}{2y} \\ \dfrac{y}{\omega}\dfrac{(1-\alpha)}{(2y-\alpha)} & \dfrac{\omega\alpha}{2y} < E < \omega \end{cases} \qquad (5.49)$$

illustrated in figure 5.5, and take the Fermi level to lie in the high density of states region. Then

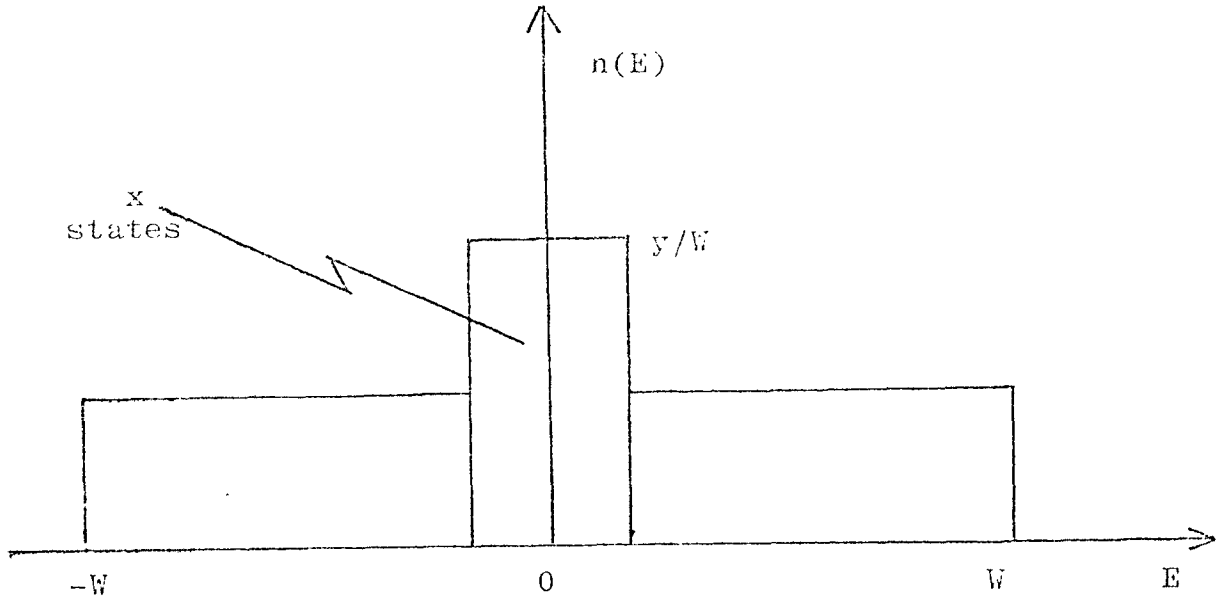

Figure 5.5. Density of states (5.49) assumed in the text.

$$E_f = \frac{W}{2y}(n-1)$$

$$n\bar{\epsilon} = \frac{W}{4y}\left[-x-2y+2xy+n^2-2n+1\right] \quad (5.50)$$

So from (5.23)

$$C_{eff} \to \frac{-W}{4y(1-n/2)^2}\left[-x-2y+2xy-n^2+4n-3\right] \text{ as } C \to \infty \quad (5.51)$$

So the non-magnetic state is unstable against ferromagnetism for sufficiently large C if

$$2y > 1 \quad (5.52)$$

From (5.48) the critical value of C at which ferromagnetism first occurs is given, for one electron/atom by

$$C_{CRIT} = \frac{2W}{y}\left[-x-2y+2xy\right]\left[1-\sqrt{\frac{-x-2y+2xy}{1-x-2y+2xy}}\right] \quad (5.53)$$

whilst the value of C at which a metal insulator transition occurs for one electron per atom is given by

$$C_o = \frac{2W}{y}\left[x+2y-2xy\right] \quad (5.54)$$

So a transition to ferromagnetism will occur before the metal insulator transition if

$$y > \frac{4-3x}{6(1-x)} \quad (5.55)$$

Ferromagnetism is thus favoured by a sharp peak in the density of states, that is by large y and small x.

5.3 Dependence of Energy upon Magnetisation

If $m \neq \mu$ minimisation of (4.21) by varying V_o gives

$$\frac{1}{\left[g(N,m,\mu,V_o)\right]^{1/2}}\frac{\partial g}{\partial V_o} = \left(N-2m-2\mu+4V_o\right) - \frac{C(N-m)(N-\mu)}{(N-\mu)\bar{\epsilon}_\uparrow + (N-m)\bar{\epsilon}_\downarrow} \quad (5.56)$$

Where $g(N,m,\mu,\nu_0) = (N-m-\mu+\nu_0)\,(m-\nu_0)(\mu-\nu_0)\nu_0$, which may be written in the form

$$\left[\frac{(\mu-\nu_0)(m-\nu_0)}{\nu_0(N-m-\mu+\nu_0)} - 1\right](N-m-\mu)^2 + \left[\frac{(N-m-\mu+\nu_0)\nu_0}{(m-\nu_0)(\mu-\nu_0)} - 1\right](m-\mu)^2$$

$$= -\frac{(N-m)(N-\mu)c}{(N-\mu)\bar{\epsilon}_\uparrow + (N-m)\bar{\epsilon}_\downarrow}\left[2(N-2m-2\mu+4\nu_0) - \frac{(N-m)(N-\mu)c}{(N-\mu)\bar{\epsilon}_\uparrow + (N-m)\bar{\epsilon}_\downarrow}\right] \quad (5.57)$$

For one electron per atom $m+\mu = N$ and zero magnetisation $m = \mu$ this is the situation discussed by Brinkman and Rice (1970) with solution (4.25), whilst if $m = \mu$ but $m+\mu \neq N$ we obtain the cubic equation (4.34) discussed in §4.3.

In §5.2 the Stoner parameter was not found to be strongly dependent upon the number of electrons per atom in the band, the important requirement for ferromagnetism being the existence of a high density of states at the Fermi level. In this section we shall investigate the dependence of the energy on the magnetisation in the presence of such a peak in the density of states for $m+\mu = N$, $m \neq \mu$ in which case (5.57) becomes

$$\left[\frac{\nu_0^2}{(m-\nu_0)(\mu-\nu_0)} - 1\right](m-\mu)^2 = \frac{m\mu c}{m\bar{\epsilon}_\uparrow + \mu\bar{\epsilon}_\downarrow}\left[2N - 8\nu_0 + \frac{m\mu c}{m\bar{\epsilon}_\uparrow + \mu\bar{\epsilon}_\downarrow}\right] \quad (5.58)$$

that is

$$4\bar{\nu}_0^3 - \left[5 + (1-\zeta^2)\frac{c}{8\bar{\epsilon}}\right]\bar{\nu}_0^2 + \left[1 + (1-\zeta^2) + (1-\zeta^2)\frac{c}{8\bar{\epsilon}} + \frac{2\bar{\epsilon}\zeta^2}{(1-\zeta^2)c}\right]\bar{\nu}_0 - \left[\frac{1}{4}(1-\zeta^2) + (1-\zeta^2)^2\frac{c}{32\bar{\epsilon}} + \frac{\bar{\epsilon}\zeta^2}{2c}\right] = 0 \quad (5.59)$$

where $n\bar{\epsilon} = m\bar{\epsilon}_\uparrow + \mu\bar{\epsilon}_\downarrow$, $\bar{V}_0 = V_0/N$ and $0 \leq \zeta^2 \leq 1$

Clearly, as $C \to 0$, $\bar{V}_0 \to \frac{1}{4}(1-\zeta^2)$ Whilst as $\zeta^2 \to 1$, $\bar{V}_0 \to 0$

If $\zeta^2 = 0$, (5.59) reduces to

$$\left(\frac{1}{2} - \bar{V}_0\right)^2 \left(4\bar{V}_0 - 1 - \frac{C}{8\bar{\epsilon}}\right) = 0 \qquad (5.60)$$

the root of interest being $\bar{V}_0 = \frac{1}{4}\left(1 + \frac{C}{8\bar{\epsilon}}\right)$

To obtain the solution in the limit $C \to 0$ to higher order we treat the non-dominant terms as known and re-arrange (5.59) into the recursive form

$$\bar{V}_0 = \frac{(1-\zeta^2)}{4} + \frac{(1-\zeta^2)C}{2\bar{\epsilon}\zeta^2}\left[\frac{1}{4}(1-\zeta^2) + (1-\zeta^2)^2\frac{C}{32\bar{\epsilon}}\right]$$
$$- \frac{(1-\zeta^2)C}{2\bar{\epsilon}\zeta^2}\left[1 + (1-\zeta^2) + (1-\zeta^2)\frac{C}{8\bar{\epsilon}}\right]\bar{V}_0 \qquad (5.61)$$
$$+ \frac{(1-\zeta^2)C}{2\bar{\epsilon}\zeta^2}\left[5 + (1-\zeta^2)\frac{C}{8\bar{\epsilon}}\right]\bar{V}_0^2 - \frac{2(1-\zeta^2)C}{\zeta^2\bar{\epsilon}}\bar{V}_0^3$$

from which we may generate better and better approximations by substituting the previous best approximation into the right hand side. Thus to first order in C

$$\bar{V}_0 = \frac{(1-\zeta^2)}{4}\left[1 + (1-\zeta^2)^2\frac{C}{8\bar{\epsilon}}\right] \qquad (5.62)$$

Thus, as in the non-magnetic case, the effect of correlations is to reduce the number of doubly occupied atoms in the ground state, but the effectiveness of correlation is reduced by the factor $(1-\zeta^2)^2$. Indeed, as $\zeta^2 \to 1$ correlation effects become ineffective in reducing the number of double occupancies. In the other limit, as $\zeta^2 \to 1$, we have to third order in $(1-\zeta^2)$

$$\nu_0 = \frac{(1-\zeta^2)}{4}\left[1 + \frac{(1-\zeta^2)^2}{\zeta^2}\,\frac{C}{8\bar{\epsilon}}\right] \tag{5.63}$$

If the correlation energy C is strong such that $\bar{\nu}_0$ is small, then

$$\bar{\nu}_0 \approx \frac{(1-\zeta^2)}{4}\,\frac{\left[1+\frac{(1-\zeta^2)}{\zeta^2}\frac{C}{2\bar{\epsilon}}\left\{1+(1-\zeta^2)\,\frac{C}{8\bar{\epsilon}}\right\}\right]}{\left[1+\frac{(1-\zeta^2)}{\zeta^2}\frac{C}{2\bar{\epsilon}}\left\{1+(1-\zeta^2)\left(1+\frac{C}{8\bar{\epsilon}}\right)\right\}\right]} \tag{5.64}$$

Thus if $\zeta^2 \neq 0$ the metal insulator transition occurs when

$$C = -4\bar{\epsilon}\,\frac{\left[1+(1-\zeta^2)^{1/2}\right]}{(1-\zeta^2)} \tag{5.65}$$

which is in agreement with (5.28) and (5.29) in the limit $\zeta^2 \to 0$. In general, we must solve the cubic equation (5.61). Defining quantities a_0, a_1 and a_2 by

$$\begin{aligned}
a_0 &= -\frac{1}{4}\left[\frac{1}{4}(1-\zeta^2) + (1-\zeta^2)^2\,\frac{C}{32\bar{\epsilon}} + \frac{\bar{\epsilon}\,\zeta^2}{2C}\right] \\
a_1 &= \frac{1}{4}\left[1 + (1-\zeta^2) + (1-\zeta^2)\,\frac{C}{8\bar{\epsilon}} + \frac{2\bar{\epsilon}\,\zeta^2}{(1-\zeta^2)C}\right] \\
a_2 &= -\frac{1}{4}\left[5 + (1-\zeta^2)\,\frac{C}{8\bar{\epsilon}}\right]
\end{aligned} \tag{5.66}$$

and making the substitution $\bar{\nu}_o = x - \frac{a_2}{3}$ we obtain the reduced equation $x^3 + px + q = 0$ where

$$p = a_1 - \frac{1}{3}a_2^2 \qquad q = \frac{2}{27}a_2^3 - \frac{1}{3}a_1a_2 + a_o \qquad (5.67)$$

The solution then proceeds according to equations (4.37) to (4.39). In particular, the quantity D in (4.38) which determines the nature of the solutions is given by

$$D = \frac{1}{(3)^3(128)^2}\left[27\frac{Co^2}{C^2}\zeta^8 - \left(122+66\frac{Co}{C} + 12\frac{Co^2}{C^2} + 4\frac{Co^3}{C^3}\right)\zeta^6 + \left(124\frac{C^2}{Co^2} + 164\frac{C}{Co} + 99 + 40\frac{Co}{C} + 8\frac{Co^2}{C^2}\right)\zeta^4 - \left(16\frac{C^4}{Co^4} + 64\frac{C^3}{Co^3} + 100\frac{C^2}{Co^2} + 76\frac{C}{Co} + 28 + 4\frac{Co}{C}\right)\zeta^2\right] \qquad (5.68)$$

where $C_o = \frac{-8\bar{\epsilon}}{(1-\zeta^2)}$ is positive. If $\zeta^2 = 0$ then all roots are real and at least two are equal in agreement with (5.66). D is negative over most of the physical domain, and because of the complexity of its behaviour it is necessary to follow the roots numerically. The complexity of the behaviour of D is illustrated in Table 5.2 which gives the coefficients of powers of C/C_o occurring in D.

Table 5.2 Terms in D.

Power of C/C_o	Coefficient	Sign
4	$-16\zeta^2$	- ve
3	$-64\zeta^2$	- ve
2	$-100\zeta^2 + 124\zeta^4$	-ve if $\zeta^2 < 100/124$
		+ve if $\zeta^2 > 100/124$
1	$-76\zeta^2 + 164\zeta^4$	-ve if $\zeta^2 < 76/164$
		+ ve if $\zeta^2 > 76/164$
0	$-28\zeta^2+99\zeta^4-112\zeta^6$	- ve
-1	$-4\zeta^2+40\zeta^4-66\zeta^6$	-ve if $\zeta^2 >$ a or $<$ b
		+ ve if b $< \zeta^2 <$ a
		$a = \frac{40+4\sqrt{34}}{132}$, $b = \frac{40-4\sqrt{34}}{132}$
-2	$8\zeta^4 - 12\zeta^6 + 27\zeta^8$	+ ve
-3	$-4\zeta^6$	- ve

We have solved equation (5.59) for $\bar{\nu}_o$ for the density of states (5.49) illustrated in figure 5.5 for which

$$
\begin{aligned}
E_{F\uparrow} &= \frac{\omega\zeta}{2y} \\
E_{F\downarrow} &= -\frac{\omega\zeta}{2y} \\
m\bar{\epsilon}_\uparrow + \mu\bar{\epsilon}_\downarrow &= \frac{\omega}{4y}\left[\zeta^2 - \alpha - 2y + 2\alpha y\right]
\end{aligned}
\qquad (5.69)
$$

if $\bar{m} + \bar{\mu} = 1, \zeta \leq \alpha$; whilst if $\zeta \geq \alpha$

$$
\begin{aligned}
E_{F\uparrow} &= \frac{\omega}{2y(1-\alpha)}\left[\alpha(1-2y) + (2y-\alpha)\zeta\right] \\
E_{F\downarrow} &= -\frac{\omega}{2y(1-\alpha)}\left[\alpha(1-2y) + (2y-\alpha)\zeta\right] \\
m\bar{\epsilon}_\uparrow + \mu\bar{\epsilon}_\downarrow &= \frac{y}{\omega}\frac{(1-\alpha)}{(2y-\alpha)}\left(E_F^2 - \omega^2\right)
\end{aligned}
\qquad (5.70)
$$

A transition to a ferromagnetic state will occur before the metal insulator transition, as C is increased, if (5.55) is satisfied, which occurs in the region of the xy plane shown in figure 5.6. Table 5.3 gives the volume of C for given x and y at which a transition to ferromagnetism first occurs, a blank in the table indicating that a metal insulator transition occurs first.

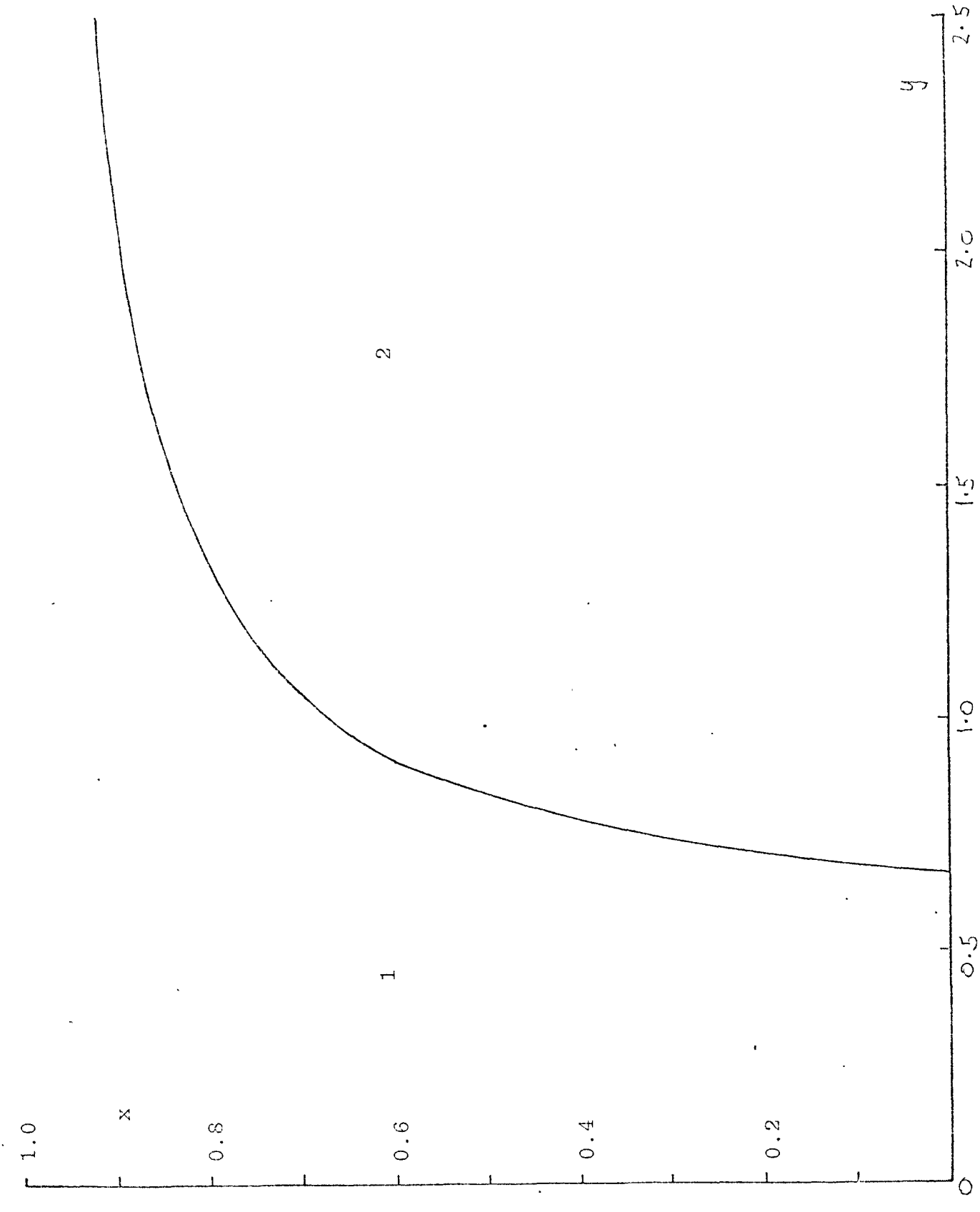

Figure 5.6. Density of states (5.49). In region 2 a transition to a ferromagnetic state occurs before the metal insulator transition as C is increased, whilst in region 1 the metal insulator transition occurs first.

Table 5.3 Value of $C/2W$ at which a transition to ferromagnetism first occurs for the density of states(5.49) & $\bar{m}+\bar{\mu} = 1$.

	y			
x	1	2	4	8
0.1	0.861	0.316	0.140	0.066
0.2	0.900	0.323	0.141	0.066
0.3	0.949	0.333	0.144	0.067
0.4	1.013	0.346	0.147	0.068
0.5	1.098	0.364	0.151	0.069
0.6	1.219	0.389	0.157	0.070
0.7		0.430	0.167	0.073
0.8		0.506	0.186	0.077
0.9			0.237	0.091

It is seen that for a given value of y, the value of $C/2W$ at which a ferromagnetic transition first occurs is lowest for a small value of x, that is if the high density of states region contains only a small number of states. The dependence of C_{CRIT} on x is, however, rather weak, particularly for large y, and the most important factor governing the appearance of a ferromagnetic transition is seen to be the density of states at the Fermi level.

Figures 5.7, 5.8, 5.9 and 5.10 show the dependence of the ground state energy on the magnetisation for the cases $x = 0.25$, $y = 2$; $x = 0.25$, $y = 4$; $x = 0.5$, $y = 2$ and $x = 0.5$, $y = 4$ respectively. It is seen that although the value of $C/2W$ at which the non-magnetic state becomes unstable, with respect to spin alignment, for a given value of y, is smallest for a small value of x, the magnetisation $\bar{\zeta}$ and the relative energy of magnetisation $(E_{\bar{\zeta}} - E_0)/E_0$

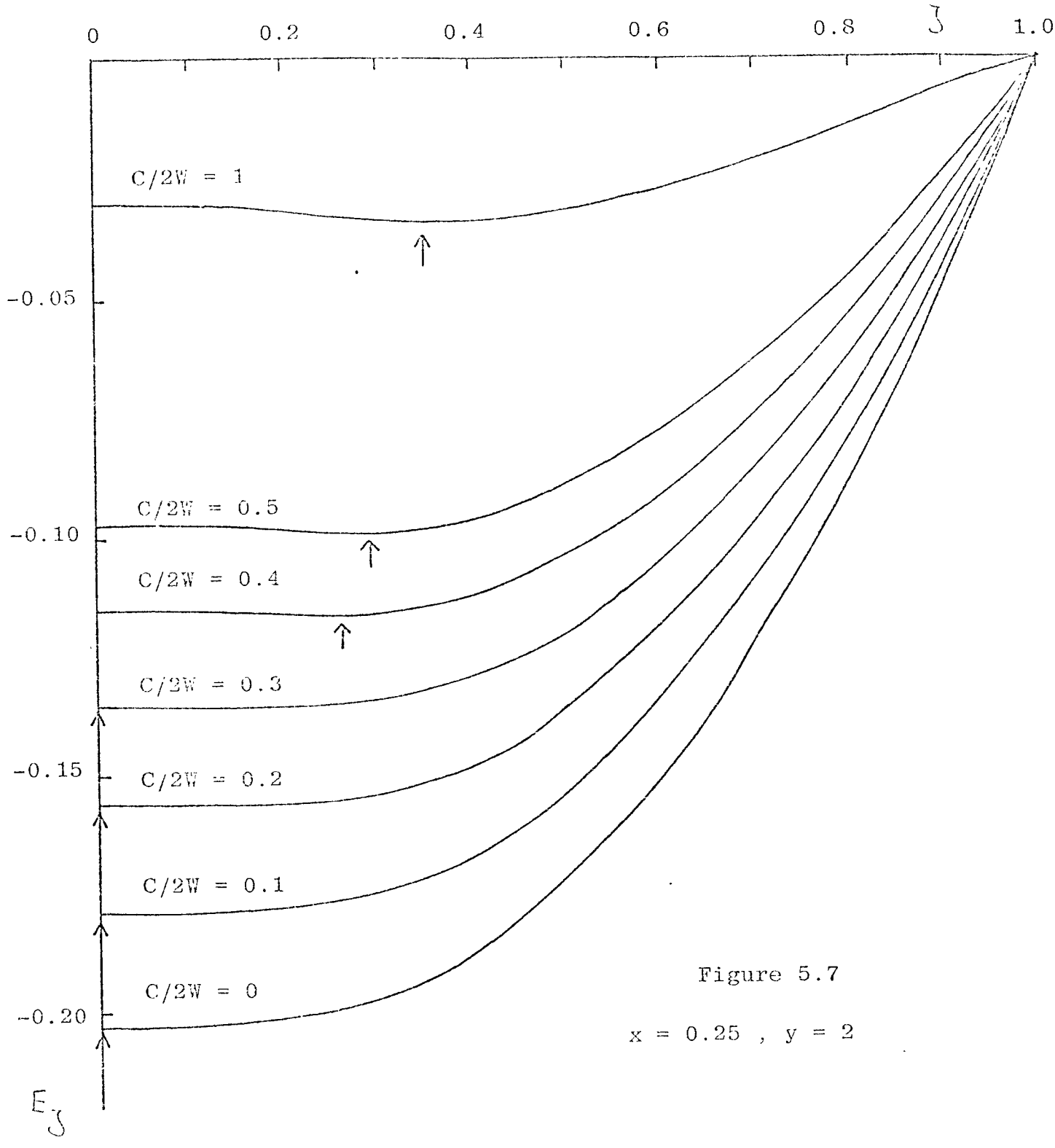

Figure 5.7

x = 0.25 , y = 2

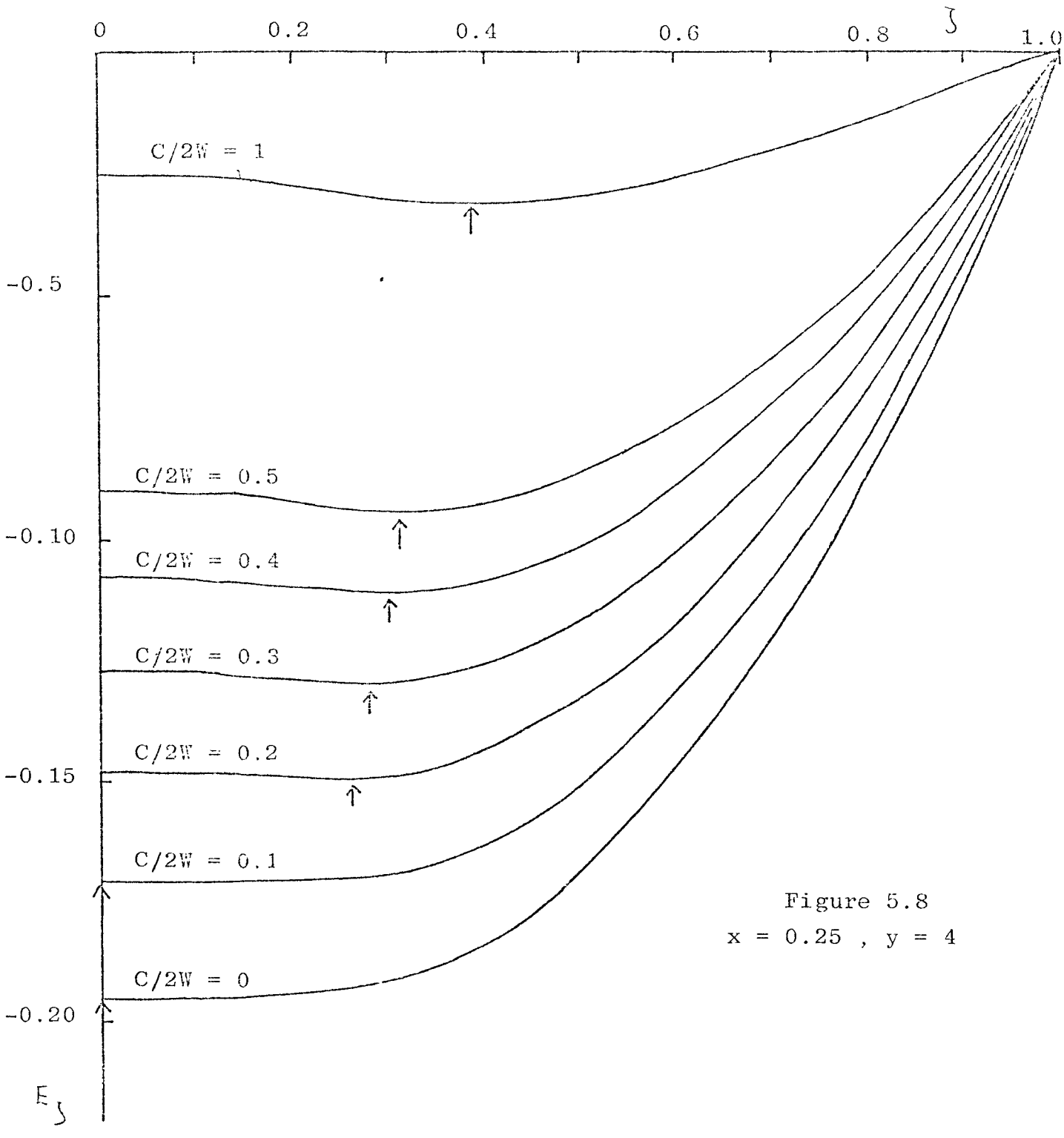

Figure 5.8
x = 0.25 , y = 4

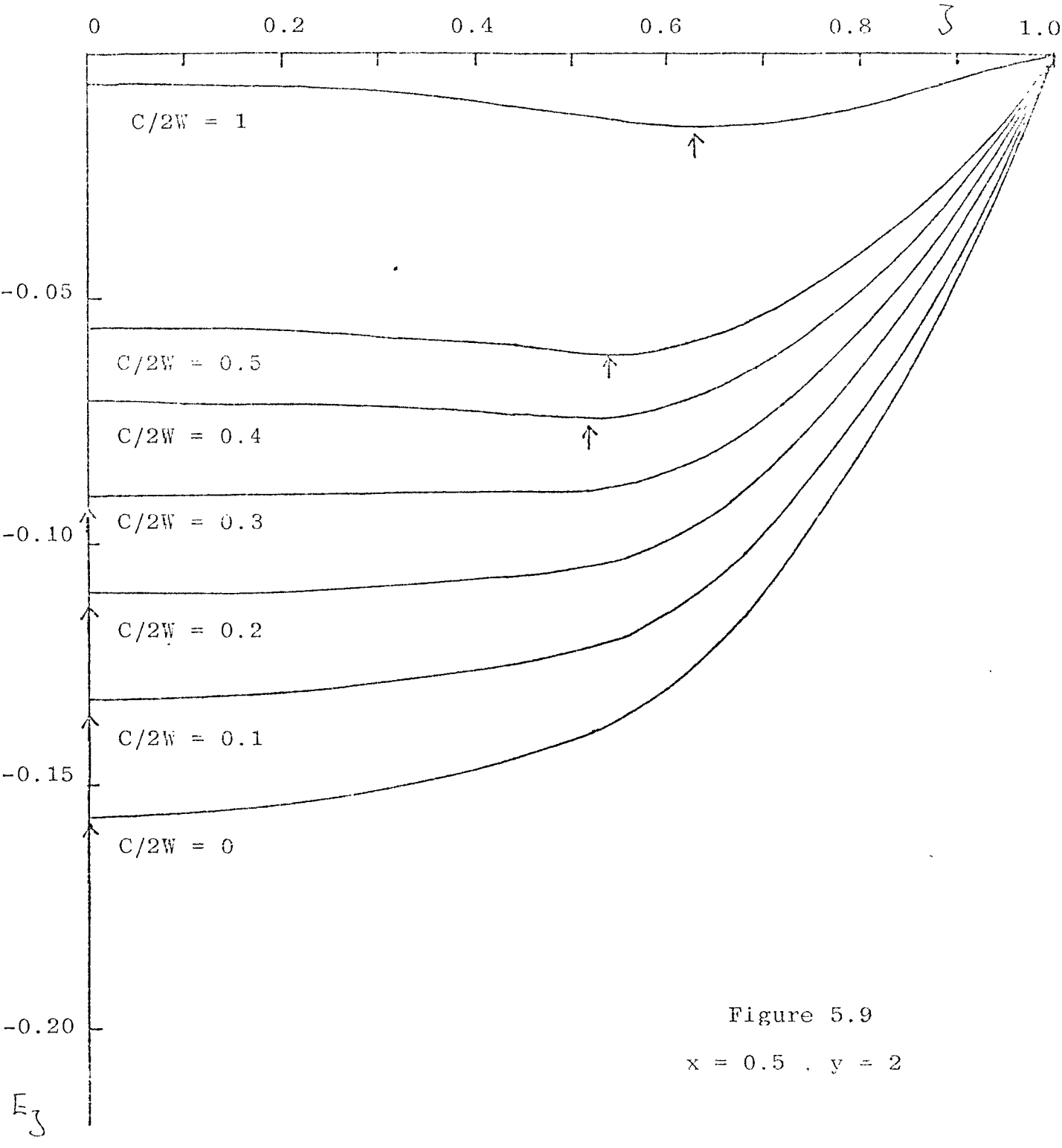

Figure 5.9

x = 0.5 , y = 2

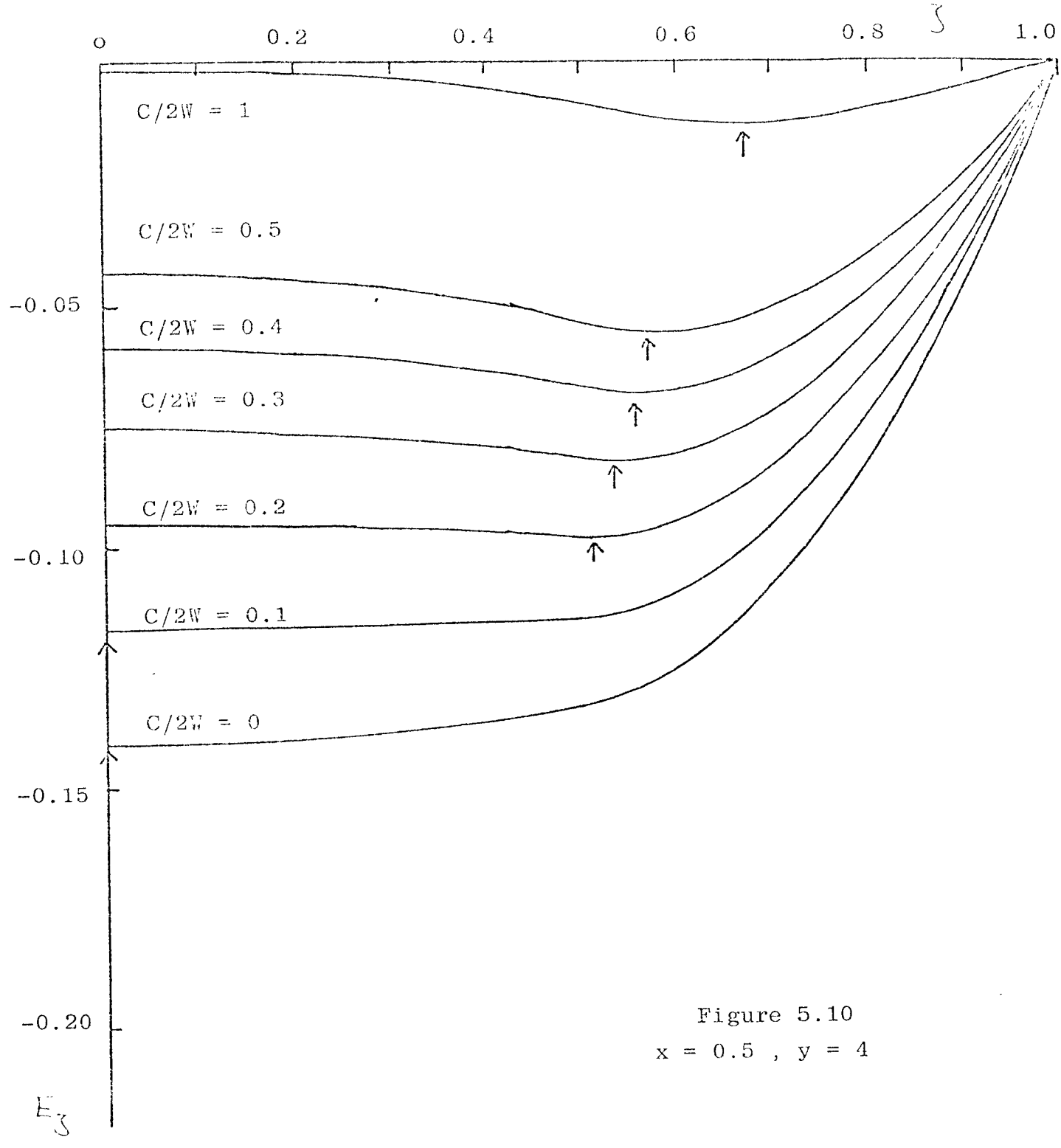

Figure 5.10

x = 0.5 , y = 4

increase with increasing x provided that $C/2W$ is large enough to cause a transition to a partially aligned state. Values of $\bar{\zeta}$ and $(E_{\bar{\zeta}} - E_o)/E_o$ are given in Table 5.4, where E_o is the energy of the non-magnetic state.

Table 5.4 Values of $\bar{\zeta}$ and $(E_{\bar{\zeta}} - E_o)/E_o$

	$\bar{\zeta}$				$(E_{\bar{\zeta}} - E_o)/E_o$			
	x = 0.25	0.25	0.5	0.5	0.25	0.25	0.5	0.5
	y = 2	4	2	4	2	4	2	4
$C/2W$								
0.1	0	0	0	0	0	0	0	0
0.2	0	0.26	0	0.51	0	0.005	0	0.025
0.3	0	0.28	0	0.53	0	0.014	0	0.084
0.4	0.26	0.30	0.52	0.56	0.006	0.026	0.025	0.162
0.5	0.29	0.31	0.54	0.58	0.015	0.041	0.080	0.272
1.0	0.35	0.39	0.63	0.67	0.122	0.223	1.301	5.971

The relative energy of magnetisation is seen to be small in agreement with the observed Curie temperatures of Fe, Ni and Co which are well below the melting points and boiling points as seen in Table 5.5.

Table 5.5 Observed values of the Curie temperature T_C, the melting point T_M and the boiling point T_B (^oK)

	T_C	T_M	T_{C/T_M}	T_B	T_{C/T_B}
Fe	1040	1808	0.58	3160	0.33
Co	1400	1765	0.79	3229	0.43
Ni	631	1726	0.37	3055	0.21

It is seen in figures 5.7 to 5.10 that the magnetisation of the lowest energy state is not strongly dependent upon the strength of the interaction provided that this is sufficient to cause a transition to a partially aligned state, the most important influence being the density of states in the region of the Fermi level. When the interaction becomes strong enough to cause a ferromagnetic transition, the Fermi level is seen to move up in energy to a position just above the top of the high density of states region for majority spin electrons, and just below for minority spins. A similar behaviour is expected in the case of the five band case of the transition metals with arbitary number of electrons per atom, although intra-atomic exchange will of course be an additional important factor in stabilising the ferromagnetic state. In Ni, it is well known from band structure calculations that there is a sharp peak in the density of states at the Fermi level. Since the number of holes in the d band of Ni is small, strong ferromagnetism is possible despite the narrowness of this peak. In iron, however, with 2.9 holes per atom in the d band, it is unlikely that a peak of sufficient width for strong ferromagnetism will occur at the Fermi level, and this would appear to explain why iron is a weak ferromagnet despite the strong stabilising influence of intra-atomic exchange.

It is interesting to enquire why Pd and Pt, which are also known to have a narrow peak in the density of states at the Fermi level, are non-magnetic, whilst Ni is a strong ferromagnet. It is possible that this peak is

significantly lower for Pd and Pt than for Ni. Thus Pt has a specific heat of 6.5 ± 0.03 mJ/mole$^{o}K^{2}$ (Shoemake and Rayne, 1968) whilst Ni has an electronic specific heat of 7.02 ± 0.06mJ/mole$^{o}K^{2}$ (Rayne and Kemp, 1956). On the other hand Pd has an electronic specific heat of 9.42 ± 0.02mJ/mole$^{o}K^{2}$ (Veal and Rayne, 1964) which is larger than that of Ni. We should, however, compare the specific heat of Pd and Pt not with that of real ferromagnetic Ni, but with that of the non-magnetic state, since figures 5.7 to 5.10 show that when the electron interaction is strong enough to form a ferromagnetic state, the Fermi level moves away from the high density of states region. Hodges et al.(1966) have calculated the total density of states at the Fermi level in both the ferromagnetic and non-magnetic state, and multiplying the experimental value of the electronic specific heat of ferromagnetic Ni by the ratio of $N(E_F)$ for the paramagnetic and ferromagnetic state, gives a value of about 14.8mJ/mole$^{o}K^{2}$ suggesting that indeed the density of states at the Fermi level is larger for Ni than for Pd and Pt. Hodges et al. (1966) investigated the effect of spin orbit coupling on the density of states at the Fermi level by calculating the band structure with the potential kept at the value appropriate for paramagnetic Ni, but using the spin orbit coupling strength appropriate for atomic Ni, Pd and Pt. This procedure permits the isolation of the effects of spin orbit interaction from those resulting from the widening of the band in the series Ni, Pd, Pt. It was found that spin orbit coupling reduced $n(E_f)$ for Pt by only 16%, whereas $n(E_f)$ deduced from the specific heat is down by 50% from that of para-

magnetic nickel. It seems, therefore, that the decrease in the height of this peak in the series Ni, Pd, Pt arises from the greater overlap of d states on neighbouring atoms.

5.4 Discussion and Comparison with Kanamori's theory

We have calculated the Stoner parameter in Gutzwiller's theory in §5.2. The result is given by equation (5.35) and is illustrated for several values of $\bar{n}$, the number of electrons per atom in the band, in figures 5.2 and 5.3 for the rectangular density of states and for the triangular density of states with $\theta = 0$ respectively. For large C, the Stoner parameter C_{eff} is reduced to a value of the order of the bandwidth, whilst as $C \to 0$, $C_{eff} \to 0$.

The dependence of C_{eff} on C is in qualitative agreement with that of the effective interaction, C_{HF}, between opposite spin electrons in the non-magnetic state, obtained in §5.1 by comparing the energy of the non-magnetic ground state in Gutzwiller's theory with that in the Hartree-Fock approximation. As $\bar{n} \to 0$ the agreement is quantitatively good, but as $\bar{n} \to 1$, $C_{HF}-C_{eff}$ increases in magnitude, C_{HF} being greater than C_{eff}. Consequently, the approximation of replacing the bare interaction C in the Stoner criterion, derived in the Hartree-Fock approximation, by the effective interaction in the non-magnetic state overestimates the tendency to ferromagnetism, particularly as $\bar{n} \to 1$.

It is interesting to compare these results with those of Kanamori (1963), who used Brueckner's theory of nuclear matter to treat correlation effects in the limit

$\bar{n} \to 0$ (Brueckner, 1955, Wada and Brueckner, 1956). In the simplest Brueckner approximation the total energy is written as the Hartree-Fock energy with the bare interaction C replaced by the sum of ladder diagrams. Galitski (1958) has shown that this is exact in the limit $\bar{n} \to 0$. Following Kanamori (1963) therefore, the effective interaction between electrons of opposite spin is, in this limit, given by

$$C_{\text{Kanamori}} = \frac{C}{1 + C g(\underset{\sim}{k}, \underset{\sim}{k}')} \tag{5.71}$$

where $$g(\underset{\sim}{k}, \underset{\sim}{k}') = \frac{1}{N} \sum_{q} \frac{(1 - \bar{n}_{\underset{\sim}{k}+\underset{\sim}{q}\uparrow})(1 - \bar{n}_{\underset{\sim}{k}'-\underset{\sim}{q}\downarrow})}{E_{\underset{\sim}{k}+\underset{\sim}{q}\uparrow} + E_{\underset{\sim}{k}'-\underset{\sim}{q}\downarrow} - E_{\underset{\sim}{k}\uparrow} - E_{\underset{\sim}{k}'\downarrow}} \tag{5.72}$$

Kanamori (1963) introduced the further approximation of replacing $g(\underline{k}, \underline{k}')$ by its value g(o,o) when $\underline{k}=\underline{k}'$ = the wavevector of the lowest energy state in the band, and evaluated g(o,o) for the non-magnetic state. If this wavevector is at a point of inversion symmetry $E_{\underline{k}+\underline{q}} = E_{\underline{k}'-\underline{q}}$, (5.70) becoming

$$g(o,o) \simeq \frac{1}{Z} \int_{E>E_f} \frac{n(E)dE}{E} \tag{5.73}$$

where E is measured from the bottom of the band. In the limit $\bar{n} \to 0$ this is just the Hilbert transform of the density of states and the result (5.71) can be understood in Koster-Slater theory as the treatment of the correlation of two electrons, neglecting all others, such that one of the electrons is assumed to be fixed on an atom for the purposes of studying the motion of the other. The problem is then reduced to that of an electron moving in a narrow band and scattered by a large atomic repulsive potential C (Friedel, 1969).

The approximation of using the value of $g(\underline{k},\underline{k}')$ at the band edge will overestimate the tendency to ferromagnetism since it would be better to use a $g(\underline{k},\underline{k}')$ for $\underline{k}$ and $\underline{k}'$ on the Fermi surface, for which the energy denominator in (5.72) would be smaller. Further, we have seen that the effective interaction energy between electrons in the non-magnetic ground state C_{HF} overestimates the Stoner parameter C_{eff} especially as $\bar{n} \to 1$, and so the approximation of using the value of $C_{Kanamori}$ evaluated in the non-magnetic state will overestimate the tendency to ferromagnetism.

$$C^{o}_{Kanamori} = \frac{C}{1 + Cg(o,0)} \qquad (5.74)$$

is easily evaluated for the model densities of states considered in §5.2. Thus for the triangular density of states (5.36), for example, with $\theta = 0$.

$$2Wg(o,o) \equiv W \int_{E_f}^{2W} \frac{n(E)dE}{E} = 2\ln 2 - n^{\frac{1}{2}} \qquad (5.75)$$

Figure 5.11 shows the variation of $C^{o}_{Kanamori}$ with C for various values of $\bar{n}$, whilst Figure 5.12 shows the variation of $1 - n(E_f)\, C^{o}_{Kanamori}$ versus C. Comparing figures 5.11 and 5.12 with 5.4 and 5.5 the behaviour is seen to be much the same as in Gutzwiller's approximation, but as $\bar{n} \to 1$ Kanamori's theory is seen to lead to ferromagnetism for much smaller values of $C/2W$ than in Gutzwiller's model. This is just what we expect from the above discussion and is illustrated more clearly in figure 5.13 which illustrates the behaviour of $C^{o}_{Kanamori}$ and $C^{Gutzwiller}_{eff}$ in the limit $C \to \infty$ as a function of $\bar{n}$.

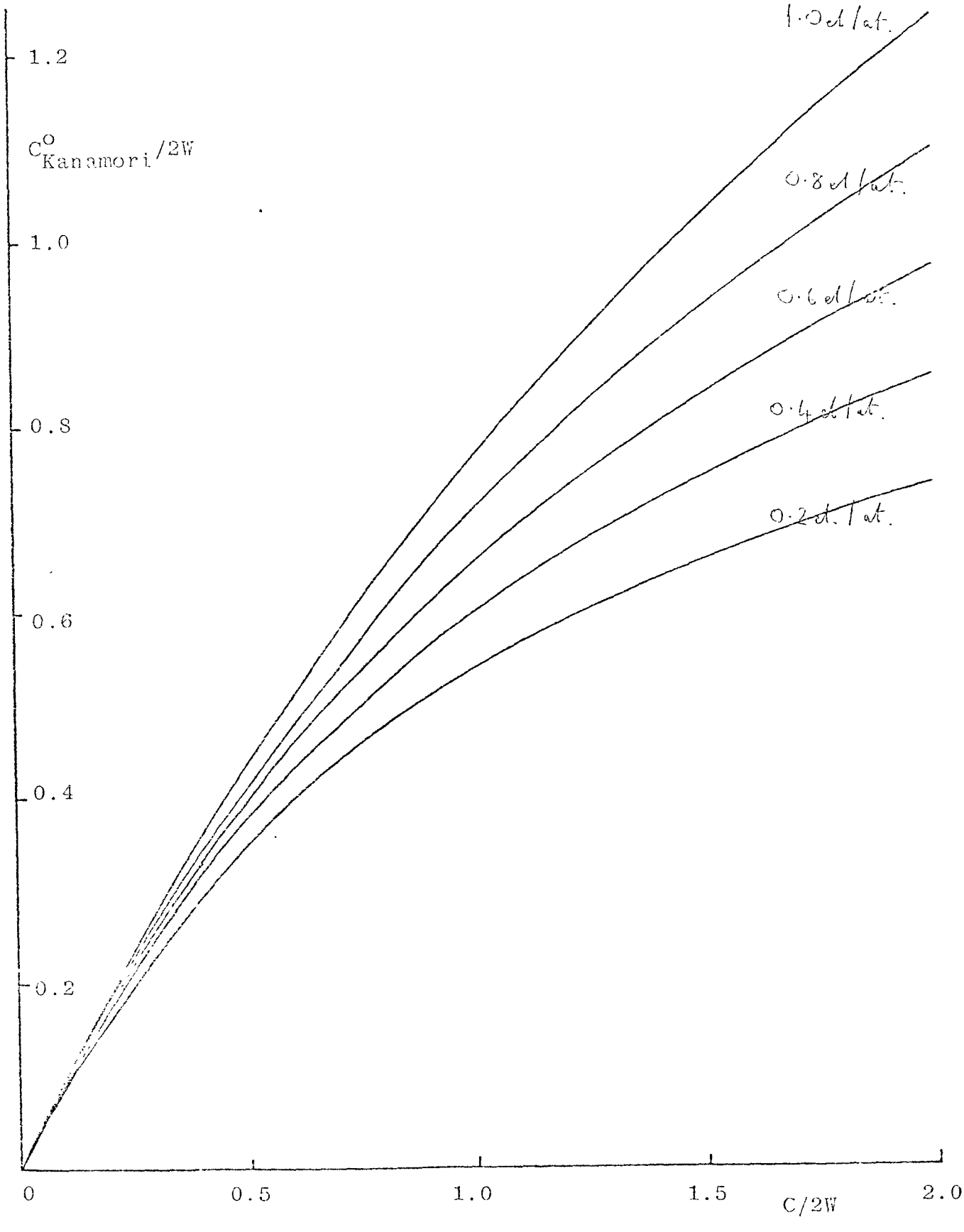

Figure 5.11. $C^{O}_{Kanamori}$ versus C for the triangular density of states (5.36).

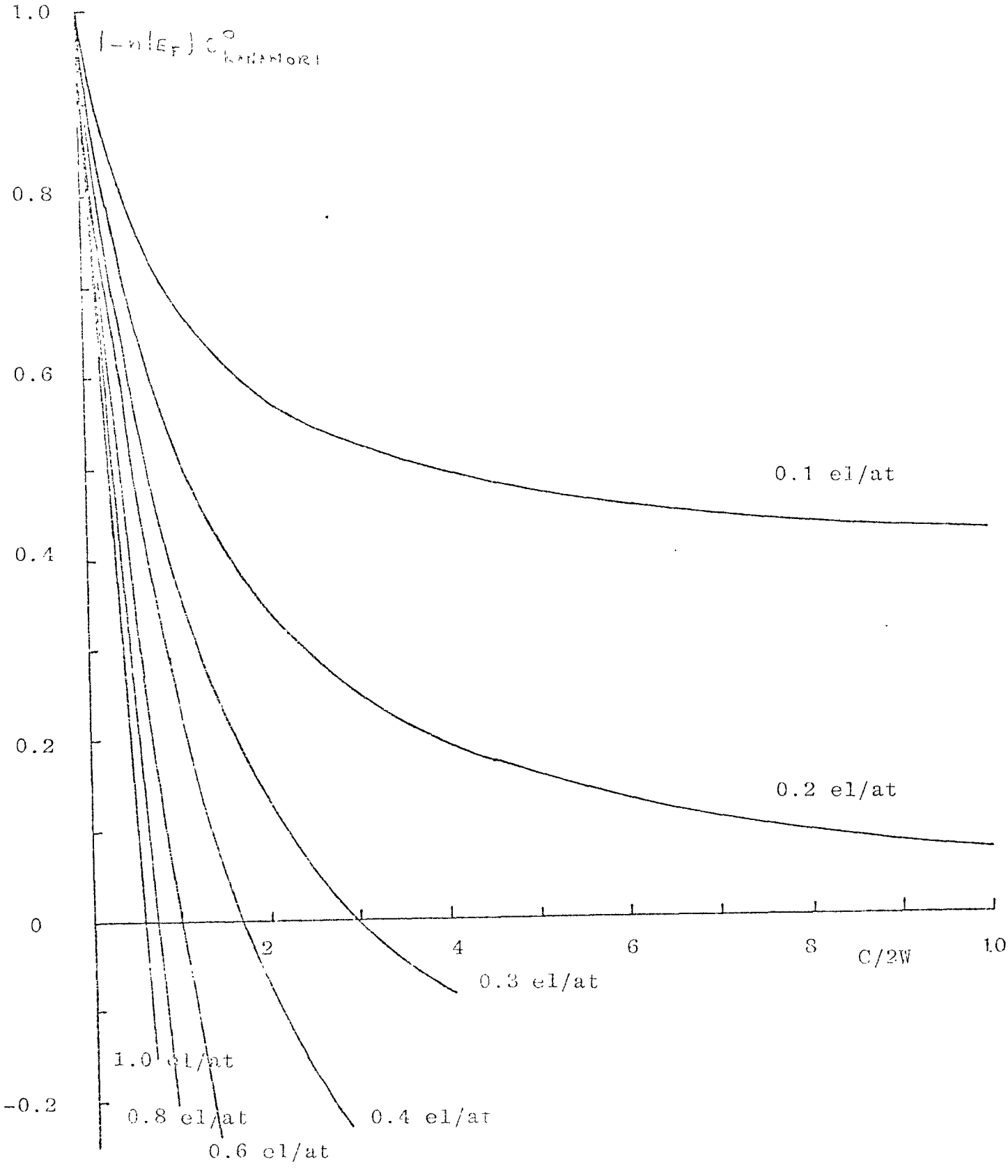

Figure 5.12. $1 - n(E_f)\ C^{o}_{Kanamori}$ versus C for the triangular density of states.

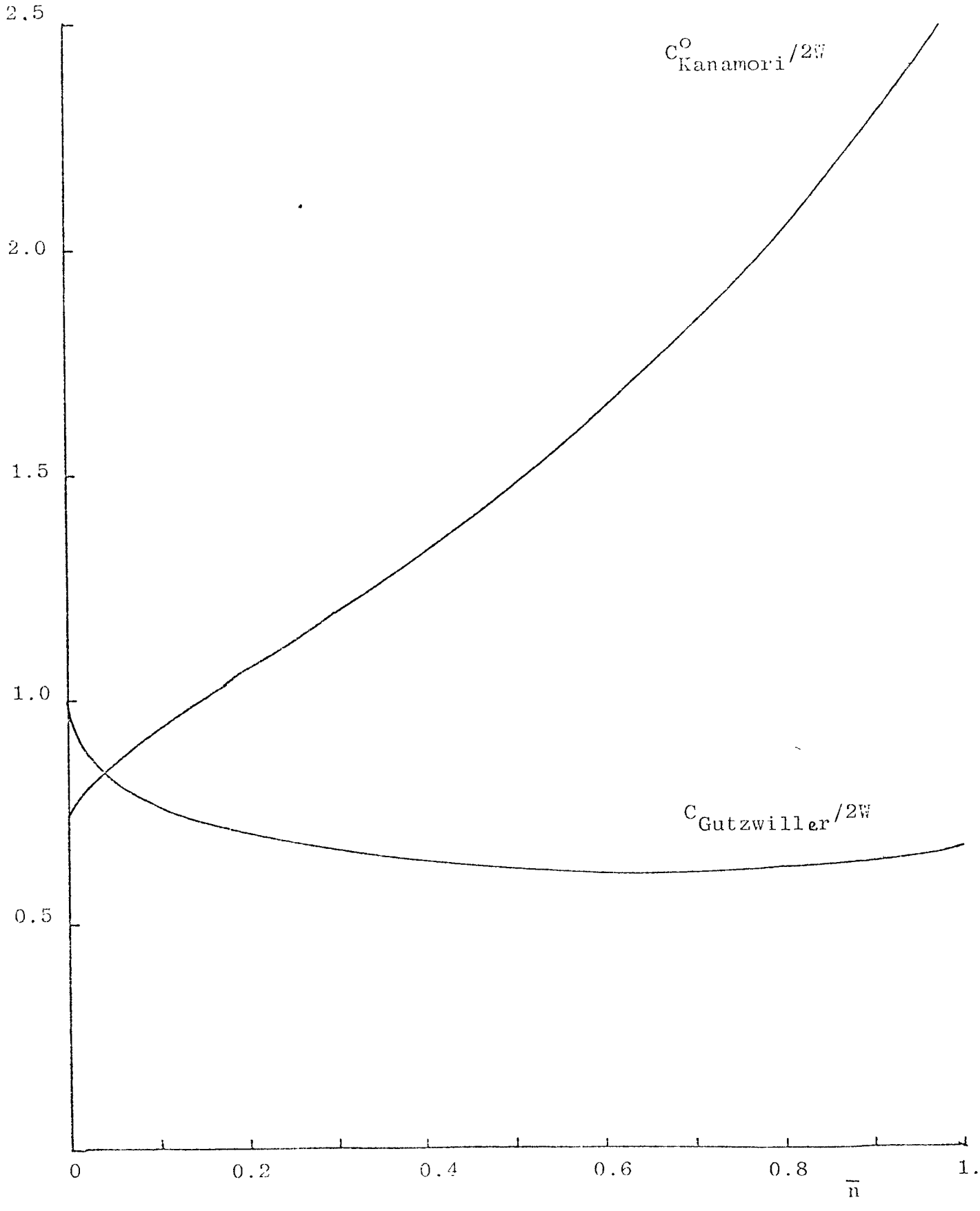

Figure 5.13. Variation of $C_{Gutzwiller}/2W$ and $C_{Kanamori}$ with $\bar{n}$ in the limit $C = \infty$ for the triangular density of states with $\Theta = 0$.

Gutzwiller (1965) was able to prove that $n_{\underline{k}}$ given by (4.21) is exact in the limit $C \to \infty$ inside the Fermi surface, but could not prove this for $E > E_f$. It seems, therefore, that Gutzwiller's theory, if not exact, in this limit, will overestimate the energy of the non-magnetic state. On the other hand, in the approximation in which inter-atomic correlations are neglected, the ferromagnetic state is an exact eigenstate of the Hamiltonian. It appears from figure 5.13, therefore, that Gutzwiller's model offers a better description of the correlated ground state than does Kanamori's for this density of states if $\bar{n} \gtrsim 0.035$.

Appendix A Extension of Hohenberg-Kohn theorem to the spin dependent case (Stoddart and March, 1971, von Barth and Hedin, 1972)

Consider a Hamiltonian written in second quantisation as

$$H = \sum_{\sigma} \int \psi_{\sigma}^{\dagger}(\underline{r}) \left(\frac{p^2}{2m} \right) \psi_{\sigma}(\underline{r}) \, d\underline{r} + \frac{1}{2} \sum_{\sigma\sigma'} \psi_{\sigma}^{\dagger}(\underline{r}) \psi_{\sigma'}^{\dagger}(\underline{r}') \frac{e^2}{|\underline{r}-\underline{r}'|} \psi_{\sigma'}(\underline{r}') \psi_{\sigma}(\underline{r}) \, d\underline{r} \, d\underline{r}' + \sum_{\sigma} \int \psi_{\sigma}^{\dagger}(\underline{r}) V_{\sigma}(\underline{r}) \psi_{\sigma}(\underline{r}) \, d\underline{r} \tag{A.1}$$

The expectation value of H in the ground state is

$$E = T + U + \sum_{\sigma} \int V_{\sigma}(\underline{r}) \rho_{\sigma}(\underline{r}) \, d\underline{r} \tag{A.2}$$

where T and U are the expectation values of the kinetic and interaction energy and where

$$\rho_{\sigma}(r) = \langle \underline{\Psi} | \psi_{\sigma}^{\dagger}(\underline{r}) \psi_{\sigma}(\underline{r}) | \underline{\Psi} \rangle \tag{A.3}$$

Let us assume there exist two different ground states $\underline{\Psi}$ and $\underline{\Psi}'$, corresponding to Hamiltonians H and H′ with potentials V and V′ in (A.1), which both give the same density ρ_{σ}. Owing to the assumed non-degeneracy of the ground state and the minimal property of the expectation value of the Hamiltonian with respect to variations in the wavefunction we have the inequality

$$\langle \underline{\Psi} | H | \underline{\Psi} \rangle < \langle \underline{\Psi}' | H | \underline{\Psi}' \rangle = \langle \underline{\Psi}' | H' | \underline{\Psi}' \rangle + \langle \underline{\Psi}' | H - H' | \underline{\Psi}' \rangle \tag{A.4}$$

or

$$E < E' + \sum_{\sigma} [V_{\sigma}(\underline{r}) - V_{\sigma}'(\underline{r})] \rho_{\sigma}(\underline{r}) \, d\underline{r} \tag{A.5}$$

Similiarly we have

$$E' < E + \sum_{\sigma} [V_{\sigma}'(\underline{r}) - V_{\sigma}(\underline{r})] \rho_{\sigma}(\underline{r}) \, d\underline{r} \tag{A.6}$$

and adding (A.5) and (A.6) gives

$$E + E' < E + E' \tag{A.7}$$

which is impossible, so the starting assumption that $\underline{\Psi}$ and $\underline{\Psi}'$ are different is false. Thus the ground state wavefunction and hence all ground state properties such as the total energy are functionals of the spin density.

Equation (A.2) assumes its minimum value for the correct $\rho_\sigma(\underline{r})$ if the admissible functions are restricted by the condition

$$n = \sum_\sigma \int \rho_\sigma(\underline{r})\, d\underline{r} \qquad (A.8)$$

where n is the total number of electrons, since a change in ρ_σ from the correct spin density corresponds to a change in the wavefunction from the ground state wavefunction, and consequently by the variational principle to a higher energy.

Appendix B Calculation of the density matrix in the quasi-chemical approximation (Gutzwiller, 1965)

In order to give the weighting factor η^{ν} in (4.14) a well defined meaning Gutzwiller (1965) assumed that configurations with different values of ν have the same average weight apart from the factor η^{ν} so that

$$\rho_{n\uparrow}(h_1 \cdots h_n, f_1 \cdots f_n) \equiv \langle \Psi_c | a^{\dagger}_{h_1\uparrow} \cdots a^{\dagger}_{h_n\uparrow} a_{f_n\uparrow} \cdots a_{f_1\uparrow} | \Psi_c \rangle$$
$$= \text{const} \left(P_f(i-j) \middle| \begin{matrix} h_1 \cdots h_n \\ f_1 \cdots f_n \end{matrix} \right) \qquad \text{(B.1)}$$

with $P_f(i-j)$ given by (4.16) and where the constant in (B.1) is taken as proportional to the number of all possible configurations of $\downarrow$ spin electrons with weight $\eta^{\nu+\nu'}$ where η is the variational parameter in (4.14), ν is the number of doubly occupied sites in $h_1 \cdots h_m$ in each configuration and ν' the number in $f_1 \cdots f_m$ where m is the number of $\uparrow$ spin electrons. Thus the coefficient of the diagonal density matrix with $h_1 = f_1, h_2 = f_2, \ldots, h_n = f_n$ is taken as

$$C_0 \sum_{\nu} \eta^{2\nu} \binom{m}{\nu} \binom{N-m}{\mu-\nu} \qquad \text{(B.2)}$$

where μ is the number of $\downarrow$ spin electrons, $m-\nu$ and $\mu-\nu$ the number of 'dissociated' spin $\uparrow$ and spin $\downarrow$ electrons and $N - m - \mu + \nu$ is the number of empty lattice sites. Similarly if $h_1 \neq f_1, h_2 = f_2 \ldots h_n = f_n$ the coefficient is taken as

$$C_0 \sum_{\nu} \left[\eta^{2(\nu+1)} \binom{m-1}{\nu} \binom{N-m-2}{\mu-\nu-2} \right.$$
$$\left. + 2\eta^{2\nu+1} \binom{m-1}{\nu} \binom{N-m-2}{\mu-\nu-1} + \eta^{2\nu} \binom{m-1}{\nu} \binom{N-m-2}{\mu-\nu} \right] \qquad \text{(B.3)}$$

where C_o is assumed to be the same as in (B.2) and is obtained from the normalisation condition $\rho_o = 1$.

The summations in (B.2) and (B.3) can be replaced by the largest term corresponding to ν_o given by

$$\eta^2 \frac{(m-\nu_0)(\mu-\nu_0)}{\nu_0(N-m-\mu+\nu_0)} = 1 \qquad (B.4)$$

since the distributions are sharply peaked about ν_o. Thus, following Gutzwiller (1965) we obtain

$$\rho_{i\uparrow}(i,i) = p_\uparrow(i-i) = \frac{m}{N}$$

$$\rho_{i\uparrow}(i,j) = q_\uparrow p_\uparrow(i-j) \quad \text{for } i \neq j \qquad (B.5)$$

with $q_\uparrow$ given by (4.17) with similar expressions for $\downarrow$ spin electrons with m replaced by μ.

It is seen from (B.4) that the quantity η^2 plays the same role as the Boltzmann factor in the law of mass action and Gutzwiller called this the 'quasi-chemical' approximation. Transforming (B.5) to reciprocal space gives equation (4.21) for $n_{k\uparrow}$, with $q_\uparrow$ being the discontinuity at the Fermi surface, which has been shown by Gutzwiller (1965) to be exact for $E \leq E_f$ in the limit $C \to \infty$.

Aldred, A.T., 1966, J.Appl.Phys. 37, 1344.

Aldred, A.T., 1968, J.Phys.C. 1, 1103.

Angadi, M.M., Fawcett, E. and Rasolt, M., 1974, Phys.Rev.Lett. 32, 613.

Arrot, A. and Sato, H., 1959, Phys.Rev. 114, 1420.

Baraff, D.R., 1973, Phys.Rev.B. 8, 3439.

Bardasis, A., Falk, D.S., Ferrell, R.A., Fullenbaum, M.S., Prange, R.E. and Mills, D.L., 1965, Phys.Rev.Lett. 14, 298.

Bates, C.A. and Stevens, K.W.H., 1961, Proc.Phys.Soc. 78, 1321.

Beck, P.A., 1964, Proc.Int.Conf.Magnetism, Nottingham, p.178.

Brinkman, W.F. and Rice, T.M., 1970, Phys.Rev. B2, 4302.

Brown, R.C. and March, N.H., 1976, Physics Reports 24, 77.

Brueckner, K.A., 1955, Phys.Rev. 97, 1353.

Callaway, J., Tawil, R.A. and Wang, C.S., 1973, Phys.Lett. 46A, 161.

Campbell, I.A. and Gomes, A.A., 1967, Proc.Phys.Soc. 91, 319.

Cheng, C.H., Gupta, K.P., Wei, C.T. and Beck, P.A., 1964, J.Phys.Chem. Solids 25, 759.

Cheng, C.H., Wei, C.T. and Beck, P.A., 1960, Phys.Rev. 120, 426.

Clogston, A.M., 1962, Phys.Rev. 125, 439.

Coleman, R.V., Morris, R.C. and Sellmyer, D.J., 1973, Phys.Rev.B8, 317.

Coles, B.R., 1958, Adv.Phys. 7, 40.

Comly, J.B., Holden, T.M. and Low, G.G., 1968, J.Phys.C.1, 458.

Coulson, C.A. and Fisher, I., 1949, Phil.Mag. 40, 386.

Crangle, J. and Martin, M.J.C., 1959, Phil.Mag. 4, 1006.

Cuthill, J.R., McAllister, A.J. and Williams, M.L., 1968, J.Appl.Phys.39,2204.

Cyrot-Lackmann, F., 1967, Adv.Phys. 16, 393.

Cyrot-Lackmann, F., 1969, Surface Science 15, 535.

Daniel, E. and Friedel, J., 1963, J.Phys.Chem.Solids 24, 1601.

Duff, K.J. and Das, T.P., 1971, Phys.Rev. B3, 2294.

Duff, K.J. and Das, T.P., 1975, Phys.Rev. B12, 3870.

References (Continued)

Edwards, D.M., 1970, Phys.Lett. 33A, 183.

Edwards, D.M. and Hewson, A.C., 1968, Rev.Mod.Phys. 40, 810.

Ericson, M. and Jacrot, B., 1960, J.Phys.Chem.Sol. 13, 235.

Fallot, M., 1936, Ann.Phys.(Paris) 6, 305.

Friedel, J., 1958, Nuovo Cimento.Suppl. 7, 287.

Friedel, J., 1964, Trans.AIME, 230, 616.

Friedel, J., 1969, The Physics of Metals Ed. J.M. Ziman (Cambridge University Press) p.340.

Friedel, J., 1976, To be published in Ann.Phys.(Paris).

Friedel, J. and Sayers, C.M., 1976, To be submitted to J.Physique.

Galitski, V.M., 1958, Sov.Phys. JETP. 7, 104.

Geldart, D.J.W., Rasolt, M. and Taylor, R., 1972, Sol.St.Comm. 10, 279.

Goodenough, J.B., 1958, J.Appl.Phys. 29, 513.

Goodenough, J.B., 1963, Magnetism and the chemical bond. (New York: Wiley).

Goodings, D.A. and Heine, V., 1960, Phys.Rev.Lett. 5, 370.

Gold, A.V., Hodges, L., Panousis, P.T. and Stone, D.R., 1971, Int.J.Mag. 2, 357.

Gschneider, K.A., 1964, Sol.St.Phys. 16, 275.

Gupta, K.P., Cheng, C.H. and Beck, P.A., 1964, J.Phys.Chem.Solids 25, 1147.

Gutzwiller, M.C., 1963, Phys.Rev.Lett. 10, 159.

Gutzwiller, M.C., 1965, Phys.Rev. 137, A1726.

Hagemann, H.J., Gudat, W. and Kunz, C., 1976, Phys.Stat.Sol. B74, 507.

Hedin, L. and Lundquist, S., 1969, Sol.St.Phys. 23, 1.

Heitler, W. and London, F., 1927, Z.f. .Phys. 44, 455.

Herring, C., 1966, Magnetism Ed. G. Rado and H. Suhl, Vol.4 (New York: Academic Press).

Hodges, L., Ehrenreich, H. and Lang, N.D., 1966, Phys.Rev. 152, 505.

Hofmann, J.A., Paskin, A., Tauer, K.J. and Weiss, R.J., 1956, J.Phys. Chem.Solids 1, 45.

Hohenberg, P.C. and Kohn, W., 1964, Phys.Rev. 136, B864.

Holden, T.M., Comly, J.B. and Low, G.G., 1967, Proc.Phys.Soc. 92, 726.

References (Continued)

Hubbard, J., 1963, Proc.Roy.Soc. A276, 238.

Hubbard, J., 1964, Proc.Roy.Soc. A277, 237.

Hund, F., 1928, Z.f.Phys. 51, 759.

Joseph, A.S. and Thorsen, A.C., 1963, Phys.Rev.Lett. 11, 554.

Kanamori, J., 1963,Prog.Theor.Phys. 30, 275.

Kapoor, Q.S., Watson, L.M. and Fabian, D.J., 1973, Band Structure Spectroscopy of Metals and Alloys Ed. D.J. Fabian and L.M. Watson (London and New York. Academic Press) p.215.

Koster, G.F. and Slater, J.C., 1954, Phys.Rev. 96, 1208.

Koster, T.A. and Shirley, D.A., 1971, Hyperfine interactions in excited nuclei, Vol.4. Ed. G. Goldring and R. Kalish (New York : Gordon and Breach) p.1239.

Kouvel, J.S. and Fisher, M.E., 1964, Phys.Rev. 136, A1626.

Kulkov, V.D., 1972, Sov.Phys.Sol.St. 14, 557.

Kumagai, K., Asayama, K. and Campbell, I.A., 1974, J.Phys.Soc.Japan 37,1460.

Kunz, C., 1973, Band Structure Spectroscopy of Metals and Alloys. Ed. D.J. Fabian and L.M. Watson (London and New York : Academic Press)p.503.

March, N.H. and Murray, A.M., 1960, Phys.Rev. 120, 830.

March, N.H. and Murray, A.M., 1961, Proc.Roy.Soc. A261, 119.

Mott, N.F., 1935, Proc.Phys.Soc. 47, 571.

Mott, N.F., 1964, Adv.Phys. 13, 325.

Mott, N.F. and Stevens, K.W.H., 1957, Phil.Mag. 2, 1364.

Mulliken, R.S., 1928, Phys.Rev. 32, 186, 761.

Nemoshkalenko, V.V., Nagornyi,V.Y. and Nikolaev, L.I, 1973, Sov.Phys. Sol.St. 14, 1835.

Noakes, J.E. and Arrot, A., 1964, J.Appl.Phys. 35, 931.

Parsons, D., Sucksmith , W. and Thompson, J.E., 1958, Phil.Mag. 3, 1174.

Pauling, L., 1938, Phys.Rev. 54, 899.

Rayne, J.A. and Kemp, W.R.G., 1956, Phil.Mag. 1, 918.

Sakoh, M. and Edwards, D.M., 1975, Phys.Stat.Sol. B70, 611.

Sayers, C.M., 1976, To be published in J.Phys.F.

Sayers, C.M., March, N.H., Dev, A., Fabian, D.J. and Watson, L.M., 1975, J.Phys. F.5, L207.

References (Continued)

Shirley, D.A. and Westenbarger, G.A., 1965, Phys.Rev. 138, A170.

Shoemake, G.E. and Rayne, J.A., 1968, Phys.Lett. 26A, 222.

Shull, C.G., 1963, Electronic Structure and Alloy Chemistry of the Transition Elements (New York : Wiley) p.69.

Shull, C.G. and Yamada, Y., 1962, J.Phys.Soc.Jap. 17 (Suppl.B-III) 1.

Slater, J.C., 1930, Phys.Rev. 36, 57.

Song, C., Trooster, J. and Benczer-Koller, N., 1974, Phys.Rev. B9, 3854.

Song, C., Trooster, J., Benczer-Koller, N. and Rothberg, G.M., 1972, Phys.Rev.Lett. 29, 1165.

Stearns, M.B., 1973, Phys.Rev. B8, 4383.

Stearns, M.B., 1974, AIP Conf.Proc. No.24, p.453.

Stoddart, J.C. and March, N.H., 1971, Ann.Phys.(N.Y) 64, 174.

Stoddart, J.C., March, N.H. and Stott, M.J., 1969, Phys.Rev. 186, 683.

Stott, M.J., 1969, J.Phys.C. 2, 1474.

Tawil, R.A. and Callaway, J., 1973, Phys.Rev. B 7, 4242.

Terakura, K., 1976, J.Phys.F.6, 1385.

Van der Woude, F. and Sawatzky, G.A., 1974, Phys.Rep. 12, 335.

Van Vleck, J.H., 1953, Rev.Mod.Phys. 25, 220.

Veal, B.W. and Rayne, J.A., 1964, Phys.Rev. 135, A442.

Vincze, I. and Aldred, A.T., 1974, Phys.Rev. B9, 3845.

Von Barth, U. and Hedin, L., 1972, J.Phys.C5, 1629.

Wada, W.W. and Brueckner, K.A., 1956, Phys.Rev. 103, 1008 (1956).

Wakoh, S. and Yamashita, J., 1968, J.Phys.Soc.Jap. 25, 1272.

Wang, C.S. and Callaway, J., 1974, Phys.Rev. B9, 4897.

Watson, R.E. and Freeman, A.J., 1961, Phys.Rev. 123, 2027.

Wenger, A., Burri, G. and Steinemann, S., 1971, Phys.Lett. 34A, 195.

White, G.K. and Woods, S.B., 1958, Phil.Trans.Roy.Soc. A251, 273.

Wolff, P.A., 1961, Phys.Rev. 124, 1030.

Wood, J.H., 1962, Phys.Rev. 126, 517 (1962).